





A facile synthesis of visible light driven Ni₃V₂O₈ nano-cube/BiVO₄ nanorod composite photocatalyst with enhanced photocatalytic activity towards degradation of acid orange 7

Swaminathan Arumugam^a, Thirugnanam Bavani^a, Mani Preeyanghaa^b, Saleh O. Alaswad^c, Bernaurdshaw Neppolian^e, Jagannathan Madhavan^a  , Sepperumal Murugesan^d

[Show more](#) 

 Share  Cite

<https://doi.org/10.1016/j.chemosphere.2022.136100> 

[Get rights and content](#) 

Highlights

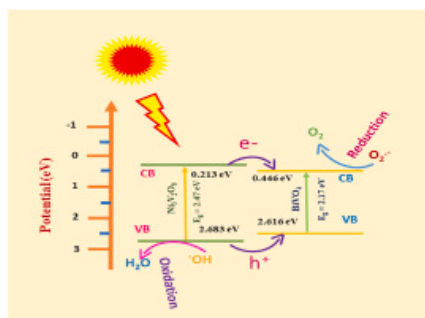
- Ni₃V₂O₈/BiVO₄ nanocomposites are prepared by facile one-pot hydrothermal method.
- Ni₃V₂O₈/BiVO₄ nanocomposites exhibits higher photocurrent intensities than pure BiVO₄ and Ni₃V₂O₈.
- h⁺ and OH[•] are playing vital role in the degradation of AO7 under VLI.
- Optimized NB-2 composite exhibits excellent photostability and reusability.

Abstract

Photocatalysis is one of the promising method to degrade harmful organic pollutants under visible light exposure. In this work, a novel Ni₃V₂O₈/BiVO₄ nanocomposite has been prepared by one-pot hydrothermal method, and investigated through X-ray diffraction, FT-IR, UV-visible diffuse reflectance spectroscopy, scanning and transmission electron microscopy and photoluminescence techniques. Subsequently, the photocatalytic performance of Ni₃V₂O₈/BiVO₄ nanocomposite has been examined by degrading AO7 under visible light illumination. The photocatalytic efficiency of the optimized 1:2 ratio of Ni₃V₂O₈/BiVO₄ nanocomposite photocatalyst is found to be 87% with a rate constant value of 0.03387 min⁻¹ which are higher than those of other prepared photocatalysts. This

nanocomposite exhibits excellent stability even after 3 three cycles, and shows 1.135- and 1.17-times higher photocurrent intensity than pure BiVO₄ and Ni₃V₂O₈ respectively. The mechanism for the degradation of AO7 over Ni₃V₂O₈/BiVO₄ nanocomposite photocatalyst has been proposed.

Graphical abstract



Download : [Download high-res image \(195KB\)](#)

Download : [Download full-size image](#)

Introduction

In the present situation, the pollutant-free water is the most essential requirement for all lives. The aquatic environment is heavily polluted by the discharge of untreated industrial effluents, which has been increasing with more modern industries and population (Saravanan et al., 2021; Ahmed et al., 2021). The highly toxic components constitute harmful pollutants that results in severe health and ecological problems. As a model, AO7 is a one of the rapidly used azo dye in the textile industries and particularly used as a hair coloring agent. After disposal, the azo compounds are reduced to form the harmful products, which are highly toxic than its mother compound. These components with wastewater might cause skin problems, mutagenic and carcinogenic diseases to the living organisms and results in severe health issues. Thus, it is essential to treat the effluents before releasing into aquatic environment, to possibly prevent all the above issues. Hence, different physical, chemical and biological treatment methods, like, chemical coagulation, carbon adsorption, membrane filtration, ion-exchange and advanced oxidation processes are employed to remove the contaminants from the polluted water (Malathi et al., 2018a, 2018b; Adeola and Forbes, 2021). Of them, except advance oxidation processes (AOPs), all treatment methods require costly additional steps and produces secondary pollutants at the time of operation. AOPs convert highly toxic organic pollutants into harmless and biodegradable products by the in-situ formation of the hydroxyl radicals (Pandis et al., 2022; Malathi et al., 2018c). Though, TiO₂ is considered as a benchmark photocatalyst, its wide bandgap energy (E_g) (~3.2eV) makes it disadvantageous for commercial applications (Chava et al., 2021, 2022; Wetchakun et al., 2015). Therefore, it is vital to design a good visible light active photocatalyst. In the recent studies, bismuth-based semiconductor photocatalysts, such as, Bi₂WO₆ (Malathi et al., 2017a), BiVO₄ (Gomes et al., 2021), BiFeO₃ (Bavani et al., 2021a), BiOX (X=F, Cl, Br, I) (Arumugam et al., 2021a; Cen et al., 2021; Bavani et al., 2021b, 2022), Bi₂O₃ (Zhao et al., 2022), Bi₂S₃ (Arumugam et al., 2021b), Bi₂MoO₆ (Stelo et al., 2020), BiFeWO₆ (Lu et al., 2021) have received much attention from researchers. Among this, BiVO₄ photocatalyst with low E_g (~2.3–2.5eV) is found to be highly visible light responsive and more economical with easy preparation. However, its photocatalytic activity is unexpectedly limited because of its low separation and migration of e^-/h^+ pairs leading to high recombination. However, it is possible to augment the photocatalytic activity of BiVO₄ by the creating heterojunction with a suitable semiconductor photocatalyst having appropriate band potential, which would possibly improve the catalytic activity under visible light exposure. Additionally, BiVO₄ based composites, like, AgVO₃/BiVO₄ (Wang and Cao, 2017), g-C₃N₄/BiVO₄ (Li et al., 2022), BiVO₄/BiOI (Huang et al., 2015), BiFeWO₆/BiVO₄ (Malathi et al., 2017b), BiVO₄/FeVO₄ (Sajid et al., 2018a), BiVO₄/InVO₄ (Guo et al., 2015), BiVO₄/BiOBr (Li et al., 2016),

BiVO₄/WO₃ (Selvarajan et al., 2017), Fe₃O₄/BiVO₄ (Ma et al., 2021), Co₃O₄/BiVO₄ (Long et al., 2006), BiVO₄/BiOCl (Ma et al., 2017) and BiVO₄/FeOOH (Sajid et al., 2018b) are reported to show excellent photocatalytic activity in the remediation of wastewater. However, Ni₃V₂O₈ is a reactive visible light semiconducting photocatalyst with narrow bandgap (~2.0eV), easily available non-toxic, inexpensive and photochemically stable with high electron mobility and hence it has been chosen to couple with BiVO₄. Recently, the Ni₃V₂O₈ composites, such as, g-C₃N₄/Ni₃V₂O₈ (Vesali-Kermani et al., 2020) and V₂O₅@Ni₃V₂O₈ (Zheng and Zhang, 2021) are found to exhibit greater photocatalytic ability under visible light irradiation (VLI). Thus, the creation of the heterojunction between BiVO₄ and Ni₃V₂O₈ is expected to increase the charge separation by reducing the fast reconnection of e⁻/h⁺ pairs. The photocatalytic activity of Ni₃V₂O₈/BiVO₄ heterojunction composite for pollutant degradation is not reported so far.

In the present study, Ni₃V₂O₈ is taken as a co-catalyst to load over the BiVO₄, due to its easy preparation, inexpensiveness and high activity in the visible region. We have constructed the Ni₃V₂O₈/BiVO₄ composite using one-step hydrothermal method by differentiating the molar ratios of Ni/Bi. The Ni₃V₂O₈/BiVO₄ heterojunction composite photocatalyst has been tested for the decomposition of acid orange-7 (AO7) under visible light illumination. The obtained photocatalytic degradation results of Ni₃V₂O₈/BiVO₄ composite are impressive and hence it could be considered as a useful material for wastewater treatment purposes.

Section snippets

Materials

Nickel nitrate hexahydrate (Ni(NO₃)₂·6H₂O), bismuth nitrate pentahydrate (Bi(NO₃)₃·5H₂O) and ammonium metavanadate (NH₄VO₃) were obtained from Sigma Aldrich. Triton X-100, acid orange-7 (AO7), isopropanol (IPA) and benzoquinone (BQ) were obtained from SD Fine Chemicals Limited, India. Ammonium oxalate (AO) and ethanol were procured from Qualigens, India. Double distilled water was used for the preparation of all solution used in this study...

Preparation of Ni₃V₂O₈/BiVO₄ composite

A simple one-step hydrothermal method was employed to...

Crystal structure and morphology

The structural units of the newly synthesized BiVO₄, Ni₃V₂O₈, NB-1, NB-2 and NB-3 nanocomposites were characterized by FT-IR spectra. As shown in Fig. 1, pure BiVO₄ shows a peak at 426cm⁻¹, due to Bi-O bond and the asymmetric V-O stretching peak appears at 676 and 841 cm⁻¹. In the case of pure Ni₃V₂O₈, the band at 925 and 797 cm⁻¹ are due to the asymmetric and symmetric stretching of VO₄, correspondingly (Zhang et al., 2010). The band at 667 and 424cm⁻¹ indicates the presence of V-O-V and...

Conclusions

In conclusion, Ni₃V₂O₈/BiVO₄ nanocomposite photocatalysts were prepared by hydrothermal method. The XRD, SEM and TEM characterization results illustrated the formation of the Ni₃V₂O₈/BiVO₄ nanocomposite without any other impurities. Furthermore, the optimized 1:2 ratio of Ni:Bi nanocomposite (NB-2) exhibited an excellent photocatalytic ability among the prepared photocatalysts. This was mainly attributed to the formation of close contact between Ni₃V₂O₈ and BiVO₄ which considerably increased...

Author contributions statement

Swaminathan Arumugam: Experimental work, Writing – original draft.; **Sepperumal Murugesan and Bavani Thirugnanam :** Methodology, Writing - review & editing.; **Jagannathan Madhavan:** Supervision, Validation, Writing – review & editing.; **Saleh O. Alaswad, Mani Preeyanghaa and Bernaurdshaw Neppolian:** Validation and Formal analysis....

Declaration of competing interest

The authors declare that they have no known competing financial interests or personal relationships that could have appeared to influence the work reported in this paper....

Acknowledgement

The authors S. Arumugam and J. Madhavan are thankful and grateful to Thiruvalluvar University, Vellore, for providing laboratory facilities....

[Special issue articles](#) [Recommended articles](#)

References (38)

S.F. Ahmed *et al.*

[Recent developments in physical, biological, chemical, and hybrid treatment techniques for removing emerging contaminants from wastewater](#)

J. Hazard Mater. (2021)

M. Arumugam *et al.*

[Recent developments on bismuth oxyhalides \(BiOX; X= Cl, Br, I\) based ternary nanocomposite photocatalysts for environmental applications](#)

Chemosphere (2021)

M. Arumugam *et al.*

[Enhanced photocatalytic activity at multidimensional interface of 1D-Bi₂S₃@2D-GO/3D-BiOI ternary nanocomposites for tetracycline degradation under visible-light](#)

J. Hazard Mater. (2021)

T. Bavani *et al.*

[A straightforward synthesis of visible light driven BiFeO₃/AgVO₃ nanocomposites with improved photocatalytic activity](#)

Environ. Pollut. (2021)

T. Bavani *et al.*

[Fabrication of novel AgVO₃/BiOI nanocomposite photocatalyst with photoelectrochemical activity towards the degradation of Rhodamine B under visible light irradiation](#)

Environ. Res. (2021)

T. Bavani *et al.*

[One-pot synthesis of bismuth yttrium tungstate nanosheet decorated 3D-BiOBr nanoflower heterostructure with enhanced visible light photocatalytic activity](#)

Chemosphere (2022)

S. Cen *et al.*

[Direct Z-scheme Ag₂WO₄/BiOCl composite photocatalyst for efficient photocatalytic degradations of dissolved organic impurities](#)

Optik (2021)

R.K. Chava *et al.*

[Surface engineering of CdS with ternary Bi/Bi₂MoO₆-MoS₂ heterojunctions for enhanced photoexcited charge separation in solar-driven hydrogen evolution reaction](#)

Appl. Surf. Sci. (2021)

R.K. Chava *et al.*

[Bismuth quantum dots anchored one-dimensional CdS as plasmonic photocatalyst for pharmaceutical tetracycline hydrochloride pollutant degradation](#)

Chemosphere (2022)

L.E. Gomes *et al.*

[Enhanced photocatalytic activity of BiVO₄/Pt/PtO_x photocatalyst: the role of Pt oxidation state](#)

Appl. Surf. Sci. (2021)



View more references

Cited by (7)

[Facile green synthesis of Ni₃V₂O₈ nanoparticles for efficient photocatalytic degradation of Rose Bengal dye under visible light irradiation](#)

2024, Chemical Physics Letters

[Show abstract](#)

[Non-noble-metal TiC-nanoparticle-promoted charge separation and photocatalytic degradation performance on Bi₂O₃ microrods: degradation pathway and mechanism investigation](#) ↗

2023, Physical Chemistry Chemical Physics

[A Novel Z-Scheme Ni₃V₂O₈/AgI Visible Light Photocatalyst with Enhanced Photocatalytic Activity](#) ↗

2023, Research Square

[Co-Doped Ni₃V₂O₈ Nanofibers Achieving d-d Orbital Coupling for Electrocatalytic Oxygen Reduction](#) ↗

2023, Inorganic Chemistry

[Microwave-assisted synthesis of ZnO nanoparticles using different capping agents and their photocatalytic application](#) ↗

2023, Environmental Science and Pollution Research

Deep Eutectic Solvent-Mediated Synthesis of Ni₃V₂O₈/N-Doped RGO for Visible-Light-Driven H₂ Evolution and Simultaneous Degradation of Dyes ↗

2023, Inorganics

[View all citing articles on Scopus ↗](#)

[View full text](#)

© 2022 Elsevier Ltd. All rights reserved.



All content on this site: Copyright © 2024 Elsevier B.V., its licensors, and contributors. All rights are reserved, including those for text and data mining, AI training, and similar technologies. For all open access content, the Creative Commons licensing terms apply.



[Home](#) [Environmental Science and Pollution Research](#) [Article](#)

A Z-scheme BiYO₃/g-C₃N₄ heterojunction photocatalyst for the degradation of organic pollutants under visible light irradiation

Research Article Published: 11 January 2023

Volume 30, pages 41095–41106, (2023) [Cite this article](#)

Environmental Science and
Pollution Research

[Aims and scope](#)[Submit manuscript](#)

[Parthasarathy Sasikala](#), [Thirugnanam Bavani](#), [Manickam Selvaraj](#), [Mani Preeyanghaa](#),
[Bernardshaw Neppolian](#), [Sepperumal Murugesan](#) & [Jagannathan Madhavan](#) 

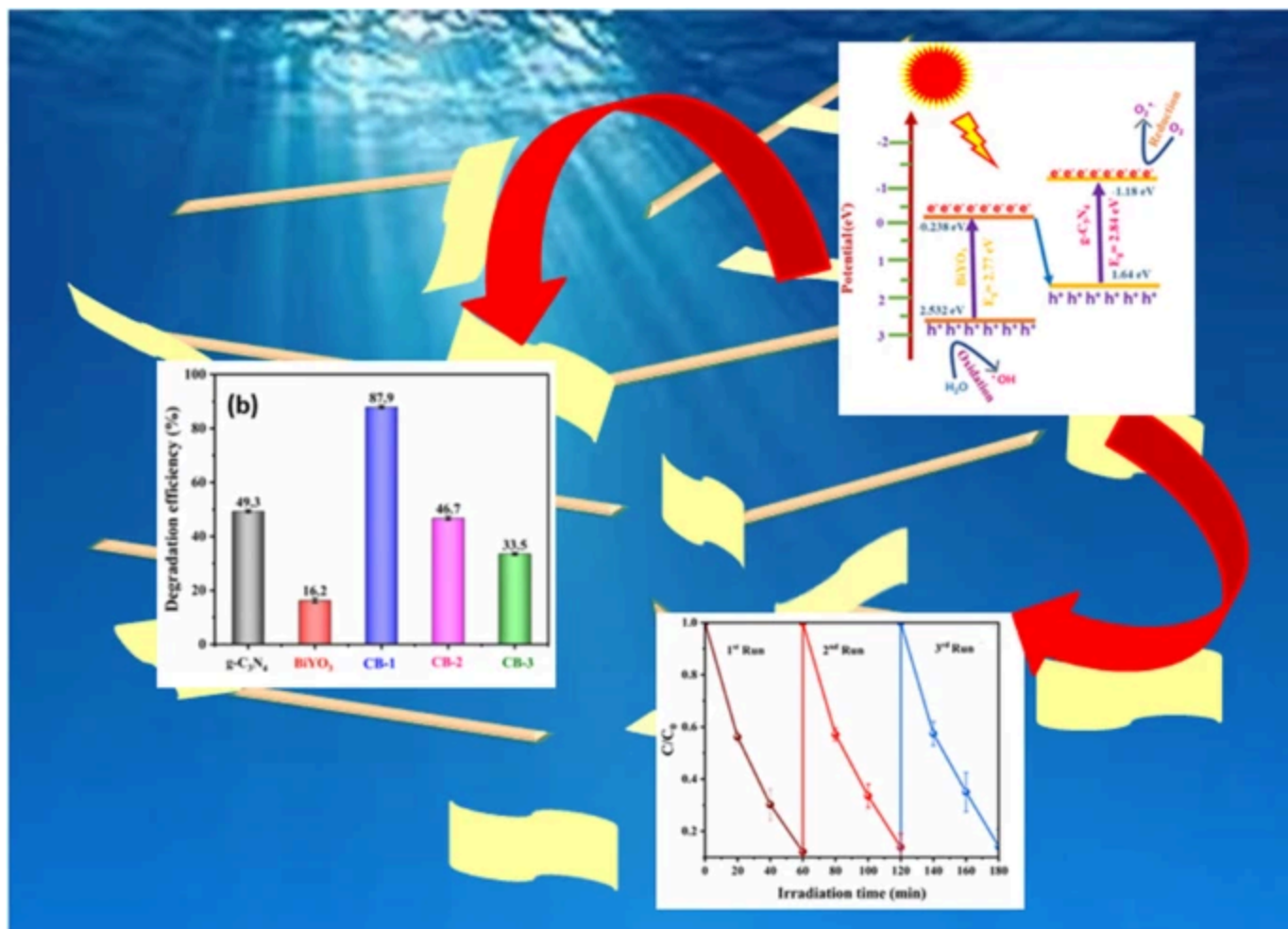
 321 Accesses  3 Citations [Explore all metrics](#) →

Abstract

Photocatalysis is one of the fascinating fields for the wastewater treatment. In this regard, the present study deals with an effective visible light active BiYO₃/g-C₃N₄ heterojunction nanocomposite photocatalyst with various ratios of BiYO₃ and g-C₃N₄ (1:3, 1:1 and 3:1), synthesised by a wet chemical approach. The as-synthesised nanocomposite photocatalysts were investigated via different physicochemical approaches like Fourier transform infrared

(FT-IR), X-ray diffraction (XRD), scanning electron microscopy (SEM), energy dispersive spectroscopy (EDS), transmission electrons microscopy (TEM), UV–vis diffuse reflectance spectroscopy (DRS), photoluminescence (PL) and photoelectrochemical studies to characterise the crystal structure, morphology, optical absorption characteristics and photoelectrochemical properties. The photocatalytic degradation ability of the prepared photocatalytic samples was also analysed through the degradation of RhB in the presence of visible light irradiation. Of all the synthesised photocatalysts, the optimised CB-1 composite showed a significant photocatalytic efficiency (88.7%), with excellent stability and recyclability after three cycles. O₂^{•-} and [•]OH radicals were found to act a major role in the RhB degradation using optimised CB-1 composite, and it possessed ~ 1 times greater photocurrent intensity than the pristine g-C₃N₄ and BiYO₃. In the present work, a direct Z-scheme heterojunction BiYO₃/g-C₃N₄ with a considerably improved photocatalytic performance is reported.

Graphical Abstract



i This is a preview of subscription content, [log in via an institution](#) to check access.

Access this article

Log in via an institution

Buy article PDF 39,95 €

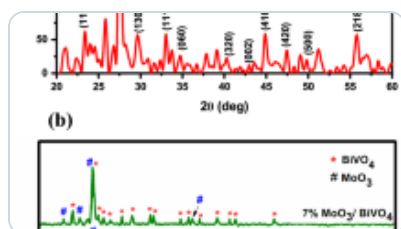
Price includes VAT (India)

Instant access to the full article PDF.

Rent this article via [DeepDyve](#)

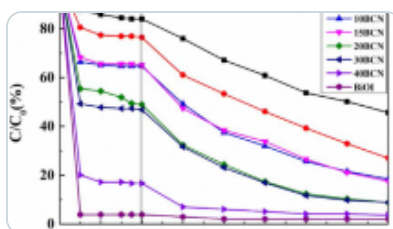
[Institutional subscriptions](#) →

Similar content being viewed by others



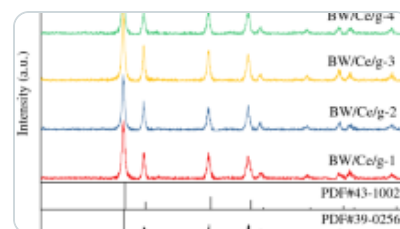
Efficient photocatalysis performance and recyclability of MoO₃/BiVO₄...

Article | 09 June 2021



Construction of Z-scheme BiOI/g-C₃N₄ heterojunction with enhanced photocatalyt...

Article | 08 June 2019



Synthesis of novel ternary Bi₂WO₆/CeO₂/g-C₃N₄ composites with...

Article | 08 September 2020

Data availability

All data related to this manuscript is incorporated in the manuscript.

References

Abdelhafeez IA, Chen J, Zhou X (2020) Scalable one-step template-free synthesis of ultralight edge-functionalized g-C₃N₄ nanosheets with enhanced visible light photocatalytic performance. *Sep Purif Technol* 250:117085

[Article](#) [CAS](#) [Google Scholar](#)

An W, Sun K, Hu J, Cui W, Liu L (2020) The Z-scheme Ag₂CO₃@ g-C₃N₄ core-shell structure for increased photoinduced charge separation and stable photocatalytic degradation. *Appl Surf Sci* 504:144345

[Article](#) [CAS](#) [Google Scholar](#)

Bashir S, Iqbal N, Jamil A, Alazmi A, Shahid M (2022) Facile synthesis of a novel photocatalyst with integrated features for industrial effluents treatment. *Ceram Int* 48(3):3172–3184

[Article](#) [CAS](#) [Google Scholar](#)

Bavani T, Madhavan J, Prasad S, AlSalhi MS, AlJaafreh MJ (2021a) A straightforward synthesis of visible lightdrivenBiFeO₃/AgVO₃ nanocomposites with improved photocatalytic activity. *Environ Poll* 269:116067

[Article](#) [CAS](#) [Google Scholar](#)

Bavani T, Madhavan J, Prasad S, AlSalhi MS, AlJaffreh M, Vijayanand S, (2021b) Fabrication of novel AgVO₃/BiOI nanocomposite photocatalyst with photoelectrochemical activity

towards the degradation of Rhodamine B under visible light irradiation. *Environ Res* 200:111365

[Article](#) [CAS](#) [Google Scholar](#)

Bavani T, Vinesh V, Neppolian B, Murugesan S, Selvaraj M, Madhavan J (2022a) One-step synthesis of rod-on-plate like 1D/2D-NiMoO₄/BiOI nanocomposite for an efficient visible light driven photocatalyst for pollutant degradation. *Environ Sci Pollut Res* 1–11

Bavani T, Madhavan J, Preeyanghaa M, Neppolian B, Murugesan S (2022b) Construction of direct Z-scheme g-C₃N₄/BiYWO₆ heterojunction photocatalyst with enhanced visible light activity towards the degradation of methylene blue. *Environ Sci Poll Res* 7:1–2

[Google Scholar](#)

Che H, Che G, Dong H, Hu W, Hu H, Liu C, Li C (2018) Fabrication of Z-scheme Bi₃O₄Cl/g-C₃N₄ 2D/2D heterojunctions with enhanced interfacial charge separation and photocatalytic degradation various organic pollutants activity. *Appl Surf Sci* 455:705–716

[Article](#) [CAS](#) [Google Scholar](#)

Danish M, Tayyab M, Akhtar A, Altaf AA, Kausar S, Ullah S, Iqbal M (2020) Effect of soft template variation on the synthesis, physical, and electrochemical properties of Mn₃O₄ nanomaterial. *Inorg Nano Metal Chem* 51(3):359–365

[Article](#) [Google Scholar](#)

Geng Y, Chen D, Li N, Xu Q, Li H, He J, Lu J (2021) Z-Scheme 2D/2D α -Fe₂O₃/g-C₃N₄ heterojunction for photocatalytic oxidation of nitric oxide. *Appl Catal B Environ* 280:119409

[Article](#) [CAS](#) [Google Scholar](#)

Hernández ADL, Durán AJC, Cortés LS, Zanella R, Soto TE, López JR (2022) Cr-doped BiYO₃ photocatalyst for degradation of oxytetracycline under visible light irradiation. *J Korean Ceram Society* 26:1–4

[Google Scholar](#)

Jia Z, Lyu F, Zhang LC, Zeng S, Liang SX, Li YY, Lu J (2019) Pt nanoparticles decorated heterostructured g-C₃N₄/Bi₂MoO₆ micropjlates with highly enhanced photocatalytic activities under visible light. *Sci Rep* 9(1):1–13

[Article](#) [Google Scholar](#)

Li T, Zhao L, He Y, Cai J, Luo M, Lin J (2013) Synthesis of g-C₃N₄/SmVO₄ composite photocatalyst with improved visible light photocatalytic activities in RhB degradation. *Appl Catal B Environ* 129:255–263

[Article](#) [CAS](#) [Google Scholar](#)

Lian X, Xue W, Dong S, Liu E, Li H, Xu K (2021) Construction of S-scheme Bi₂WO₆/g-C₃N₄ heterostructure nanosheets with enhanced visible-light photocatalytic degradation for ammonium dinitramide. *J Hazard Mater* 412:125217

[Article](#) [CAS](#) [Google Scholar](#)

Liu J, Liu Y, Liu N, Han Y, Zhang X, Huang H, Lifshitz Y, Lee ST, Zhong J, Kang Z (2015) Metal-free efficient photocatalyst for stable visible water splitting via a two-electron pathway. *Sci* 347(6225):970–4

Liu Y, Zhu Q, Tayyab M, Zhou L, Lei J, Zhang J (2021a) Single-atom Pt loaded zinc vacancies ZnO–ZnS induced type-V electron transport for efficiency photocatalytic H₂ evolution. *Solar Rrl* 5(11):2100536

[Article](#) [CAS](#) [Google Scholar](#)

Liu G, Feng M, Tayyab M, Gong J, Zhang M, Yang M, Lin K (2021b) Direct and efficient reduction of perfluorooctanoic acid using bimetallic catalyst supported on carbon. *J Hazard Mater* 412:125224

[Article](#) [CAS](#) [Google Scholar](#)

Liu X, Chen J, Yang L, Yun S, Que M, Zheng H, Zhao Y, Yang T, Liu Z (2022) 2D/2D g-C₃N₄/TiO₂ with exposed (001) facets Z-scheme composites accelerating separation of interfacial charge and visible photocatalytic degradation of Rhodamine B. *J Phys Chem Solids* 160:110339

[Article](#) [CAS](#) [Google Scholar](#)

Long M, Cai W, Cai J, Zhou B, Chai X, Wu Y (2006) Efficient photocatalytic degradation of phenol over Co O /BiVO composite under visible light irradiation. *J Phys Chem B* 110(41):20211–20216

Lv J, Dai K, Zhang J, Geng L, Liang C, Liu Q, Zhu G, Chen C (2015) Facile synthesis of Z-scheme graphitic-C₃N₄/Bi₂MoO₆ nanocomposite for enhanced visible photocatalytic properties. *Appl Surf Sci* 358:377–384

[Article](#) [CAS](#) [Google Scholar](#)

Malathi A, Arunachalam P, Grace AN, Madhavan J, Al-Mayouf AM (2017) A robust visible-light driven BiFeWO₆/BiOI nanohybrid with efficient photocatalytic and photoelectrochemical performance. *Appl Surf Sci* 412:85–95

[Article](#) [CAS](#) [Google Scholar](#)

Mondal KUNAL, Sharma A (2014) Photocatalytic oxidation of pollutant dyes in wastewater by TiO₂ and ZnO nano-materials—a mini-review. *Nanosci Technol* 36–72

Palanisamy G, Bhuvaneshwari K, Srinivasan M, Vignesh S, Elavarasan N, Venkatesh G, Pazhanivel T, Ramasamy P (2021) Two-dimensional g-C₃N₄ nanosheets supporting Co₃O₄-V₂O₅ nanocomposite for remarkable photodegradation of mixed organic dyes based on a dual Z-scheme photocatalytic system. *Diam Relat Mater* 118:108540

[Article](#) [CAS](#) [Google Scholar](#)

Preeyanghaa M, Dhileepan MD, Madhavan J, Neppolian B (2022a) Revealing the charge transfer mechanism in magnetically recyclable ternary g-C₃N₄/BiOBr/Fe₃O₄ nanocomposite for efficient photocatalytic degradation of tetracycline antibiotics. *Chemosphere* 303:135070

[Article](#) [CAS](#) [Google Scholar](#)

Preeyanghaa M, Vinesh V, Sabarikirishwaran P, Rajkamal A, Ashokkumar M, Neppolian B (2022b) Investigating the role of ultrasound in improving the photocatalytic ability of CQD decorated boron-doped g-C₃N₄ for tetracycline degradation and first-principles study of nitrogen-vacancy formation. *Carbon* 192:405–417

[Article](#) [CAS](#) [Google Scholar](#)

Priya A, Arumugam M, Arunachalam P, Al-Mayouf AM, Madhavan J, Theerthagiri J, Choi MY (2020a) Fabrication of visible-light active BiFeWO₆/ZnO nanocomposites with enhanced photocatalytic activity. *Colloids Surf A Physicochem Eng* 586:124294

[Article](#) [CAS](#) [Google Scholar](#)

Priya A, Arunachalam P, Selvi A, Madhavan J, Al-Mayouf AM (2018) Synthesis of BiFeWO₆/WO₃ nanocomposite and its enhanced photocatalytic activity towards degradation

of dye under irradiation of light. *Colloids Surf A Physicochem Eng Asp* 559:83–91

[Article](#) [Google Scholar](#)

Priya A, Senthil RA, Selvi A, Arunachalam P, Kumar CS, Madhavan J, Boddula R, Pothu R, Al-Mayouf AM (2020b) A study of photocatalytic and photoelectrochemical activity of as-synthesized WO₃/g-C₃N₄ composite photocatalysts for AO7 degradation. *Mater Sci Energy Technol* 3:43–50

[CAS](#) [Google Scholar](#)

Qin Z, Chen L, Ma R, Tomovska R, Luo X, Xie X, Su T, Ji H (2020) TiO₂/BiYO₃ composites for enhanced photocatalytic hydrogen production. *J Alloys Compd* 836:155428

[Article](#) [CAS](#) [Google Scholar](#)

Qin ZZ, Liu ZL, Liu YB (2009) Synthesis of BiYO₃ for degradation of organic compounds under visible-light irradiation. *Catal Commun* 10(12):1604–1608

[Article](#) [CAS](#) [Google Scholar](#)

Saravanan A, Kumar P.S, Jeevanantham S, Karishma S, Tajsabreen B, Yaashikaa P.R, Reshma B (2021) Effective water/wastewater treatment methodologies for toxic pollutants removal: Processes and applications towards sustainable development. *Chemosphere* 280:130595

Senthil RA, Osman S, Pan J, Sun Y, Kumar TR, Manikandan A (2019a) A facile hydrothermal synthesis of visible-light responsive BiFeWO₆/MoS₂ composite as superior photocatalyst for degradation of organic pollutants. *Ceram Int* 45(15):18683–18690

[Article](#) [CAS](#) [Google Scholar](#)

Senthil RA, Sun M, Pan J, Osman S, Khan A, Sun Y (2019b) Facile fabrication of a new BiFeWO₆/α-AgVO₃ composite with efficient visible-light photocatalytic activity for dye-degradation. *Opt Mater* 92:284–293

[Article](#) [CAS](#) [Google Scholar](#)

Senthil RA, Theerthagiri J, Selvi A, Madhavan J (2017) Synthesis and characterization of low-cost g-C₃N₄/TiO₂ composite with enhanced photocatalytic performance under visible-light irradiation. *Opt Mater* 64:533–539

[Article](#) [CAS](#) [Google Scholar](#)

Sirimahachai U, Harome H, Wongnawa S (2017) Facile synthesis of AgCl/BiYO₃ composite for efficient photodegradation of RO16 under UV and visible light irradiation. *Sains Malaysiana* 46(9):1393–1399

[Article](#) [CAS](#) [Google Scholar](#)

Sun Y, Qi X, Li R, Xie Y, Tang Q, Ren B (2020) Hydrothermal synthesis of 2D/2D BiOCl/g-C₃N₄ Z-scheme: for TC degradation and antimicrobial activity evaluation. *Opt Mate* 108:110170

[Article](#) [CAS](#) [Google Scholar](#)

Tayyab M, Liu Y, Liu Z, Pan L, Xu Z, Yue W, Zhou L, Lei J, Zhang J (2022a) One-pot in-situ hydrothermal synthesis of ternary In₂S₃/Nb₂O₅/Nb₂C Schottky/S-scheme integrated heterojunction for efficient photocatalytic hydrogen production. *J Colloid Interface Sci* 628:500–512

[Article](#) [CAS](#) [Google Scholar](#)

Tayyab M, Liu Y, Min S, Irfan RM, Zhu Q, Zhou L, Lei J, Zhang J (2022b) Simultaneous hydrogen production with the selective oxidation of benzyl alcohol to benzaldehyde by a noble-metal-free photocatalyst VC/CdS nanowires. *Chinese J Catal* 43(4):1165–1175

[Article](#) [CAS](#) [Google Scholar](#)

Theerthagiri J, Senthil R.A, Priya A, Madhavan J, Michael R.JV, Ashokkumar M (2014) Photocatalytic and photoelectrochemical studies of visible-light active α -Fe₂O₃-g-C₃N₄ nanocomposites. *Rsc Adv* 4(72):38222–38229

Ullah R, Dutta J (2008) Photocatalytic degradation of organic dyes with manganese-doped ZnO nanoparticles. *J Hazard Mater* 156(1–3):194–200

[Article](#) [CAS](#) [Google Scholar](#)

Vinitha V, Preeyanghaa M, Anbarasu M, Jeya G, Neppolian B, Sivamurugan V (2022) Aminolytic depolymerization of polyethylene terephthalate wastes using Sn-doped ZnO nanoparticles. *J Polymers Environ* 1–16

Wang JC, Yao HC, Fan ZY, Zhang L, Wang JS, Zang SQ, Li ZJ (2016) Indirect Z-scheme BiOI/g-C₃N₄ photocatalysts with enhanced photoreduction CO₂ activity under visible light irradiation. *ACS Appl Mater Interface* 8(6):3765–3775

[Article](#) [CAS](#) [Google Scholar](#)

Wongli H, Goodwin CM, Beebe TP Jr, Wongnawa S, Sirimahachai U (2017) AgI-BiYO₃ photocatalyst: synthesis, characterization, and its photocatalytic degradation of dye. *Mater Chem Phys* 202:120–126

[Article](#) [CAS](#) [Google Scholar](#)

Wu Y, Zhao X, Huang S, Li Y, Zhang X, Zeng G, Niu L, Ling Y, Zhang Y (2021) Facile construction of 2D g-C₃N₄ supported nanoflower-like NaBiO₃ with direct Z-scheme heterojunctions and insight into its photocatalytic degradation of tetracycline. *J Hazard Mater* 414:125547

[Article](#) [CAS](#) [Google Scholar](#)

Yin Z, Wang H, Jian M, Li Y, Xia K, Zhang M, Wang C, Wang Q, Ma M, Zheng Q.S, Zhang Y (2017) Extremely black vertically aligned carbon nanotube arrays for solar steam generation. *ACS Appl Mater Interfaces* 9(34):28596–28603

Zhao Z, Ma H, Feng M, Li Z, Cao D, Guo Z (2019) In situ preparation of WO₃/g-C₃N₄ composite and its enhanced photocatalytic ability, a comparative study on the preparation methods. *Engineered Sci* 7(4):52–58

[Google Scholar](#)

Zhao Y, Shi H, Yang D, Fan J, Hu X, Liu E (2020) Fabrication of a Sb₂MoO₆/g-C₃N₄ photocatalyst for enhanced RhB degradation and H₂ generation. *J Phys Chem C* 124(25):13771–13778

[Article](#) [CAS](#) [Google Scholar](#)

Zhou Z, Zhang L, Su W, Li Y, Zhang G (2021) Facile fabrication of AgI/Sb₂O₃ heterojunction photocatalyst with enhanced visible-light driven photocatalytic performance for efficient degradation of organic pollutants in water. *Environ Res* 197:111143

Acknowledgements

The authors J. Madhavan and P. Sasikala are grateful to Thiruvalluvar University, Vellore, for the laboratory facilities.

Author information

Authors and Affiliations

Solar Energy Lab, Department of Chemistry, Thiruvalluvar University, Vellore, 632 115, India

Parthasarathy Sasikala, Thirugnanam Bavani & Jagannathan Madhavan

Department of Chemistry, Faculty of Science, King Khalid University, Abha, 61413, Saudi Arabia

Manickam Selvaraj

Department of Physics and Nanotechnology, SRM Institute of Science and Technology, Kattankulathur, 603 203, Chennai, India

Mani Preeyanghaa

Department of Chemistry, SRM Institute of Science and Technology, Kattankulathur, 603 203, Chennai, India

Bernaurdshaw Neppolian

School of Chemistry, Madurai Kamaraj University, Madurai, 625 021, India

Sepperumal Murugesan

Contributions

All authors contributed to the study conception and design. Material preparation, data collection, analysis and the first draft of the manuscript were written by Parthasarathy Sasikala. Analysis, interpretation and review by Thirugnanam Bavani. Characterisation, interpretation of data and validation are conducted by Mani Preeyanghaa, Bernaurdshaw Neppolian, Manickam Selvaraj and Sepperumal Murugesan. Supervision, validation and review by Jagannathan Madhavan. All authors read and approved the final manuscript.

Corresponding author

Correspondence to [Jagannathan Madhavan](#).

Ethics declarations

Ethical approval

Not applicable.

Consent to participate

All authors have approved the final version of the manuscript and have given their consent for publication.

Consent for publication

All authors have approved the final version of the manuscript and have given their consent for publication.

Competing interests

The authors declare no competing interests.

Additional information

Responsible Editor: Sami Rtimi

Publisher's note

Springer Nature remains neutral with regard to jurisdictional claims in published maps and institutional affiliations.

Supplementary Information

Below is the link to the electronic supplementary material.

[Supplementary file1 \(DOC 729 KB\)](#)

Rights and permissions

Springer Nature or its licensor (e.g. a society or other partner) holds exclusive rights to this article under a publishing agreement with the author(s) or other rightsholder(s); author self-archiving of the accepted manuscript version of this article is solely governed by the terms of such publishing agreement and applicable law.

[Reprints and permissions](#)

About this article

Cite this article

Sasikala, P., Bavani, T., Selvaraj, M. *et al.* A Z-scheme BiYO₃/g-C₃N₄ heterojunction photocatalyst for the degradation of organic pollutants under visible light irradiation. *Environ Sci Pollut Res* 30, 41095–41106 (2023). <https://doi.org/10.1007/s11356-022-25027-9>

Received

17 August 2022

Accepted

23 December 2022

Published

11 January 2023

Issue Date

March 2023

DOI

<https://doi.org/10.1007/s11356-022-25027-9>

Keywords

[1D/2D-BiYO₃/g-C₃N₄](#)

[Nanocomposite](#)





[Visible light: Advanced oxidation process](#)

[Z-scheme](#)

[Photodegradation](#)



Construction of direct FeMoO₄/g-C₃N₄-2D/2D Z-scheme heterojunction with enhanced photocatalytic treatment of textile wastewater to eliminate the toxic effect in marine environment

Swaminathan Arumugam^a, Thirugnanam Bavani^a, Manickam Selvaraj^{b c}, Badria M. Al-Shehri^{b c d}, Mani Preeyanghaa^e, Sieon Jung^f, Jayaraman Theerthagiri^f, Bernaurdshaw Neppolian^g, Sepperumal Murugesan^h, Jagannathan Madhavan^a  , Myong Yong Choi^f  

Show more 

 Share  Cite

<https://doi.org/10.1016/j.chemosphere.2022.137552> 

[Get rights and content](#) 

Highlights

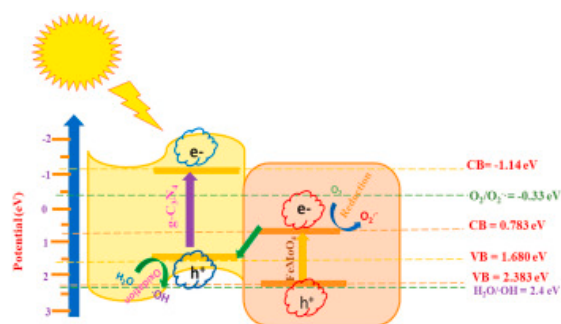
- Novel Z-scheme FeMoO₄/g-C₃N₄ heterojunction photocatalysts were constructed.
- Optimal FeMoO₄/g-C₃N₄ show excellent degradation of Rhodamine B.
- Optimal FeMoO₄/g-C₃N₄ exhibits excellent photostability under visible light.
- h⁺ and O₂^{•-} radicals are playing major role in the degradation of RhB.
- Plausible mechanism for direct Z-scheme FeMoO₄/g-C₃N₄ heterojunction was proposed.

Abstract

A novel FeMoO₄/g-C₃N₄-2D/2D Z-scheme heterojunction photocatalyst was prepared via wet chemical method. The observed structural morphology of FeMoO₄/g-C₃N₄ reveals the 2D-iron molybdate (FeMoO₄) nanoplates compiled with the 2D-graphitic carbon nitride (g-C₃N₄) nanosheets like structure. The photocatalytic activity of the g-C₃N₄, FeMoO₄, and FeMoO₄/g-C₃N₄ composites were studied via the degradation of Rhodamine B (RhB) as targeted textile dye under

visible light irradiation (VLI). The optimal FeMoO₄/g-C₃N₄ (1:3 ratio of g-C₃N₄ and FeMoO₄) composite show an enhanced degradation performance with rate constant value of 0.02226 min⁻¹ and good stability even after three cycles. Thus, the h⁺ and O₂^{•-} are the key radicals in the degradation of RhB under VLI. It is proposed that the FeMoO₄/g-C₃N₄ Z-scheme heterojunction effectively enhances the transfer and separation ability of e⁻/h⁺ pairs, by the way increasing the photocatalytic efficiency towards the RhB degradation. Thus, the newly constructed Z-scheme FeMoO₄/g-C₃N₄ heterojunction photocatalyst is a promising material for the remediation of wastewater relevant to elimination of toxic effect in marine environment.

Graphical abstract



[Download : Download high-res image \(264KB\)](#)

[Download : Download full-size image](#)

Introduction

Recently, a large number of synthetic dyes were used by the developing modern industries like textiles this and printing industries, etc., using highly hazardous chemicals during the production processes (Jayaraman et al., 2015; Arumugam et al., 2021; Theerthagiri et al., 2014, 2019, 2021; Naing et al., 2020; Hojjati-Najafabadi et al., 2022a, 2022b; Mansoorianfar et al., 2022). The generated wastes after the production process containing huge number of synthetic dyes were directly discharged into the waterbodies without any treatment, which contaminates the aquatic environment and presents harmful threats to living organisms (Bavani et al., 2021a; Theerthagiri et al., 2017; P. A et al., 2020; Theerthagiri et al., 2018; Zhang et al., 2022; Baladi et al., 2022; Akhoondi et al., 2021; Rao et al., 2022). Various biological, physical and chemical methods are employed for the wastewater remediation, some of these methods are operated with high cost and some other processes produce secondary pollutants. It is more essential to adopt a treatment without secondary pollutants generation (Senthil et al., 2018; Karuppasamy et al., 2021; Lee et al., 2020; Madhavan et al., 2019). Semiconductor photocatalysts in the advanced oxidation processes (AOPs) is considered as a cost effective and environmentally friendly method without producing secondary by-products (Yu et al., 2021; Mohammadi et al., 2022). Conventionally, titanium dioxide (TiO₂) and zinc oxide (ZnO) are benchmark photocatalyst, owing its inexpensiveness, non-toxicity and greater stability. However, its wide bandgap energy (E_g) is unfavourable for visible light absorption (VLA), to address this issue, its essential to develop semiconductors with more VLA. For that, more research attention has been devoted by the researchers worldwide (Senthil et al., 2017; Pasternak and Paz, 2016; Nemiwal et al., 2021). Recently, g-C₃N₄ has gained significant consideration, due to its high stability, strong reduction ability, specific electronic properties and inexpensiveness. However, the metal free g-C₃N₄ has moderate E_g values (~2.7–3.0eV), photocatalytic ability is still not satisfactory, due to the fast reconnection rate of photoexcited e⁻/h⁺ pairs, which is major barrier of the single semiconductor photocatalyst (Jiang et al., 2018; Theerthagiri et al., 2015). For this, construction of heterojunction with another semiconductor photocatalyst is an operative strategy to increase the photocatalytic degradation efficiency. Various composite like g-C₃N₄/Ni₃V₂O₈ (Vesali-Kermani et al., 2020a), g-C₃N₄/BiVO₄ (Li et al., 2019), g-C₃N₄/BiOBr (Shi et al., 2020), g-C₃N₄/BiOI (Liang et al., 2021), g-C₃N₄/Bi₂MoO₆ (Vesali-

Kermani et al., 2020b), V₂O₅/g-C₃N₄ (Shawky et al., 2021) and Bi₂WO₆/g-C₃N₄ (Guo et al., 2018) exhibits superior photocatalytic performance towards the organic and inorganic pollutant degradation under VLI. Recently, Guang et al. designed Z-scheme Bi₂O₃/g-C₃N₄ heterojunctions using in-situ thermal polymerization method for the degradation of methylene blue under VLI. As a result, Z-scheme Bi₂O₃/g-C₃N₄ heterojunction photocatalyst possesses greater photocatalytic degradation performance compared than pure Bi₂O₃ and g-C₃N₄ (Fan et al., 2021). Similarly, Yuzhen et al. used impregnation-calcination method to prepare BiVO₄/g-C₃N₄ heterojunction Z-scheme photocatalyst to evaluate the catalytic degradation of malachite green under VLI (Li et al., 2021). On the basis of obtained results, the constructed Z-scheme heterojunction between BiVO₄ and g-C₃N₄ exposed an improving photocatalytic activity by an efficient separation of charge carriers. The FeMoO₄ is a semiconductor with excellent redox nature, thereof it is used as electrode material in supercapacitor and photocatalytic degradation as well as hydrogen production reactions. Due to low cost and easy availability with appropriate bandgap energy value ($E_g \sim 1.6\text{ eV}$) of FeMoO₄, it is chosen to combine with g-C₃N₄.

Herein, we fabricated the FeMoO₄/g-C₃N₄-2D/2D Z-scheme heterojunction photocatalyst using wet impregnation method. A series of FeMoO₄/g-C₃N₄ composite are synthesized through differentiating the ratio 1:3, 1:1, 3:1 of FeMoO₄ and g-C₃N₄. Further the synthesized FeMoO₄/g-C₃N₄ composites are employed to the RhB degradation in the existence of VLI. The experimental outcomes reveal that the prepared FeMoO₄/g-C₃N₄ composite possess excellent photocatalytic ability towards RhB degradation. Furthermore, a feasible mechanism for Z-scheme FeMoO₄/g-C₃N₄ heterojunction towards the RhB as targeted textile dye degradation under VLI also been included.

Section snippets

Synthesis of g-C₃N₄

g-C₃N₄ was synthesized using thermal condensation method by heating 5g of melamine at heating ramp of 15°C per minute in a tubular furnace at 550°C for 4h. Then, the attained yellow colour of g-C₃N₄ was powdered for further use...

Preparation of FeMoO₄ photocatalyst

FeMoO₄ nanocomposite was synthesized by taking equal ratio of ferrous sulfate heptahydrate (FeSO₄·7H₂O) and sodium molybdate dihydrate (NaMoO₄·2H₂O) and separately dissolved in 30mL of deionised (DI) water. After that, these two solutions were mixed well with 60min ...

Structural analysis

FTIR was studies conducted to classify the functional groups of photocatalytic samples. Fig. 1 shows the FTIR spectra of pristine FeMoO₄, g-C₃N₄, and FeMoO₄/g-C₃N₄ composite photocatalysts. g-C₃N₄ shows the broad absorption peaks observed at 3078 to 3246cm⁻¹ corresponds to the presence of -N-H and -O-H stretching vibrations (Fig. 1a). The sharp peaks appeared at 1203 and 1312cm⁻¹ are owing to the -C-N stretching vibration and 1471 and 1532cm⁻¹ reveals the existence of -C=N stretching band...

Conclusions

In conclusion, the Z-scheme 2D/2D-FeMoO₄/g-C₃N₄ heterojunction composite was constructed through wet chemical process and its photocatalytic ability on the RhB degradation was evaluated under VLI. Morphological studies illustrate the 2D/2D-FeMoO₄ nanoplate on g-C₃N₄ nanosheet structure. The optimized FMCN-1 composite presents higher

photocatalytic degradation efficiency (79%) with 0.02226 min⁻¹ apparent rate constant value. Also, it possesses 1.24- and 1.13-times higher photocurrent intensity...

Credit author statement

Swaminathan Arumugam: Conceptualization, Investigation, Original draft preparation. **Thirugnanam Bavani:** Data curation, Methodology, Investigation, Visualization. **Manickam Selvaraj:** Data curation, Conceptualization, Methodology, Investigation. **Badria M. Al-Shehri:** Reviewing and Data curation. **Mani Preeyanghaa:** Reviewing and Editing. **Sieon Jung:** Reviewing and Data curation. **Jayaraman Theerthagiri:** Reviewing and Data curation. **Bernaardshaw Neppolian:** Reviewing and Data curation. **Sepperumal...**

Declaration of competing interest

The authors declare that they have no known competing financial interests or personal relationships that could have appeared to influence the work reported in this paper....

Acknowledgement

The authors Mr. S. Arumugam and Dr. J. Madhavan be thankful to Thiruvalluvar University, Vellore, for their lab facilities. The authors, Prof. M. Y. Choi, Dr. J. Theerthagiri acknowledge the support by Korea Basic Science Institute (National research Facilities and Equipment Center) grant funded by the Ministry of Education (No. 2019R1A6C1010042, 2021R1A6C103A427) and National Research Foundation of Korea (NRF), (2021R111A1A01060380, 2019H1D3A1A01071209)....

[Special issue articles](#) [Recommended articles](#)

References (48)

M. Arumugam *et al.*

[Enhanced photocatalytic activity at multidimensional interface of 1D-Bi₂S₃@2D-GO/3D-BiOI ternary nanocomposites for tetracycline degradation under visible-light](#)

J. Hazard Mater. (2021)

E. Baladi *et al.*

[Synthesis and characterization of g-C₃N₄-CoFe₂O₄-ZnO magnetic nanocomposites for enhancing photocatalytic activity with visible light for degradation of penicillin G antibiotic](#)

Environ. Res. (2022)

T. Bavani *et al.*

[Fabrication of novel AgVO₃/BiOI nanocomposite photocatalyst with photoelectrochemical activity towards the degradation of Rhodamine B under visible light irradiation](#)

Environ. Res. (2021)

T. Bavani *et al.*

[A straightforward synthesis of visible light driven BiFeO₃/AgVO₃ nanocomposites with improved photocatalytic activity](#)

Environ. Pollut. (2021)

T. Bavani *et al.*

[One-pot synthesis of bismuth yttrium tungstate nanosheet decorated 3D-BiOBr nanoflower heterostructure with enhanced visible light photocatalytic activity](#)

Chemosphere (2022)

G. Fan *et al.*

[Coupling of Bi₂O₃ nanoparticles with g-C₃N₄ for enhanced photocatalytic degradation of methylene blue](#)

Ceram. Int. (2021)

W. Guo *et al.*

[2D/2D Z-scheme Bi₂WO₆/Porous-g-C₃N₄ with synergy of adsorption and visible-light-driven photodegradation](#)

Appl. Surf. Sci. (2018)

R. He *et al.*

[Room-temperature in situ fabrication of Bi₂O₃/g-C₃N₄ direct Z-scheme photocatalyst with enhanced photocatalytic activity](#)

Appl. Surf. Sci. (2018)

A. Hojjati-Najafabadi *et al.*

[A review on magnetic sensors for monitoring of hazardous pollutants in water resources](#)

Sci. Total Environ. (2022)

A. Hojjati-Najafabadi *et al.*

[Magnetic-MXene-based nanocomposites for water and wastewater treatment: a review](#)

J. Water Proc. Eng. (2022)



View more references

Cited by (8)

[High-performance antibacterial tight ultrafiltration membrane constructed by co-deposition of dopamine and tobramycin for sustainable high-salinity textile wastewater management](#)

2024, Desalination

[Show abstract](#) ✓

[Photocatalytic hydrogen evolution and tetracycline degradation over a novel Z-scheme Ni-MOF/g-C₃N₄ heterojunction](#)

2024, Colloids and Surfaces A: Physicochemical and Engineering Aspects

[Show abstract](#) ✓

[MOF-derived ZnO/g-C₃N₄ nanophotocatalyst for efficient degradation of organic pollutant](#)

2024, Journal of Saudi Chemical Society

[Show abstract](#) ✓

Oxygen vacancy-enhanced magnesium-doped ferrous molybdate photocatalytic-peroxymonosulfate synergistic degradation of pollutants

2024, Applied Surface Science

[Show abstract](#) 

Nanosheet g-C₃N₄ enhanced by Bi₂MoO₆ for highly efficient photocatalysts toward photodegradation of Rhodamine-B dye

2023, Heliyon

[Show abstract](#) 

Persulfate promoted visible photocatalytic elimination of bisphenol A by g-C₃N₄-CeO₂ S-scheme heterojunction: The dominant role of photo-induced holes

2023, Chemosphere

[Show abstract](#) 



[View all citing articles on Scopus](#) 

[View full text](#)

© 2022 Elsevier Ltd. All rights reserved.



All content on this site: Copyright © 2024 Elsevier B.V., its licensors, and contributors. All rights are reserved, including those for text and data mining, AI training, and similar technologies. For all open access content, the Creative Commons licensing terms apply.



[Home](#) [Environmental Science and Pollution Research](#) [Article](#)

Construction of direct Z-scheme g-C₃N₄/BiYWO₆ heterojunction photocatalyst with enhanced visible light activity towards the degradation of methylene blue

Research Article Published: 07 September 2022

Volume 30, pages 10179–10190, (2023) [Cite this article](#)

Environmental Science and
Pollution Research

[Aims and scope](#)[Submit manuscript](#)


[Thirugnanam Bavani](#), [Jagannathan Madhavan](#) , [Mani Preeyanghaa](#), [Bernaurdshaw Neppolian](#) & [Sepperumal Murugesan](#)

 458 Accesses  10 Citations [Explore all metrics](#) →

Abstract

Construction of the Z-scheme heterojunction photocatalyst achieved highly improved photocatalytic ability by its high redox ability of the photoinduced e⁻-h⁺ pairs. In the study, Z-scheme g-C₃N₄/BiYWO₆ heterojunction photocatalyst is prepared by the single-step hydrothermal method. Further, its photocatalytic ability was assessed by degrading

methylene blue under visible light exposure. Particularly, the optimized 30 wt% of g-C₃N₄ in the g-C₃N₄/BiYWO₆ composite exposes almost complete degradation after 90 min, that is ~ 3.0 times greater than the bare BiYWO₆ and g-C₃N₄ with the rate constant value 0.032 min⁻¹. Experimentally, the radical trapping studies indicate O₂^{·-} and ·OH radicals are playing a vital role in the photocatalytic degradation process. Also, the Z-scheme g-C₃N₄/BiYWO₆ heterojunction photocatalyst exhibits excellent photoelectrochemical property and it is stable after 5 cycles, which indicates its good reusability nature. These enhancements are due to the newly formed heterostructure that facilitates the migration and separation efficiency of the photoproduced e⁻ -h⁺ pairs. Hence, the synthesized Z-scheme g-C₃N₄/BiYWO₆ heterostructure could be an excellent material for wastewater remediation works.

 This is a preview of subscription content, [log in via an institution](#)  to check access.

Access this article

[Log in via an institution](#)

[Buy article PDF 39,95 €](#)

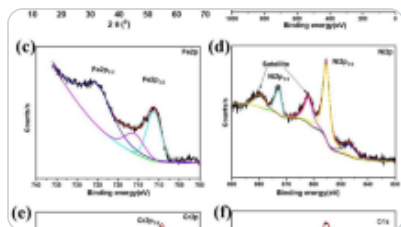
Price includes VAT (India)

Instant access to the full article PDF.

Rent this article via [DeepDyve](#) 

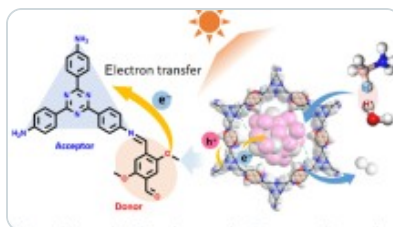
[Institutional subscriptions](#) →

Similar content being viewed by others



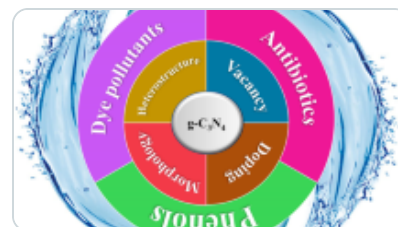
Sol-gel assisted incremental substitution of Ni with Ba in barium ferrichromites and thei...

Article | 15 April 2024



Donor-acceptor covalent organic frameworks-confined ultrafine bimetallic Pt-...

Article | 07 March 2024



g-C₃N₄-based photocatalysts for organic pollutant removal: a critical review

Article | Open access
06 April 2023

Data availability

All data related to this manuscript are incorporated in the manuscript.

References

Abdelkader S, Gross F, Winter D, Went J, Koschikowski J, Geissen SU, Bousselmi L (2019) Application of direct contact membrane distillation for saline dairy effluent treatment: performance and fouling analysis. *Environ Sci Polut Res* 26(19):18979–18992

[Article](#) [CAS](#) [Google Scholar](#)

Alanazi HS, Ahmad N, Alharthi FA (2021) Synthesis of Gd/N co-doped ZnO for enhanced UV-vis and direct solar-light-driven photocatalytic degradation. *RSC Adv* 11(17):10194–10202

[Article](#) [CAS](#) [Google Scholar](#)

Al-Zaqri N, Ahmed MA, Alsalmeh A, Alharthi F, Alsyahi A, Elmahgary MG, Galal AH (2021) Synthesis of novel direct Z-scheme AgVO₃-g-C₃N₄ heterojunction for photocatalytic

hydrogen production and bisphenol degradation. *J Mater Sci Mater Elect* 32(2):2601–17

[Article](#) [CAS](#) [Google Scholar](#)

An W, Sun K, Hu J, Cui W, Liu L (2020) The Z-scheme Ag₂CO₃@ g-C₃N₄ core-shell structure for increased photoinduced charge separation and stable photocatalytic degradation. *Appl Surf Sci* 504:144345

[Article](#) [CAS](#) [Google Scholar](#)

Bavani T, Madhavan J, Prasad S, AlSalhi MS, AlJaafreh MJ (2021) A straightforward synthesis of visible light driven BiFeO₃/AgVO₃ nanocomposites with improved photocatalytic activity. *Environ Poll* 269:116067

[Article](#) [CAS](#) [Google Scholar](#)

Bavani T, Madhavan J, Prasad S, AlSalhi MS, ALJaffreh M, Vijayanand S (2021) Fabrication of novel AgVO₃/BiOI nanocomposite photocatalyst with photoelectrochemical activity towards the degradation of rhodamine B under visible light irradiation. *Environ Res* 200:111365

[Article](#) [CAS](#) [Google Scholar](#)

Bavani T, Vinesh V, Neppolian B, Murugesan S, Selvaraj M, Madhavan J (2022a) One-step synthesis of rod-on-plate like 1D/2D-NiMoO₄/BiOI nanocomposite for an efficient visible light driven photocatalyst for pollutant degradation. *Environ Sci Poll Res* 29:1–1

Bavani T, Selvi A, Madhavan J, Selvaraj M, Vinesh V, Neppolian B, Vijayanand S, Murugesan S (2022b) One-pot synthesis of bismuth yttrium tungstate nanosheet decorated 3D-BiOBr nanoflower heterostructure with enhanced visible light photocatalytic activity. *Chemosphere* 297:133993

Dadigala R, Bandi R, Gangapuram BR, Dasari A, Belay HH, Guttena V (2019) Fabrication of novel 1D/2D V₂O₅/g-C₃N₄ composites as Z-scheme photocatalysts for CR degradation and Cr (VI) reduction under sunlight irradiation. *J Environ Chem Eng* 7(1):102822

[Article](#) [CAS](#) [Google Scholar](#)

Geng Y, Chen D, Li N, Xu Q, Li H, He J, Lu J (2021) Z-scheme 2D/2D α -Fe₂O₃/g-C₃N₄ heterojunction for photocatalytic oxidation of nitric oxide. *Appl Catal B Environ* 280:119409

[Article](#) [CAS](#) [Google Scholar](#)

Han Q, Wang R, Xing B, Chi H, Wu D, Wei Q (2018) Label-free photoelectrochemical aptasensor for tetracycline detection based on cerium doped CdS sensitized BiYWO₆. *Biosens Bioelectron* 106:7–13

[Article](#) [CAS](#) [Google Scholar](#)

Hao R, Xiao X, Zuo X, Nan J, Zhang W (2012) Efficient adsorption and visible-light photocatalytic degradation of tetracycline hydrochloride using mesoporous BiOI microspheres. *J Hazard Mater* 209:137–145

[Article](#) [Google Scholar](#)

He R, Zhou J, Fu H, Zhang S, Jiang C (2018) Room-temperature in situ fabrication of Bi₂O₃/g-C₃N₄ direct Z-scheme photocatalyst with enhanced photocatalytic activity. *Appl Surf Sci* 430:273–282

[Article](#) [CAS](#) [Google Scholar](#)

Jayaraman T, Raja SA, Priya A, Jagannathan M, Ashokkumar M (2015) Synthesis of a visible-light active V₂O₅-gC₃N₄ heterojunction as an efficient photocatalytic and photoelectrochemical material. *New J Chem* 39(2):1367–1374

[Article](#) [CAS](#) [Google Scholar](#)

Jiang L, Yuan X, Zeng G, Liang J, Wu Z, Wang H (2018) Construction of an all-solid-state Z-scheme photocatalyst based on graphite carbon nitride and its enhancement to catalytic activity. *Environ Sci Nano* 5(3):599–615

[Article](#) [CAS](#) [Google Scholar](#)

Li Z, Jin C, Wang M, Kang J, Wu Z, Yang D, Zhu T (2020) Novel rugby-like g-C₃N₄/BiVO₄ core/shell Z-scheme composites prepared via low-temperature hydrothermal method for enhanced photocatalytic performance. *Separation Purif Technol* 232:115937

[Article](#) [CAS](#) [Google Scholar](#)

Lian X, Xue W, Dong S, Liu E, Li H, Xu K (2021) Construction of S-scheme Bi₂WO₆/g-C₃N₄ heterostructure nanosheets with enhanced visible-light photocatalytic degradation for ammonium dinitramide. *J Hazard Mater* 412:125217

[Article](#) [CAS](#) [Google Scholar](#)

Liu Y, Zhu Q, Tayyab M, Zhou L, Lei J, Zhang J (2021) Single-atom Pt loaded zinc vacancies ZnO–ZnS induced type-V electron transport for efficiency photocatalytic H₂ evolution. *Solar Rrl* 5(11):2100536

[Article](#) [CAS](#) [Google Scholar](#)

Liu G, Feng M, Tayyab M, Gong J, Zhang M, Yang M, Lin K (2021) Direct and efficient reduction of perfluorooctanoic acid using bimetallic catalyst supported on carbon. *J Hazard Mater* 412:125224

[Article](#) [CAS](#) [Google Scholar](#)

Luo J, Ning X, Zhan L, Zhou X (2021) Facile construction of a fascinating Z-scheme AgI/Zn₃V₂O₈ photocatalyst for the photocatalytic degradation of tetracycline under visible light irradiation. *Sep Purif Technol* 255:117691

[Article](#) [CAS](#) [Google Scholar](#)

Ma C, Lee J, Kim Y, Seo WC, Jung H, Yang W (2021) Rational design of α -Fe₂O₃ nanocubes supported BiVO₄ Z-scheme photocatalyst for photocatalytic degradation of antibiotic under visible light. *J Colloid Interface Sci* 581:514–522

[Article](#) [CAS](#) [Google Scholar](#)

Malathi A, Arunachalam P, Grace AN, Madhavan J, Al-Mayouf AM (2017) A robust visible-light driven BiFeWO₆/BiOI nanohybrid with efficient photocatalytic and photoelectrochemical performance. *Appl Surf Sci* 412:85–95

[Article](#) [CAS](#) [Google Scholar](#)

Malathi A, Arunachalam P, Madhavan J, Al-Mayouf AM, Ghanem MA (2018) Rod-on-flake α -FeOOH/BiOI nanocomposite: facile synthesis, characterization and enhanced photocatalytic performance. *Colloids Surf A Physicochem Eng Asp* 537:435–445

[Article](#) [CAS](#) [Google Scholar](#)

Pasternak S, Paz Y (2016) BiYWO₆: Novel synthetic routes and their effect on visible-light photocatalysis. *J Photochem Photobiol A Chem* 318:14–24.

<https://doi.org/10.1016/j.jphotochem.2015.11.024>

[Article](#) [CAS](#) [Google Scholar](#)

Pattnaik SP, Behera A, Martha S, Acharya R, Parida K (2019) Facile synthesis of exfoliated graphitic carbon nitride for photocatalytic degradation of ciprofloxacin under solar

irradiation. *J Mater Sci* 54(7):5726–5742

[Article](#) [CAS](#) [Google Scholar](#)

Priya A, Arunachalam P, Selvi A, Madhavan J, Al-Mayouf AM, Ghanem MA (2018) A low-cost visible light active BiFeWO₆/TiO₂ nanocomposite with an efficient photocatalytic and photoelectrochemical performance. *Opt Mater* 81:84–92

[Article](#) [CAS](#) [Google Scholar](#)

Priya A, Arumugam M, Arunachalam P, Al-Mayouf AM, Madhavan J, Theerthagiri J, Choi MY (2020a) Fabrication of visible-light active BiFeWO₆/ZnO nanocomposites with enhanced photocatalytic activity. *Colloids Surf A Physicochem Eng Asp* 586:124294

[Article](#) [CAS](#) [Google Scholar](#)

Priya A, Senthil RA, Selvi A, Arunachalam P, Kumar CS, Madhavan J, Boddula R, Pothu R, Al-Mayouf AM (2020b) A study of photocatalytic and photoelectrochemical activity of as-synthesized WO₃/g-C₃N₄ composite photocatalysts for AO7 degradation. *Mater Sci Energy Technol* 3:43–50

[CAS](#) [Google Scholar](#)

Rosset A, Bartolomei V, Laisney J, Shandilya N, Voisin H, Morin J, Michaud-Soret I, Capron I, Wortham H, Brochard G, Bergé V (2021) Towards the development of safer by design TiO₂-based photocatalytic paint: impacts and performances. *Environ Sci Nano* 8(3):758–772

[Article](#) [CAS](#) [Google Scholar](#)

Senthil RA, Priya A, Theerthagiri J, Selvi A, Nithyadharseni P, Madhavan J (2018) Facile synthesis of α -Fe₂O₃/WO₃ composite with an enhanced photocatalytic and photo-

electrochemical performance. *Ionics* 24(11):3673–3684

[Article](#) [CAS](#) [Google Scholar](#)

Shi Z, Zhang Y, Shen X, Duoerkun G, Zhu B, Zhang L, Li M, Chen Z (2020) Fabrication of g-C₃N₄/BiOBr heterojunctions on carbon fibers as weaveable photocatalyst for degrading tetracycline hydrochloride under visible light. *Chem Eng J* 386:124010

[Article](#) [CAS](#) [Google Scholar](#)

Shi W, Yang S, Sun H, Wang J, Lin X, Guo F, Shi J (2021) Carbon dots anchored high-crystalline g-C₃N₄ as a metal-free composite photocatalyst for boosted photocatalytic degradation of tetracycline under visible light. *J Mater Sci* 56(3):2226–2240

[Article](#) [CAS](#) [Google Scholar](#)

Sun Y, Qi X, Li R, Xie Y, Tang Q, Ren B (2020) Hydrothermal synthesis of 2D/2D BiOCl/g-C₃N₄ Z-scheme: for TC degradation and antimicrobial activity evaluation. *Opt Mater* 108:110170

[Article](#) [CAS](#) [Google Scholar](#)

Tayyab M, Liu Y, Min S, Irfan RM, Zhu Q, Zhou L, Lei J, Zhang J (2022) Simultaneous hydrogen production with the selective oxidation of benzyl alcohol to benzaldehyde by a noble-metal-free photocatalyst VC/CdS nanowires. *Chinese J Catal* 43(4):1165–1175

[Article](#) [CAS](#) [Google Scholar](#)

Theerthagiri J, Duraimurugan K, Kim HS, Madhavan J (2019) Graphitic Carbon Nitride-Based Nanostructured Materials for Photocatalytic Applications. *Photocatalytic Functional Materials for Environmental Remediation* 23:291–307

[Article](#) [Google Scholar](#)

Vinitha V, Preeyanghaa M, Vinesh V, Dhanalakshmi R, Neppolian B, Sivamurugan V (2021) Two is better than one: catalytic, sensing and optical applications of doped zinc oxide nanostructures. *Emerg Mater* 4(5):1093–1124

[Article](#) [CAS](#) [Google Scholar](#)

Wu H, Meng F, Liu X, Yu B (2021) Carbon nanotubes as electronic mediators combined with Bi₂MoO₆ and g-C₃N₄ to form Z-scheme heterojunctions to enhance visible light photocatalysis. *Nanotechnology* 33(11):115203

[Article](#) [Google Scholar](#)

Yi J, Song J, Mo H, Yang Y (2018) One step pyridine-assisted synthesis of visible-light-driven photocatalyst Ag/AgVO₃. *Adv Powder Technol* 29(2):319–324

[Article](#) [CAS](#) [Google Scholar](#)

Zhang J, Fu J, Wang Z, Cheng B, Dai K, Ho W (2018) Direct Z-scheme porous g-C₃N₄/BiOI heterojunction for enhanced visible-light photocatalytic activity. *J Alloys Compd* 766:841–850

[Article](#) [CAS](#) [Google Scholar](#)

Zhang X, Yi J, Chen H, Mao M, Liu L, She X, Ji H, Wu X, Yuan S, Xu H, Li H (2019) Construction of a few-layer g-C₃N₄/α-MoO₃ nanoneedles all-solid-state Z-scheme photocatalytic system for photocatalytic degradation. *J Ener Chem* 29:65–71

[Article](#) [Google Scholar](#)

Zhang W, Li H, Xiao Q, Jiang S, Li X (2020) Surface nitrous oxide (N₂O) concentrations and fluxes from different rivers draining contrasting landscapes: spatio-temporal variability, controls, and implications based on IPCC emission factor. *Environ Poll* 263:114457

[Article](#) [CAS](#) [Google Scholar](#)

Zhao X, Xu Y, Wang X, Liang Q, Zhou M, Xu S, Li Z (2021) Construction and enhanced efficiency of Z-scheme-based ZnCdS/Bi₂WO₆ composites for visible-light-driven photocatalytic dye degradation. *J Phys Chem Solids* 154:110075

[Article](#) [CAS](#) [Google Scholar](#)

Zheng X, Wang Z, Chen T, Ran J, Wu Y, Tan C, Zhang Q, Chen P, Wang F, Liu H, Lv W (2021) One-step synthesis of carbon nitride nanobelts for the enhanced photocatalytic degradation of organic pollutants through peroxydisulfate activation. *Environ Sci Nano* 8(1):245–257

[Article](#) [CAS](#) [Google Scholar](#)

Zhou S, Wang Y, Zhou K, Ba D, Ao Y, Wang P (2021) In-situ construction of Z-scheme g-C₃N₄/WO₃ composite with enhanced visible-light responsive performance for nitenpyram degradation. *Chinese Chem Lett* 32(7):2179–2182

[Article](#) [CAS](#) [Google Scholar](#)

Zhou S, Wang Y, Zhao G, Li C, Liu L, Jiao F (2021) Enhanced visible light photocatalytic degradation of rhodamine B by Z-scheme CuWO₄/g-C₃N₄ heterojunction. *J Mater Sci Mater Electron* 32(3):2731–2743

[Article](#) [CAS](#) [Google Scholar](#)

Zhu X, Guo F, Pan J, Sun H, Gao L, Deng J, Zhu X, Shi W (2021) Fabrication of visible-light-response face-contact ZnSnO₃@g-C₃N₄ core-shell heterojunction for highly efficient

photocatalytic degradation of tetracycline contaminant and mechanism insight. *J Mater Sci* 56(6):4366–4379

[Article](#) [CAS](#) [Google Scholar](#)

Acknowledgements

The authors J. Madhavan and T. Bavani are grateful to Thiruvalluvar University, Vellore, India, for the laboratory facilities.

Author information

Authors and Affiliations

Solar Energy Lab, Department of Chemistry, Thiruvalluvar University, Vellore, 632115, India

Thirugnanam Bavani & Jagannathan Madhavan

Department of Physics and Nanotechnology, SRM Research Institute, SRM Institute of Science and Technology, Kattankulathur, Chennai, 603203, India

Mani Preeyanghaa & Bernaurdshaw Neppolian

School of Chemistry, Madurai Kamaraj University, Madurai, 625021, India

Sepperumal Murugesan

Contributions

All authors contributed to the study conception and design. Material preparation, data collection and analysis, and preparation of the first draft of the manuscript were done by Thirugnanam Bavani. Characterization, interpretation, and validation of the data are conducted by Mani Preeyanghaa and Bernaurdshaw Neppolian. Supervision, validation, and review were performed by Jagannathan Madhavan. Analysis, interpretation, and review were performed by Sepperumal Murugesan. All authors read and approved the final manuscript.

Corresponding author

Correspondence to [Jagannathan Madhavan](#).

Ethics declarations

Ethics approval and consent to participate

Not applicable.

Consent for publication

All authors have approved the final version of the manuscript and have given their consent for publication.

Competing interests

The authors declare no competing interests.

Additional information

Responsible editor: Sami Rtimi

Publisher's note

Springer Nature remains neutral with regard to jurisdictional claims in published maps and institutional affiliations.

Supplementary Information

[ESM 1](#)

(DOC 246 KB)

Rights and permissions

Springer Nature or its licensor holds exclusive rights to this article under a publishing agreement with the author(s) or other rightsholder(s); author self-archiving of the accepted manuscript version of this article is solely governed by the terms of such publishing agreement and applicable law.

[Reprints and permissions](#)

About this article

Cite this article

Bavani, T., Madhavan, J., Preeyanghaa, M. *et al.* Construction of direct Z-scheme g-C₃N₄/BiYWO₆ heterojunction photocatalyst with enhanced visible light activity towards the degradation of methylene blue. *Environ Sci Pollut Res* **30**, 10179–10190 (2023).

<https://doi.org/10.1007/s11356-022-22756-9>

Received

02 June 2022

Accepted

23 August 2022

Published

07 September 2022

Issue Date

January 2023

DOI

<https://doi.org/10.1007/s11356-022-22756-9>

Keywords

[Z-scheme](#)

[g-C₃N₄/BiYWO₆](#)



[Methylene blue](#)

[Visible light](#)

[Photocatalyst](#)



Graphene supported flower-like NiS₂/MoS₂ mixed phase nano-composites as a low cost electrode material for hydrogen evolution reaction in alkaline media

Dhandapani Balaji ^a, Jagannathan Madhavan ^a  , Vasudevan Vinesh ^b, Bernaurdshaw Neppolian ^b, Mohamad S. ALSalhi ^c, Saradh Prasad ^c

Show more 

 Share  Cite

<https://doi.org/10.1016/j.matchemphys.2022.125839> 

[Get rights and content](#) 

Highlights

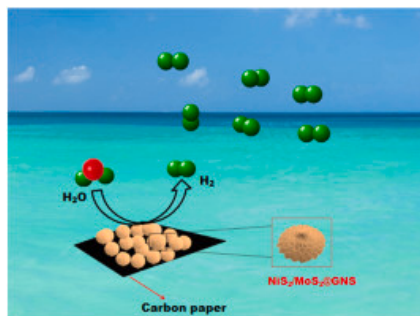
- A cost effective graphene supported NiS₂/MoS₂ heterostructure were prepared by hydrothermal and wet-chemical method.
- The NiS₂/MoS₂@GNS showed good catalytic behavior for HER in 1.0M KOH.
- The catalyst achieved low overpotential of 130mV at 10mAcm⁻² in 1.0M KOH.
- The NiS₂/MoS₂@GNS exhibited long-term stability for 10h.
- The NiS₂/MoS₂@GNS composite has been used good alternative for hydrogen evolution reaction.

Abstract

Modified bimetallic chalcogenides with numerous active sites of appropriate structures for extensive water splitting in alkaline hydrogen evolution reaction (HER) are quite challenging. In this study, we have designed a graphene nano-sheet anchored NiS₂/MoS₂ heterostructure through a facile two-step method and have employed them towards HER. To evaluate the performance of the NiS₂/MoS₂@GNS, The crystalline phase, morphology and material purity are evaluated by XRD, SEM, high resolution transmission microscopy HR-TEM and EDS. In addition, the electrochemical performance of the as-synthesized NiS₂/MoS₂@GNS composites and other electrocatalysts are tested towards the HER in 1M KOH electrolyte. It is noted that the graphene nano-sheet (GNS) anchored NiS₂/MoS₂ composite shows an excellent

electrocatalytic activity with a less overpotential of 130mV at current density ($|j|$) of 10mAcm⁻² and a low Tafel slope of 40mV dec⁻¹ compared with pristine NiS₂/MoS₂ material (141 mV at 10mAcm⁻² and Tafel slope of 48mV dec⁻¹). Furthermore, it possessed good stability for 1000 cycles and performed time-dependant current density for 10h at a limited overpotential of 130mV. The high synergistic effect between NiS₂/MoS₂ and GNS in promotion of hydrogen (H₂) generation efficiency is ascribed to more active sites, low charge transfer resistance and great electrochemical kinetics which justified the use of NiS₂/MoS₂@GNS hybrid material as a best alternative to replace noble metal for efficient HER.

Graphical abstract



Download : [Download high-res image \(261KB\)](#)

Download : [Download full-size image](#)

Introduction

The usage of fossil fuel energy and environmental pollution stimulated the great attention of alternative and sustainable energy sources. In this context, hydrogen has been considered as a source of green energy with the benefits of free-carbon emission, high energy density, renewability and ecological sustainability. It can be applied as a promising candidate to moderate climate change and to improve energy utilization productivity [1,2]. The electrochemical water splitting is most promising research hotspot to generate molecular hydrogen (H₂) in recent years [[3], [4], [5]]. Achieving large-scale and economic water splitting depends on efficient electrocatalyst with cost effectiveness and great durable properties that can greatly speed up the two half-cell reactions comprising of hydrogen evolution reaction (HER) and oxygen evolution reaction (OER) [[6], [7], [8], [9]]. So far, noble metal based catalysts such as Pt, Ru, Rh, Ir and Pd are regarded as the most promising HER candidates. Among them, Pt and Pt based materials have been confirmed as significant candidate for efficient HER [[10], [11], [12]]. In general, hydrogen generation by electrolysis of water have been great challenge, owing to the restriction of noble metal usage, cost effectiveness and low natural abundance. Therefore, the new material design with high stability, activity and less expensive non-noble metals is the best option for the wide practical application of water electrolysis.

Transition metal sulphides (TMS) such as NiS₂, CoS₂ and MoS₂ have been widely reported in different application due to its exclusive electronic and mechanical properties that provides an enormous potential in catalysis behaviours, supercapacitors, photocatalysis and hydrogen storage devices [[13], [14], [15], [16], [17], [18], [19], [20]]. Among TMS, 2-D layered transition metal sulphides with coupled layer through a weak Van-der waals force had quietly developed as effective catalytic materials for HER due to its high electrochemical stability and less expensive in price [21]. Recently, bimetal sulphides and their heterostructures have shown accessible HER properties due to the easy reliability and high abundancy of the active sites delivered by both the metal sulphide constituents [[22], [23], [24]]. Moreover, the structure modification between the two components in heterostructure establishes a synergistic effect owing to more active surface area and remodification of the electronic structure that also improves the HER behaviour, correlated to their individual counterpart [[25], [26], [27]]. For instance, Zhang et al. [28] has demonstrated an excellent

electrocatalytic water splitting reaction on MoS₂/Ni₃S₂ heterostructure interface in alkaline condition. Likewise, the lattice interfaces in NiS₂/MoS₂ heterojunctions were reported to be optimum in separation of water under broad pH condition [29]. Chen et al. [30] have developed an interface engineering strategy on NiS@MoS₂ microsphere to construct an excellent and stable electrocatalyst for efficient HER in both acid and alkaline media. They reported on the synergy between MoS₂ nano-sheet and NiS₂ plates, favour the chemical sorption of hydrogen. Which minimized the reaction barriers and enhanced the HER process.

Carbon based materials have adjustable molecular structure, great surface area and excellent electrical transfer and nontoxicity, and are widely utilized in the energy conversion field in both OER and HER [31]. In this context, graphene and graphene-based nanocomposites have been utilized as heterogeneous electrocatalysts due to their unique physicochemical properties such as superior electrical conductivity, tunable pore size, adequate mechanical strength, and specific surface area, inertness toward side reactions, and able to synthesize in various shapes and sizes. However, compared with transition metal-based catalysts, the carbon substance still endows low catalysis function and requires more overpotential to reach a maximum $|j|$ of 10 mAcm⁻². In order to further modify the electrocatalyst, carbon nanocomposite materials are essential for the design of active metal phase structures. Various cost effective less expensive transition metal based carbon composites such as FeSe₂/GO [32], Ni_{0.5}Fe_{0.5}Se₂/MWCNT [33], Ni₃N/Ni@C [34], Co-NRCNTs [35], and WON@NC are been reported in the work [36]. Recently, many researchers have reported that the graphene made by a simple hydrothermal approach, provides good electrical conductivity, easy modifiable characteristics and a good supporting material for transition metal-based catalyst in efficient water electrolysis process. Ji et al. [37] developed MoS₂/CoS₂ heterostructure embedded on N-doped carbon nanosheets. This material has showed excellent catalytic activity at an optimum potential range of 215 mV to attain a maximum $|j|$ of 10 mAcm⁻². Zhou et al. [38] designed a NiS/NiS₂ heterostructure grown on N-rGO nano-sheets, which exhibited superior catalytic performance by interfacial contact between NiS/NiS₂ and N-rGO for enhanced HER application.

In this study, we have designed a graphene-supported NiS₂/MoS₂ heterostructure using hydrothermal and wet-chemical approaches for HER application under alkaline medium. The electrocatalytic HER performance of as-prepared material was tested via CV half-cell technique in alkaline electrolyte and the achieved results revealed the well formation of desired alternate electrocatalyst for hydrogen generation.

Section snippets

Materials and reagents

Sodium molybdate dihydrate (Na₂MoO₄·2H₂O) was received from Sigma-Aldrich, India. Nickel nitrate hexahydrate (Ni(NO₃)₂·6H₂O), Thiourea (CH₄N₂S), Chloroform (CHCl₃) and metallic copper powder (Cu) were obtained through SD Fine-Chem Ltd, India. Nafion solution (5%) was received through Sigma-Aldrich, India to make the catalytic ink. Ethanol (C₂H₅OH) was bought from Merck Specialties Pvt. Ltd, India. Deionized (DI) water was served as a solvent in the entire synthesis and purification process....

Synthesis of NiS₂/MoS₂ heterostructure

In...

Powder XRD studies

The XRD pattern of the as-acquired powder of MoS₂, NiS₂/MoS₂ and NiS₂/MoS₂@GNS were exclusively studied by X-ray powder diffraction method. As presented in Fig. 2, the XRD peaks at 2θ position clearly indicated the planes indexed to (111) (200) (201) (211) (220) (311) (222) (023) of the cubic phase of NiS₂ [PDF 65–3325], [40]. The typical diffraction

peaks of MoS₂ [PDF 37–1492] are confirmed to corresponding lattice planes of (002) (100) (103) and (110) respectively [41]. In another spectrum of ...

Conclusions

In summary, we have synthesized a non-noble metal and effective NiS₂/MoS₂ nano-sphere using one step hydrothermal method. The NiS₂/MoS₂ heterostructure was composited with carbon network of graphene nano-sheet to form NiS₂/MoS₂@GNS nano-flower by a simple wet-chemical method. The NiS₂/MoS₂@GNS composite was further utilized as an excellent electrode material towards HER in 1 M KOH electrolyte. The obtained electrochemical results exposed the enhanced NiS₂/MoS₂@GNS qualities of the composite...

Author statements

D. Balaji - Carried out the experiments. J. Madhavan – Designed the experiential scheme and guided the throughout the work. V. Vinesh, characterization and analysis of results. B. Neppolian-characterization and analysis of results. Mohamad S. AlSalhi, Saradh Prasad–Experiential, Manuscript preparation, editing, and funding....

Declaration of competing interest

The authors declare that they have no known competing financial interests or personal relationships that could have appeared to influence the work reported in this paper...

Acknowledgements

The authors D. Balaji, and Dr. J. Madhavan are thankful to the Thiruvalluvar University for the lab facilities and support. The authors V. Vinesh and B. Neppolian are grateful to the Deanship of Scientific Research, Department of physics and nanotechnology, SRM Institute of Science and Technology for characterization through Deanship of Scientific Research Chairs. The authors Mohamad S. AlSalhi, and Saradh Prasad are grateful to the Deanship of Scientific Research, King Saud University for...

[Recommended articles](#)

References (50)

Q.Y. Jin *et al.*

[In situ promoting water dissociation kinetic of Co-based electrocatalyst for unprecedentedly enhanced hydrogen evolution reaction in alkaline media](#)

Nano Energy (2018)

W.J. Zhou *et al.*

[Recent developments of carbon-based electrocatalysts for hydrogen evolution reaction](#)

Nano Energy (2016)

S. Ghosh *et al.*

[Development of carbon coated NiS₂ as positive electrode material for high performance asymmetric supercapacitor](#)

Compos. B Eng. (2019)

A.K. Thakur *et al.*

[MoS₂ flakes integrated with boron and nitrogen-doped carbon: striking gravimetric and volumetric capacitive performance for supercapacitor applications](#)

J. Power Sources (2018)

S. Huang *et al.*

[Photocatalytic degradation of thiobencarb by a visible light-driven MoS₂ photocatalyst](#)

Separ. Purif. Technol. (2018)

S Jun Lee *et al.*

[Heteroatom-doped graphene-based materials for sustainable energy applications: a review](#)

Renew. Sustain. Energy Rev. (2021)

J.W. Li *et al.*

[Three-dimensional lily-like CoNi₂S₄ as an advanced bifunctional electrocatalyst for hydrogen and oxygen evolution reaction](#)

J. Catal. (2018)

J.W. Li *et al.*

[Co₉S₈-Ni₃S₂ heterointerfaced nanotubes on Ni foam as highly efficient and flexible bifunctional electrodes for water splitting](#)

Electrochim. Acta (2019)

Z. Chen *et al.*

[Interface engineering of NiS@MoS₂ core-shell microspheres as an efficient catalyst for hydrogen evolution reaction in both acidic and alkaline medium](#)

J. Alloys Compd. (2021)

J. Theerthagiri *et al.*

[Growth of iron diselenide nanorods on graphene oxide nano sheets as advanced electrocatalyst for hydrogen evolution reaction](#)

Int. J. Hydrogen Energy (2017)



View more references

Cited by (15)

[Self-standing Ni-Cu-Ti/NCNTs electrocatalyst with porous structure for hydrogen evolution reaction](#)

2024, International Journal of Hydrogen Energy

[Show abstract](#) ✓

[Turning trash to treasure: Innovative use of exhausted desiccant waste supported zinc indium sulphide for sustainable photocatalytic abatement of tetracycline](#)

2024, Chemosphere

[Show abstract](#) ✓

Preparation and hydrogen evolution performance of porous Ni-Cu-Ti/CNTs-Ni electrode

2023, Vacuum

[Show abstract](#) 

NiS@CuBi₂O₄/ERGO heterostructured electro-catalyst for enhanced hydrogen evolution reaction

2023, Micro and Nanostructures

[Show abstract](#) 

Filling the gaps on the relation between electronic conductivity and catalysis of electrocatalysts for water splitting using computational modelling

2023, Current Opinion in Electrochemistry

[Show abstract](#) 

Design and construction of 1D/2D/3D fabric-based wearable micro-supercapacitors

2023, Journal of Power Sources

[Show abstract](#) 

[View all citing articles on Scopus](#) 

[View full text](#)

© 2022 Elsevier B.V. All rights reserved.





All content on this site: Copyright © 2024 Elsevier B.V., its licensors, and contributors. All rights are reserved, including those for text and data mining, AI training, and similar technologies. For all open access content, the Creative Commons licensing terms apply.





One-pot synthesis of bismuth yttrium tungstate nanosheet decorated 3D-BiOBr nanoflower heterostructure with enhanced visible light photocatalytic activity

Thirungnanam Bavani ^a, Adikesavan Selvi ^b, Jagannathan Madhavan ^a  , Manickam Selvaraj ^e, Vasudevan Vinesh ^c, Bernardshaw Neppolian ^c, Selvaraj Vijayanand ^b, Sepperumal Murugesan ^d

Show more 

 Share  Cite

<https://doi.org/10.1016/j.chemosphere.2022.133993> 

[Get rights and content](#) 

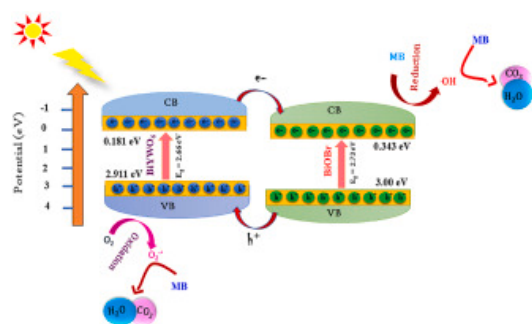
Highlights

- BiOBr/Bi_xY_{1-x}WO₆ nanocomposites are prepared by one-pot hydrothermal method.
- BiOBr/Bi_xY_{1-x}WO₆ shows remarkable photocatalytic degradation activity towards MB under visible light.
- •OH and h⁺ radicals are playing major part in the MB degradation process.

Abstract

A visible light driven BiOBr/Bi_xY_{1-x}WO₆ nanocomposite photocatalyst of various compositions are prepared by the addition of different amounts of KBr (0.5, 1.0, 1.5, 2.0 mmol) in Bi_xY_{1-x}WO₆ by a one-pot hydrothermal method. Furthermore, the photocatalytic properties of the as-prepared materials are analyzed by the decomposition of methylene blue under visible light illumination. In particular, the BiOBr/Bi_xY_{1-x}WO₆ nanocomposite prepared by taking 1.5 mmol of KBr present a superior photocatalytic ability (78.3%) with the rate constant value 0.016 min⁻¹, a low bandgap (E_g=2.51 eV) as well as photoluminescence emission intensity than other photocatalysts prepared in this study. The radical scavenging studies revealed that •OH and h⁺ performed an imperative role in the decomposition of methylene blue. Furthermore, the optimized photocatalyst is stable even after four cycles, which exposes the excellent photostability and reusability properties of the photocatalyst. In addition, a plausible mechanism of decomposition of methylene blue under visible light irradiation is also proposed.

Graphical abstract



Download : [Download high-res image \(248KB\)](#)

Download : [Download full-size image](#)

Introduction

Water is the vital source to the human being. Nowadays, the need of the resource increases with increasing industries and population. Currently, modern industries use large amount of synthetic organic dyes to improve their product quality, which ends up toxicity and diseases threatening to human being and animals (Leena and Rajubhai, 2017; Ge et al., 2019; Koutavarapu et al., 2021, 2022a, 2022b). Dye waste effluents contain high quantity of hazardous organic water pollutants that are directly released into the aquatic environment, thus limiting the sufficiency of the potable water. So, it is needed to eliminate the waste contaminants of the discharged effluents from the water bodies.

Nowadays, the development of material science is prominently connected with the saving of energy, low cost and natural approachability (Babu et al., 2021; Babu et al., 2020; Theerthagiri et al., 2019; Ray et al., 2020; Bavani et al., 2021a). The advanced oxidation process (AOP) is one such method that is extensively used to degrade the contaminants without producing secondary pollutants and has been considered as a potential solution to tackle environmental crises (Bavani et al., 2021b; Senthil et al., 2018, 2019a; Wu et al., 2017; Landge et al., 2021; Caglar et al., 2021). To imply this method, semiconductor oxide photocatalysts like TiO_2 and ZnO are commonly used. However, due to their wide bandgap energy their degradation efficiency is limited in the visible region. This disadvantage led to a strong impetus to the growth of the visible light active photocatalysts (Chowdhury and Shambharkar, 2020; Palanisamy et al., 2021; Liu et al., 2021; Priya et al., 2019).

Presently, bismuth-based semiconductor photocatalysts BiFeO_3 (Malathi et al., 2018a), BiFeWO_6 (Priya et al., 2018), Bi_2MoO_6 (Lia et al., 2019), BiYWO_6 (Han et al., 2018a), Bi_2S_3 (Xu et al., 2018), BiVO_4 (Chala et al., 2014), BiPO_4 (Zhu et al., 2017), Bi_2WO_6 (Ju et al., 2014) and BiOX ($X=\text{F}, \text{Cl}, \text{Br}, \text{I}$) (Alzamly et al., 2019; Han et al., 2018b; Hao et al., 2020; Malathi et al., 2018b) are getting quite consideration, owing to its low cost, greater stability, high activity and nontoxicity. Specially, BiYWO_6 has perovskite layered structure with low bandgap energy and a wide visible light absorption (VLA) characteristic. But, the photocatalytic activity (PCA) of BiYWO_6 is still constricted by its low charge separation and rapid rejoining of the photoexcited e^-/h^+ . Hence, it is imperative to devise an operative approach to improve the separation ability and to reduce the rejoining of photoproduced e^-/h^+ pairs, to stand with greater photocatalytic degradation ability of BYW in the visible region. The literature survey revealed the construction of heterojunction would considerably improve the charge migration and suppress the rapid rejoining of the e^-/h^+ pairs. Thereby, various heterostructured materials like WO_3/AgCl (Senthil et al., 2019b), NiO/BiOI (Hu et al., 2020a), $\text{BiFeWO}_6/\text{BiOI}$ (Malathi et al., 2017), MoS_2/BiOI (Hu et al., 2020b), BiOCl/AgBr (Chang et al., 2018), $\text{CdWO}_4/\text{BiOI}$ (Song et al., 2017), $\text{Bi}_2\text{MoO}_6/\text{ZnO}$ (Zhang et al., 2019) composite photocatalysts were reported to exhibit an enhanced photocatalytic ability and greater photostability.

Of the above mentioned photocatalysts, BiOX (X=F, Cl, Br, I) are gaining popularity among researchers, owing to its nontoxic, environmental friendly, low cost, nature and greater photodegradation efficiency towards the pollutants (Priya et al., 2018). In particular, the BiOBr possesses unique layered structure with suitable bandgap (~2.75 eV) and greater photostability as a good visible-light driven photocatalyst. Hence, BiOBr is chosen to combine with BiYWO₆, which is expected to show an excellent photodegradation efficiency by reducing electron-hole rejoining rate and improved charge transfer kinetics. Additionally, the previous reports of BR based composite photocatalysts like BiOBr/ZnO/BiOI (Zarezadeh et al., 2019), BiSbO₄/BiOBr (Wang et al., 2019), CuBi₂O₄/BiOBr (Huang et al., 2020), BiOBr/ZnO (Geng et al., 2017), BiOBr/ β -Bi₂O₃ (Xu et al., 2019), WO₃/BiOBr (Ling and Dai, 2020), SrTiO₃-BiOBr (Kanagaraj and Thiripuranthagan, 2017), etc., were proved to show excellent PCA towards the decomposition of organic waste in the aquatic environment. Recently Wang et al. prepared Sb₂WO₆/BiOBr 2D-nanocomposite photocatalyst by precipitation-deposition method at room temperature. Further, its photocatalytic activity was evaluated towards the oxidation of NO. Here, the formation of S-scheme between the Sb₂WO₆ and BiOBr enhances the photocatalytic activity under VLI (Wang et al., 2020). Meng et al. fabricate BiOBr/Bi₂WO₆ heterojunction photocatalyst by one-step hydrothermal method. Then, the photocatalytic performance of BiOBr/Bi₂WO₆ heterojunction photocatalyst was investigated by the degradation of RhB under visible light exposure and its photocatalytic activity was significantly improved than the pure BiOBr and BiWO₆ (Meng and Zhang, 2015). Hence, the BiOBr is a suitable material to couple with the BiYWO₆, which may expected to reduce the rapid reconnection of the e⁻/h⁺ pairs to improve the photocatalytic activity of the composite photocatalyst than the pure BiYWO₆ and BiOBr. In the present study, we have prepared series of BiOBr/Bi_xY_{1-x}WO₆ composite (BYWBR) photocatalysts by one-pot hydrothermal method by varying the amount of KBr (0.5–2.0 mmol). Finally, the PCA of the BYWBR composite was explored against the decomposing methylene blue dye, which revealed the BYWBR composite with enhanced PCA and stability than the pure Bi_xY_{1-x}WO₆ and BiOBr photocatalysts. Currently, there are lot of research works related to BiOBr and a few on Bi_xY_{1-x}WO₆, but no reports on the compiste between these two materials i.e., BYWBR for the degradation of organic dyes. Therefore, the newly designed BYWBR composite photocatalyst could be contemplated as a promising material to imply towards the remediation of wastewater. A plausible mechanism explaining the degradation of methylene blue using BYWBR composite photocatalyst has also been presented.

Section snippets

Materials

Sodium tungstate dihydrate (Na₂WO₄·2H₂O), potassium bromide (KBr), yttrium nitrate hexahydrate (Y(NO₃)₃·6H₂O) and bismuth nitrate pentahydrate (Bi(NO₃)₃·5H₂O) were acquired from Sigma-Aldrich. Ammonium oxalate, sodium hydroxide (NaOH) and isopropyl alcohol (IPA) were obtained from SDFCL. Nitric acid (HNO₃), methylene blue (MB), Triton X-100 and benzoquinone were procured from Qualigens. All these chemicals were used without any purification....

Synthesis of BiOBr nanoparticles

The pure bismuth oxybromide (BiOBr) nanoparticles were ...

FT-IR studies

The Fourier transformation infrared spectroscopy is a versatile method to identify the functional groups of the materials. In Fig. 2 the pure BYW shows peaks at 546, 1350 and 716 cm⁻¹ corresponding to Bi–O and Y–O symmetric stretching and W–O–W bending vibrations respectively. The peaks located at 1610 and 3466 cm⁻¹ are owing to the O–H

bending and stretching vibrations. In the case of bare BR, the peak obtained at $500\text{--}1000\text{cm}^{-1}$ codes to the symmetric stretching of Bi–O bond and the band at...

Conclusions

In this work, a novel BiOBr/Bi_xY_{1-x}WO₆ nanocomposite was fabricated using a simple one-pot hydrothermal synthesis method by varying the amount of KBr (0.5–2 mmol) and its PCA is assessed through the decomposition of MB under VLI. Here, the PCA of the BYWBR nanocomposite photocatalyst has shown greater degradation ability than that of bare BR and BYW. Among all photocatalysts, BYWBR with 1.5 mmol KBr showed a superior photocatalytic degradation performance of 78.3% with higher rate constant...

Author contributions statement

Bavani Thirungnanam: Experimental work, Field collection, Writing - original draft. Methodology, Writing - review & editing. **Jagannathan Madhavan** and **Adikesavan Selvi:** Supervision, Validation, Writing – review & editing.

Sepperumal Murugesan, Manickam Selvaraj and **Selvaraj Vijayanand:** Resources, Funding acquisition. **Vasudevan Vinesh** and **Bernaardshaw Neppolian:** Validation, Formal analysis....

Declaration of competing interest

The authors declare that they have no known competing financial interests or personal relationships that could have appeared to influence the work reported in this paper....

Acknowledgement

The authors T. Bavani, and J. Madhavan are thankful to the Thiruvalluvar University for the lab facilities and support. Prof. M. Selvaraj extends his appreciation to the deanship of scientific research at King Khalid University for the support through general research project under grant number, GRP : 81/1443....

[Special issue articles](#) [Recommended articles](#)

References (57)

A. Alzamy *et al.*

[Construction of BiOF/BiOI nanocomposites with tunable band gaps as efficient visible-light photocatalysts](#)

J. Photochem. Photobiol. Chem. (2019)

W. An *et al.*

[Surface decoration of BiPO₄ with BiOBr nanoflakes to build heterostructure photocatalysts with enhanced photocatalytic activity](#)

Appl. Surf. Sci. (2015)

B. Babu *et al.*

[Enhanced solar light-driven photocatalytic degradation of tetracycline and organic pollutants by novel one-dimensional ZnWO₄ nanorod-decorated two-dimensional Bi₂WO₆ nanoflakes](#)

J. Taiwan Inst. Chem. Eng. (2020)

B. Babu *et al.*

[Enhanced solar-light-driven photocatalytic and photoelectrochemical properties of zinc tungsten oxide nanorods anchored on bismuth tungsten oxide nanoflakes](#)

Chemosphere (2021)

T. Bavani *et al.*

[A straightforward synthesis of visible light driven BiFeO₃/AgVO₃ nanocomposites with improved photocatalytic activity](#)

Environ. Pol. (2021)

T. Bavani *et al.*

[Fabrication of novel AgVO₃/BiOI nanocomposite photocatalyst with photoelectrochemical activity towards the degradation of Rhodamine B under visible light irradiation](#)

Environ. Res. (2021)

B. Caglar *et al.*

[Bi₂S₃ nanorods decorated on bentonite nanocomposite for enhanced visible-light-driven photocatalytic performance towards degradation of organic dyes](#)

J. Alloys Compd. (2021)

J. Cao *et al.*

[Novel BiOI/BiOBr heterojunction photocatalysts with enhanced visible light photocatalytic properties](#)

Catal. Commun. (2011)

S. Chala *et al.*

[Enhanced visible-light-response photocatalytic degradation of methylene blue on Fe-loaded BiVO₄ photocatalyst](#)

J. Alloys Compd. (2014)

J.Q. Chang *et al.*

[Synthesis and significantly enhanced visible light photocatalytic activity of BiOCl/AgBr heterostructured composites](#)

Inorg. Chem. Commun. (2018)



View more references

Cited by (13)

[The core-shell structure of C/BiOBr@Co-MOF for efficient degradation of organic dyes under visible light](#)

2024, Surfaces and Interfaces

[Show abstract](#) ✓

[Recent progress on Bi⁴⁺O⁵⁺Br²⁻-based photocatalysts for environmental remediation and energy conversion](#)

2024, Catalysis Science and Technology

[Show abstract](#) ✓

Development of niobium doped tin oxide nanostructure via hydrothermal route for photocatalytic degradation of methylene blue and antimicrobial study

2023, Ceramics International

[Show abstract](#) 

Integrating magnetized bentonite and pinecone-like BiOBr/BiOI Step-scheme heterojunctions as novel recyclable photocatalyst for efficient antibiotic degradation

2023, Journal of Industrial and Engineering Chemistry

[Show abstract](#) 

Synergistic combination of BiFeO₃ nanorods and CeVO₄ nanoparticles for enhanced visible light driven photocatalytic activity


2023, Alexandria Engineering Journal

[Show abstract](#) 

Construction of direct FeMoO₄/g-C₃N₄-2D/2D Z-scheme heterojunction with enhanced photocatalytic treatment of textile wastewater to eliminate the toxic effect in marine environment

2023, Chemosphere

[Show abstract](#) 

[View all citing articles on Scopus](#) 

[View full text](#)

© 2022 Elsevier Ltd. All rights reserved.



All content on this site: Copyright © 2024 Elsevier B.V., its licensors, and contributors. All rights are reserved, including those for text and data mining, AI training, and similar technologies. For all open access content, the Creative Commons licensing terms apply.



[Home](#) [Environmental Science and Pollution Research](#) [Article](#)


One-step synthesis of rod-on-plate like 1D/2D-NiMoO₄/BiOI nanocomposite for an efficient visible light driven photocatalyst for pollutant degradation

Research Article Published: 29 April 2022

Volume 29, pages 65222–65232, (2022) [Cite this article](#)

Environmental Science and
Pollution Research

[Aims and scope](#)[Submit manuscript](#)

[Thirungnanam Bavani](#), [Vasudevan Vinesh](#), [Bernardshaw Neppolian](#), [Sepperumal Murugesan](#),
[Manickam Selvaraj](#) & [Jagannathan Madhavan](#) 

 504 Accesses  4 Citations [Explore all metrics](#) →

Abstract

Visible light active 1D/2D-NiMoO₄/BiOI nanocomposite photocatalyst has been constructed by single step solvothermal method. Various compositions of NiMoO₄/BiOI nanocomposites are prepared by loading different amounts of nickel molybdate (NiMoO₄) (1, 2, 3 wt%) to the bismuth oxy iodide (BiOI) and investigated by XRD, FTIR, SEM, EDAX, TEM, UV-vis DRS,

and PL analysis. Among the as-prepared photocatalysts, 1 wt% NiMoO₄ incorporated BiOI (NMBI-1) showed superior photocatalytic activity with a rate constant of 0.0442 min⁻¹ for methylene blue degradation. While the bandgap values of pure BiOI and NiMoO₄ are 1.94 and 2.43 eV, respectively, the optimized NMBI-1 exhibited a lower bandgap energy of 1.64 eV, and showed about 2 and 3.7 times higher photodegradation ability than the pure NiMoO₄ and BiOI, respectively, towards MB removal under visible light. The NMBI-1 nanocomposite photocatalyst is stable even after four cycles, indicating an excellent photostability and recyclability. Charge carriers on the interface of NiMoO₄ and BiOI easily transferred via the newly formed heterojunction, thereby increasing the photocatalytic performance. Photochemically formed h⁺ and ·OH are found to be the major species in the MB removal under visible light illumination. Therefore, the 1D/2D-NiMoO₄/BiOI nanocomposite photocatalyst materials may be considered for the wastewater remediation processes.

 This is a preview of subscription content, [log in via an institution](#)  to check access.

Access this article

[Log in via an institution](#)

Buy article PDF 39,95 €

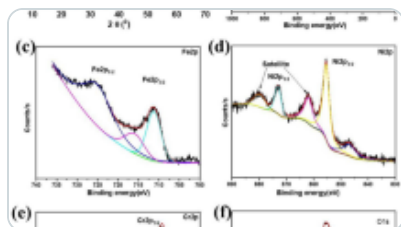
Price includes VAT (India)

Instant access to the full article PDF.

Rent this article via [DeepDyve](#) 

[Institutional subscriptions](#) →

Similar content being viewed by others



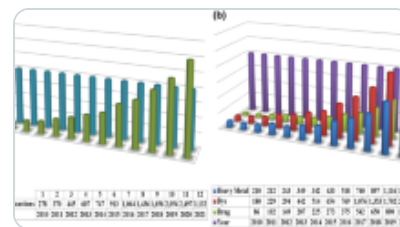
Sol-gel assisted incremental substitution of Ni with Ba in barium ferrichromites and thei...

Article | 15 April 2024



g-C₃N₄-based photocatalysts for organic pollutant removal: a critical review

Article | Open access
06 April 2023



ZnO-based heterostructures as photocatalysts for hydrogen generation...

Article | 14 January 2022

Data availability

All data related to this manuscript is incorporated in the manuscript.

References

Abdelkader S, Gross F, Winter D, Went J, Koschikowski J, Geissen SU, Bousselmi L (2019) Application of direct contact membrane distillation for saline dairy effluent treatment: performance and fouling analysis. *Environ Sci Polut Res* 26(19):18979–18992.

<https://doi.org/10.1007/s11356-018-2475-3>

[Article](#) [CAS](#) [Google Scholar](#)

Alzamly A, Bakiro M, Ahmed SH, Sallabi SM, Al Ajeil RA, Alawadhi SA, Selem HA, Al Meshayei SSM, Khaleel A, Al-Shamsi N, Saleh NI (2019) Construction of BiOF/BiOI nanocomposites with tunable band gaps as efficient visible-light photocatalysts. *J Photochem Photobiol A Chem* 375:30–39. <https://doi.org/10.1016/j.jphotochem.2019.01.031>

[Article](#) [CAS](#) [Google Scholar](#)

Bavani T, Madhavan J, Prasad S, AlSalhi MS, AlJaafreh MJ (2021a) A straightforward synthesis of visible light driven BiFeO₃/AgVO₃ nanocomposites with improved photocatalytic activity. Environ Poll 269:116067.

<https://doi.org/10.1016/j.envpol.2020.116067>

[Article](#) [CAS](#) [Google Scholar](#)

Bavani T, Madhavan J, Prasad S, AlSalhi MS, AlJaffreh M, Anand SV (2021b) Fabrication of novel AgVO₃/BiOI nanocomposite photocatalyst with photoelectrochemical activity towards the degradation of Rhodamine B under visible light irradiation. Environ Res

111365. <https://doi.org/10.1016/j.envres.2021b.111365>

Chang JQ, Zhong Y, Hu CH, Luo JL, Wang PG (2018) Synthesis and significantly enhanced visible light photocatalytic activity of BiOCl/AgBr heterostructured composites. Inorg Chem Commun 96:145–152. <https://doi.org/10.1016/j.inoche.2018.08.010>

[Article](#) [CAS](#) [Google Scholar](#)

He HY, Chen P, Cao LY, Lu J (2014) Surface alkaline–acidic and photocatalytic properties of MMoO₄ (M= Fe²⁺, Co²⁺, Ni²⁺) nanoparticles in different media conditions. Res Chem Intermed 40(4):1525–1536. <https://doi.org/10.1007/s11164-013-1057-8>

[Article](#) [CAS](#) [Google Scholar](#)

Hou D, Tang F, Ma B, Deng M, Qiao XQ, Li DS (2019) Exploring improvement of photocatalytic and catalytic performance in Nd-doped BiYO₃ nanotube systems. Inorg Chem Commun 106:151–157

[Article](#) [CAS](#) [Google Scholar](#)

Hu M, Lou H, Yan X, Hu X, Feng R, Zhou M (2018) In-situ fabrication of ZIF-8 decorated layered double oxides for adsorption and photocatalytic degradation of methylene blue.

Microporous Mesoporous Mater 271:68–72

Hu X, Wang G, Wang J, Hu Z, Su Y (2020) Step-scheme NiO/BiOI heterojunction photocatalyst for rhodamine photodegradation. Appl Surf Sci 511:145499.

<https://doi.org/10.1016/j.apsusc.2020.145499>

[Article](#) [CAS](#) [Google Scholar](#)

Hu L, Li M, Cheng L, Jiang B, Ai J (2021) Solvothermal synthesis of octahedral and magnetic CoFe₂O₄-reduced graphene oxide hybrids and their photo-Fenton-like behavior under visible-light irradiation. RSC Adv 11(36):22250–22263.

<https://doi.org/10.1016/j.inoche.2019.06.008>

[Article](#) [CAS](#) [Google Scholar](#)

Ju P, Wang P, Li B, Fan H, Ai S, Zhang D, Wang Y (2014) A novel calcined Bi₂WO₆/BiVO₄ heterojunction photocatalyst with highly enhanced photocatalytic activity. Chem Eng J 236:430–437. <https://doi.org/10.1016/j.cej.2013.10.001>

[Article](#) [CAS](#) [Google Scholar](#)

Khatri J, Nidheesh PV, Singh TA, Kumar MS (2018) Advanced oxidation processes based on zero-valent aluminum for treating textile wastewater. Chem Eng J 348:67–73.

<https://doi.org/10.1016/j.cej.2018.04.074>

[Article](#) [CAS](#) [Google Scholar](#)

Koe WS, Lee JW, Chong WC, Pang YL, Sim LC (2020) An overview of photocatalytic degradation: photocatalysts, mechanisms, and development of photocatalytic membrane.

Environ Sci Polut Res 27(3):2522–2565. <https://doi.org/10.1007/s11356-019-07193-5>

[Article](#) [CAS](#) [Google Scholar](#)

Li Y, Shen Q, Guan R, Xue J, Liu X, Jia H, Xu B, Wu Y (2020) AC@ TiO₂ yolk–shell heterostructure for synchronous photothermal–photocatalytic degradation of organic pollutants. *J Mater Chem C* 8(3):1025–1040. <https://doi.org/10.1039/C9TC05504E>

[Article](#) [CAS](#) [Google Scholar](#)

Louhichi G, Bousselmi L, Ghrabi A, Khouni I (2019) Process optimization via response surface methodology in the physico–chemical treatment of vegetable oil refinery wastewater. *Environ Sci Polut Res* 26(19):18993–19011. <https://doi.org/10.1007/s11356-018-2657-z>

[Article](#) [CAS](#) [Google Scholar](#)

Malathi A, Arunachalam P, Kirankumar VS, Madhavan J, Al-Mayouf AM (2018a) An efficient visible light driven bismuth ferrite incorporated bismuth oxyiodide (BiFeO₃/BiOI) composite photocatalytic material for degradation of pollutants. *Opt Mater* 84:227–235. <https://doi.org/10.1016/j.optmat.2018.06.067>

[Article](#) [CAS](#) [Google Scholar](#)

Malathi A, Arunachalam P, Madhavan J, Al-Mayouf AM, Ghanem MA (2018b) Rod-on-flake α -FeOOH/BiOI nanocomposite: facile synthesis, characterization and enhanced photocatalytic performance. *Colloids Surf A Physicochem Eng Asp* 537:435–445. <https://doi.org/10.1016/j.colsurfa.2017.10.036>

[Article](#) [CAS](#) [Google Scholar](#)

Malathi A, Madhavan J, Ashokkumar M, Arunachalam P (2018c) A review on BiVO₄ photocatalyst: activity enhancement methods for solar photocatalytic applications. Appl Catal A Gen 555:47–74. <https://doi.org/10.1016/j.apcata.2018.02.010>

[Article](#) [CAS](#) [Google Scholar](#)

Mansouri L, Jellali S, Akrouit H (2019) Recent advances on advanced oxidation process for sustainable water management. Environ Sci Polut Res 26(19):18939–18941.

<https://doi.org/10.1007/s11356-019-05210-1>

[Article](#) [Google Scholar](#)

Mengting Z, Kurniawan TA, Yanping Y, Othman MHD, Avtar R, Fu D, Hwang GH (2020) Fabrication, characterization, and application of ternary magnetic recyclable Bi₂WO₆/BiOI@Fe₃O₄ composite for photodegradation of tetracycline in aqueous solutions. J Environ Manage 270:110839. <https://doi.org/10.1016/j.jenvman.2020.110839>

[Article](#) [CAS](#) [Google Scholar](#)

Priya A, Arunachalam P, Selvi A, Madhavan J, Al-Mayouf AM (2018a) Synthesis of BiFeWO₆/WO₃ nanocomposite and its enhanced photocatalytic activity towards degradation of dye under irradiation of light. Colloids Surf A Physicochem Eng Asp 559:83–91.

<https://doi.org/10.1016/j.colsurfa.2018.09.031>

[Article](#) [CAS](#) [Google Scholar](#)

Priya A, Arunachalam P, Selvi A, Madhavan J, Al-Mayouf AM, Ghanem MA (2018b) A low-cost visible light active BiFeWO₆/TiO₂ nanocomposite with an efficient photocatalytic and photoelectrochemical performance. Opt Mater 81:84–92.

<https://doi.org/10.1016/j.optmat.2018.05.022>

[Article](#) [CAS](#) [Google Scholar](#)

Priya A, Arumugam M, Arunachalam P, Al-Mayouf AM, Madhavan J, Theerthagiri J, Choi MY (2020a) Fabrication of visible-light active BiFeWO₆/ZnO nanocomposites with enhanced photocatalytic activity. *Colloids Surf A Physicochem Eng Asp* 586:124294. <https://doi.org/10.1016/j.colsurfa.2019.124294>

[Article](#) [CAS](#) [Google Scholar](#)

Priya A, Senthil RA, Selvi A, Arunachalam P, Kumar CS, Madhavan J, Boddula R, Pothu R, Al-Mayouf AM (2020b) A study of photocatalytic and photoelectrochemical activity of as-synthesized WO₃/g-C₃N₄ composite photocatalysts for AO7 degradation. *Mater Sci Ener Technol* 3:43–50. <https://doi.org/10.1016/j.mset.2019.09.013>

[Article](#) [CAS](#) [Google Scholar](#)

Senthil RA, Osman S, Pan J, Sun M, Khan A, Yang V, Sun Y (2019a) A facile single-pot synthesis of WO₃/AgCl composite with enhanced photocatalytic and photoelectrochemical performance under visible-light irradiation. *Colloids Surf A Physicochem Eng Asp* 567:171–183. <https://doi.org/10.1016/j.colsurfa.2019.01.056>

[Article](#) [CAS](#) [Google Scholar](#)

Senthil RA, Osman S, Pan J, Sun Y, Kumar TR, Manikandan A (2019b) A facile hydrothermal synthesis of visible-light responsive BiFeWO₆/MoS₂ composite as superior photocatalyst for degradation of organic pollutants. *Ceram Int* 45(15):18683–18690. <https://doi.org/10.1016/j.ceramint.2019.06.093>

[Article](#) [CAS](#) [Google Scholar](#)

Senthil RA, Wu Y, Liu X, Pan J (2021) A facile synthesis of nano AgBr attached potato-like Ag₂MoO₄ composite as highly visible-light active photocatalyst for purification of industrial waste-water. *Environ Poll* 269:116034. <https://doi.org/10.1016/j.envpol.2020.116034>

[Article](#) [CAS](#) [Google Scholar](#)

Thiagarajan K, Bavani T, Arunachalam P, Lee SJ, Theerthagiri J, Madhavan J, Pollet BG, Choi MY (2020) Nanofiber NiMoO₄/g-C₃N₄ composite electrode materials for redox supercapacitor applications. *Nanomaterials* 10(2):392.

<https://doi.org/10.3390/nano10020392>

[Article](#) [CAS](#) [Google Scholar](#)

Tran VA, Kadam AN, Lee SW (2020) Adsorption-assisted photocatalytic degradation of methyl orange dye by zeolite-imidazole-framework-derived nanoparticles. *J Alloys Compd* 835:155414. <https://doi.org/10.1016/j.jallcom.2020.155414>

[Article](#) [CAS](#) [Google Scholar](#)

Xu F, Xu C, Chen H, Wu D, Gao Z, Ma X, Zhang Q, Jiang K (2019) The synthesis of Bi₂S₃/2D-Bi₂WO₆ composite materials with enhanced photocatalytic activities. *J Alloys Compd* 780:634–642. <https://doi.org/10.1016/j.jallcom.2018.11.397>

[Article](#) [CAS](#) [Google Scholar](#)

Xu M, Ye M, Zhou X, Cheng J, Huang C, Wong W, Wang Z, Wang Y, Li C (2020) One-pot controllable synthesis of BiOBr/β-Bi₂O₃ nanocomposites with enhanced photocatalytic degradation of norfloxacin under simulated solar irradiation. *J Alloys Compd* 816:152664.

<https://doi.org/10.1016/j.jallcom.2019.152664>

[Article](#) [CAS](#) [Google Scholar](#)

Zhang H, Wang X, Li N, Xia J, Meng Q, Ding J, Lu J (2018) Synthesis and characterization of TiO₂/graphene oxide nanocomposites for photoreduction of heavy metal ions in reverse osmosis concentrate. *RSC Adv* 8(60):34241–34251. <https://doi.org/10.1039/C8RA06681G>

[Article](#) [CAS](#) [Google Scholar](#)

Zhang G, Chen D, Li N, Xu Q, Li H, He J, Lu J (2019) Fabrication of Bi₂MoO₆/ZnO hierarchical heterostructures with enhanced visible-light photocatalytic activity. *Appl Catal B Environ* 250:313–324. <https://doi.org/10.1016/j.apcatb.2019.03.055>

[Article](#) [CAS](#) [Google Scholar](#)

Acknowledgements

The authors J. Madhavan and T. Bavani are grateful to Thiruvalluvar University, Vellore, for the laboratory facilities. M. Selvaraj extends his appreciation to the deanship of scientific research at King Khalid University for the support through the Large Research Group Project under grant number R.G.P: 2/97/1443.

Funding

This work was partially supported by King Khalid University (Large Research Group Project number R.G.P: 2/97/1443).

Author information

Authors and Affiliations

Solar Energy Lab, Department of Chemistry, Thiruvalluvar University, Vellore, 632115, India

Thirungnanam Bavani & Jagannathan Madhavan

Department of Physics and Nanotechnology, SRM Research Institute, SRM Institute of Science and Technology, Kattankulathur, 603203, Chennai, India

Vasudevan Vinesh & Bernaurdshaw Neppolian

**Department of Inorganic Chemistry, School of Chemistry, Madurai Kamaraj University,
Madurai, 625021, India**

Sepperumal Murugesan

**Department of Chemistry, Faculty of Science, King Khalid University, Abha, 61413, Saudi
Arabia**

Manickam Selvaraj

Contributions

All authors contributed to the study conception and design. Material preparation, data collection, analysis, and the first draft of the manuscript were done by Thirungnanam Bavani. Characterization, interpretation of data, and validation are conducted by Vasudevan Vinesh and Bernaurdshaw Neppolian. Supervision, validation, and review by Jagannathan Madhavan. Analysis, interpretation, and review by Sepperumal Murugesan. Funds, review, and editing by Manickam Selvaraj. All authors read and approved the final manuscript.

Corresponding author

Correspondence to [Jagannathan Madhavan](#).

Ethics declarations

Ethics approval

Not applicable.

Consent to participate

All authors have approved the final version of the manuscript and have given their consent for publication.

Competing interests

The authors declare no competing interests.

Additional information

Responsible Editor: George Z. Kyzas

Publisher's note

Springer Nature remains neutral with regard to jurisdictional claims in published maps and institutional affiliations.

Rights and permissions

[Reprints and permissions](#)

About this article

Cite this article

Bavani, T., Vinesh, V., Neppolian, B. *et al.* One-step synthesis of rod-on-plate like 1D/2D-NiMoO₄/BiOI nanocomposite for an efficient visible light driven photocatalyst for pollutant degradation. *Environ Sci Pollut Res* **29**, 65222–65232 (2022).

<https://doi.org/10.1007/s11356-022-19982-6>

Received

11 February 2022

Accepted

25 March 2022

Published

29 April 2022

Issue Date

September 2022

DOI

<https://doi.org/10.1007/s11356-022-19982-6>

Keywords

[NiMoO₄/BiOI](#)

[Nanocomposite](#)

[Photocatalyst](#)

[Visible light](#)

[Advanced oxidation process](#)

[Degradation](#)



Research Article

Phosphorus co-doped reduced graphene oxide embedded flower-like CoS/CoS₂ heterostructure as an efficient electrocatalyst for hydrogen evolution reaction in acidic media

Dhandapani Balaji^a, Jagannathan Madhavan^a  , Mani Preeyanga^b, Mohamed Hussien^{c,d}, Manickam Selvaraj^c, Sepperumal Murugesan^e, Bernaurdshaw Neppolian^b

Show more 

 Share  Cite

<https://doi.org/10.1016/j.jallcom.2022.164506> 

[Get rights and content](#) 

Highlights

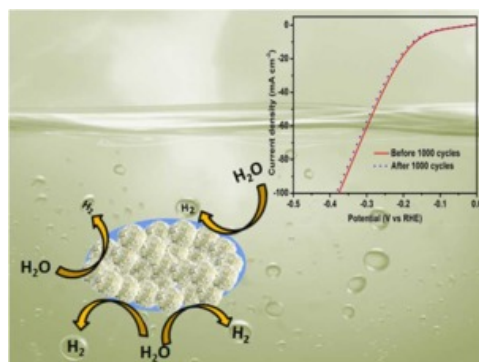
- Flower-like P-doped rGO supported CoS/CoS₂ heterostructure were obtained via simple hydrothermal method.
- The rGO-CoS/CoS₂ @P5 delivered superior HER activity at low overpotential of 148mV in acid electrolyte.
- Excellent long-term durability with negligible variation in current density after 20h chronoamperometry analysis.
- The rGO-CoS/CoS₂ @P5 composite can be used as a good alternative for water splitting process.

Abstract

The electrochemical efficacy of an electrocatalyst can be improved by an elaborate surface modification. In this study, phosphorus co-doped reduced graphene oxide embedded (rGO) flower like CoS/CoS₂ heterostructures have been prepared, via one step hydrothermal process, by taking different mole ratio of phosphorus source for excellent hydrogen evolution reaction (HER) in acid solution. The as-fabricated catalysts are studied by XRD, FT-IR, XPS, SEM,

EDS, and HR-TEM analyses. The rGO-CoS/CoS₂@P5 (5 mmol) catalyst exhibits a superior catalytic behavior for HER with a less overpotential (148 mV), low Tafel slope (44 mV dec⁻¹) and enhanced cyclic durability (1000 cycles) in acid condition in comparison with other composition. The synergetic effect of hetero-interface and rapid charge transfer through rGO on the active sites of CoS/CoS₂ have improved the HER efficiency. This study demonstrated that the component of rGO and P-incorporation on CoS/CoS₂ interface offered an achievable yet easy strategy to synthesize platinum (Pt) free metal-based heterostructured catalyst as the favorable electrode material in sustainable energy applications.

Graphical Abstract



[Download : Download high-res image \(144KB\)](#)

[Download : Download full-size image](#)

Introduction

With rapidly increasing human population and extensive usage of fossil fuels, environmental pollution and energy demand are considered as the most significant universal issues [1], [2], [3]. As a clean energy source with high density and zero carbon emission (CO₂), hydrogen (H₂) is considered to be the best potential candidate to replace fossil fuels in the future [4]. Among different methods of hydrogen production, electrocatalytic water splitting has proven to be a sustainable approach for producing hydrogen with high purity. In this field, the performance of the electrocatalyst is highly significant. Generally, Pt is the most efficient and stable electrocatalyst for hydrogen evolution reaction (HER) in acidic media. However, due to scarcity and high cost, the practical use of Pt-based catalysts has been severely hampered [5]. So there exists an urgency to prepare affordable, highly efficient and high active catalysts for hydrogen evolution reaction (HER) in acid media in order to bring this process to commercial level [6], [7].

Recently, several research attempts to replace Pt-based materials have been reported [8], [9]. Among the various noble metal-based catalysts, transition metals, such as, Ni or Co have attracted significant attention since they exhibit good catalytic activity in the acid media HER process owing to their unoccupied and unpaired electrons in the d-orbitals [10], [11], [12]. In particular, Co-based catalytic materials are recognized as promising non-noble metal catalysts for HER with a robust current density with low overpotential and notable long-term stability [13]. Interface engineering is one such most promising method to achieve high efficiency HER catalyst through heterojunction that generates concerted electric field, thus improving the electron conductivity and charge distribution on the heterointerface [14], [15], [16], [17], [18]. By means of electronic modification, the heterostructure can be explored to activate its intrinsic behavior. Information on extensive physical properties of the heterostructures have been broadly used in the catalyst field, and also helps in improving the electrocatalytic activity [19], [20], [21], [22]. Yang et al. reported NiS@CoS heterostructure on a carbon cloth substrate which resulted in a maximum number of widely distributed tiny pores all over the core-shell structure [23]. The free energy of hydrogen absorption and more active edge sites are essential

properties for an efficient electrocatalyst towards HER. Tang et al. [24] developed a facile self-assembled and self-supported MoS₂/CoS₂ heterostructure with a remarkable HER activity in a broad pH electrolyte. They reported that Gibbs's free energy of hydrogen adsorption and energy barrier for water dissociation are dramatically reduced by strong crystal interactions between MoS₂ and CoS₂. Wang et al. fabricated a 3D hierarchical NiS₂/MoS₂ heterostructure on carbon fiber paper via facile two-step method which demonstrated an efficient hydrogen evolution reaction with superior catalytic behavior through efficient electron transfer on the active edge sites [25].

Various modifications, such as, incorporation of other materials, doping non-metallic elements and compositing with carbon supports are reported to improve the HER activity [26], [27], [28], [29]. Among them, doping of elements has been considered as the most promising approaches in the development of the electrocatalyst with increased electron conductivity and active sites [30], [31]. The hetero atoms, such as, nitrogen (N), phosphorus (P) and sulphur (S) are usually employed as a dopant to metal sulphides for sustainable energy storage and conversion applications [32], [33], [34], [35]. Among these, P-doping for altering the electron density of metal sulphide is beneficial for electrocatalytic activity [36], [37], [38], [39]. Further, combining the carbon based materials, such as, carbon fiber paper (CFP) [40], [41], [42], reduced graphene oxide (GO) [43], [44], multiwalled carbon nanotube (MWCNT) [45], [46], [47] and carbon cloth (CC) [48], [49], [50] with transition metal based catalysts improves the surface area of the electrocatalyst. The P atom creates a close connection to S element in metal sulphide as its atomic radius and electronegativity are closer to those of S [51]. Hence, the synthesis of materials by compositing P and C with CoS₂ is expected to increase the active sites and electron conductivity to enhance the electrochemical efficiency towards HER.

In this work, we have followed a facile route for the fabrication of phosphorus co-doped reduced graphene oxide embedded CoS/CoS₂ heterostructure as an effective electrocatalyst for HER in acid solution. A series of rGO-CoS/CoS₂@P materials with different mole ratios (1, 3, 5, and 7 mmol) of P were prepared through a simple hydrothermal method and their electrochemical activities for HER were explored in 0.5MH₂SO₄ electrolyte.

Section snippets

Chemicals

Chemicals and reagents of analytical grade, without any further purification, were used to prepare aqueous solutions. Cobalt nitrate hexahydrate (Co(NO₃)₂·6H₂O) and sodium dihydrogen phosphate (NaH₂PO₄·H₂O) were bought from Himedia Chemical Laboratories Pvt. Ltd, India. Thiourea (CH₄N₂S) was purchased from SD Fine-Chem. Ltd, India. Ethanol (C₂H₅OH) was obtained from Merck Specialties Pvt Ltd, India. Nafion solution (5%) was procured from Sigma-Aldrich, India to make the catalytic ink. Double...

X-ray diffraction studies

The crystalline structure of rGO-CoS/CoS₂@P composites were investigated using XRD studies. As shown in Fig. 2, the sharp diffraction peaks noted for rGO-CoS/CoS₂@P are clearly matching with the characteristic JCPDS patterns for hexagonal phase of CoS (JCPDS No. 65-0407) and cubic phase of CoS₂ (JCPDS No. 65-3322). The crystalline peaks at 2θ = 30.6, 35.3, 46.9 and 54.4° are indexed to the (100), (101), (102) and (110) planes of CoS and the peaks appearing at 2θ = 27.8, 32.3, 36.2, 39.8,...

Conclusions

Phosphorus co-doped reduced graphene oxide embedded flower-like CoS/CoS₂ heterostructure has been investigated as an efficient HER catalyst in acid media. The catalysts were synthesized using a fixed concentration of rGO and different ratios of NaH₂PO₄ (1, 3, 5, 7 mmol) by a simple one step hydrothermal method. The synthesised materials

were characterized through different techniques, viz., XRD, FT-IR, SEM, HR-TEM, XPS and EDS analyses. The prepared rGO-CoS/CoS₂@P5 composite exhibited a flower ...

Credit authorship contribution statement

D. Balaji: Carried out the experiments. **J. Madhavan:** Designed the experiential scheme and guided throughout the work. **M. Preeyanghaa, B. Neppolian:** Characterization and analysis of the results. **M. Selvaraj, S. Murugesan:** Characterization and Funding speciality....

Declaration of Competing Interest

The authors declare that they have no known competing financial interests or personal relationships that could have appeared to influence the work reported in this paper....

Acknowledgements

S. Murugesan acknowledges RUSA Madurai Kamaraj University, India for the support through a research project (No. 002/RUSA/MKU/2020-2021)....

[Recommended articles](#)

References (68)

Z.C. Li *et al.*

[Synthesis of sulfur-rich MoS₂ nanoflowers for enhanced hydrogen evolution reaction performance](#)

Electrochim. Acta (2018)

S.Y. ShajaripourJaberi *et al.*

[The effect of annealing temperature, reaction time, and cobalt precursor on the structural properties and catalytic performance of CoS₂ for hydrogen evolution reaction](#)

Int. J. Hydrog. Energy (2021)

J. Lin *et al.*

[In-situ selenization of Co-based metal-organic frameworks as a highly efficient electrocatalyst for hydrogen evolution reaction](#)

Electrochim. Acta (2017)

Y. Cui *et al.*

[Highly active and stable electrocatalytic hydrogen evolution catalyzed by nickel, iron-doped cobalt disulfide@reduced graphene oxide nanohybrid electrocatalysts](#)

Mater. Today Energy (2018)

S. Li *et al.*

[Heterojunction engineering of MoSe₂/MoS₂ with electronic modulation towards synergetic hydrogen evolution reaction and super capacitance performance](#)

Chem. Eng. J. (2019)

Y. Jing *et al.*

[Enhanced hydrogen evolution reaction of WS₂-CoS₂ heterostructure by synergistic effect](#)

Int. J. Hydrog. Energy (2019)

T. Jayaraman *et al.*

[Recent development on carbon-based heterostructures for their applications in energy and environment: a review](#)

J. Ind. Eng. Chem. (2018)

R.A. Senthil *et al.*

[Facile one-pot synthesis of microspherical-shaped CoS₂/CNT composite as Pt-free electrocatalyst for efficient hydrogen evolution reaction](#)

Int. J. Hydrog. Energy (2019)

B. Chen *et al.*

[Electronic coupling induced high performance of N, S-codoped graphene supported CoS₂ nanoparticles for catalytic reduction and evolution of oxygen](#)

J. Power Sources (2018)

J.Q. Chi *et al.*

[N, P dual-doped hollow carbon spheres supported MoS₂ hybrid electrocatalyst for enhanced hydrogen evolution reaction](#)

Catal. Today (2019)



View more references

Cited by (22)

[Co, N, and P co-doped few-layer graphene derived from cobalt phthalocyanine-based covalent organic polymers as bifunctional electrocatalysts for overall water splitting](#)

2024, Journal of Physics and Chemistry of Solids

[Show abstract](#)

[Elevating hydrogen evolution performance with plasma-induced sulfur vacancies and heteroatom doping in hollow-structured MnS-CoS catalysts](#)

2024, Journal of Alloys and Compounds

[Show abstract](#)

[Hollow nanoparticles doped hierarchical hexagonal star shaped cobalt-based phosphosulfides for water splitting](#)

2024, Journal of Alloys and Compounds

[Show abstract](#)

[NiS@CuBi₂O₄/ERGO heterostructured electro-catalyst for enhanced hydrogen evolution reaction](#)

2023, Micro and Nanostructures

[Show abstract](#) 

[Hetero-interface-engineered sulfur vacancy and oxygen doping in hollow Co₉S₈/Fe₇S₈ nanospheres towards monopersulfate activation for boosting intrinsic electron transfer in paracetamol degradation](#)


2023, Applied Catalysis B: Environmental

[Show abstract](#) 

[Regulating charge distribution of Ru atoms in ruthenium phosphide/carbon nitride/carbon for promoting hydrogen evolution reaction](#)

2023, Journal of Alloys and Compounds

[Show abstract](#) 

[View all citing articles on Scopus](#) 

[View full text](#)

© 2022 Elsevier B.V. All rights reserved.







All content on this site: Copyright © 2024 Elsevier B.V., its licensors, and contributors. All rights are reserved, including those for text and data mining, AI training, and similar technologies. For all open access content, the Creative Commons licensing terms apply.





Original Article

Synergistic combination of BiFeO₃ nanorods and CeVO₄ nanoparticles for enhanced visible light driven photocatalytic activity

Velu Venugopal^a, Dhandapani Balaji^b, Mani Preeyanghaa^c, Cheol Joo Moon^d, Bernaurdshaw Neppolian^e, Govarthanam Muthusamy^{f,g}, Jayaraman Theerthagiri^d, Jagannathan Madhavan^a  , Myong Yong Choi^d  

[Show more](#) [Outline](#) | [Share](#)  [Cite](#) <https://doi.org/10.1016/j.aej.2023.04.024> [Get rights and content](#) Under a Creative Commons [license](#) 

open access

Abstract

Eliminating harmful organic pollutants from contaminated water remains an urgent problem to be solved. Taking Rhodamine B (RhB) as a representative organic water pollutant we sought to design a facile and scalable synthesis of a BiFeO₃/CeVO₄ (BFO/CVO) nanocomposite catalyst for the degradation of organic pollutant under visible light. BFO nanorods and CVO nanoparticles were fabricated using single-step hydrothermal routes and the resulting materials could be easily combined using a simple wet-chemical precipitation method. From the morphological studies, pure BiFeO₃ and CeVO₄ revealed the 1D-nanorod and 0D-nanoparticles, respectively. For the BFO/CVO composite, 0D-nanoparticles were well attached on the 1D-nanorods of BiFeO₃. Also, the 10% BFO/CVO composite provided efficient photodegradation efficiency (92%) of RhB with 0.0225 min⁻¹ rate constant. Furthermore, the obtained photocatalyst had a low band gap energy value (2.01 eV) and photoluminescence intensity when compared to pure BFO and CVO under visible light illumination. The radical scavenging experiments proposed that the [•]OH acted a substantial role in the RhB decomposition pathway. The optimized BFO/CVO composite photocatalyst exhibits superior recyclability and photostability. The superior photocatalytic action of the 10% BFO/CVO composite could be explained by the development of a heterojunction among BFO and CVO where electrons can migrate at the BFO/CVO interface. These results imply that BiFeO₃/CeVO₄ composites are suitable photocatalysts for the elimination of organic toxins from water.



Keywords

1. Introduction

Rapid increases in population and industrialization are considered to be significant sources of land and surface water pollution [[1], [2], [3], [4]]. Speaking in generalities, the cosmetics, pharmaceutical, textile, leather, pesticide, food industries contribute the most to environmental water contamination. One of the biggest pollutants from the textile industry are organic dyes. Even the very small concentrations that are discharged are hazardous because these molecules are carcinogenic and mutagenic in nature. These discharges severely affect the aquatic environment, and as many food chains link back to an aquatic environment, many living organisms can also be affected. To date, several approaches have been evaluated for reducing organic contaminants, such as dyes, from water, including: activated carbon, reverse osmosis, and ultrafiltration. However, these techniques do not destroy the water pollutants and tend to produce other types of secondary pollution instead [[5], [6], [7], [8], [9]]. For eliminating the organic pollutants, several methods have been explored, such as photocatalytic degradation using an oxidation treatment using visible light irradiation (VLI) in the presence of effective semiconductor material [[10], [11], [12], [13], [14], [15]]. Several research groups have focused on developing semiconductor materials for photocatalytic degradation because these reactions tend to be faster and highly eco-friendly [[16], [17], [18], [19], [20]]. Visible light is readily available from green sources and can convert the organic pollutant into harmless products without further environmental toxification. Semiconductor materials like TiO₂ and ZnO are commonly utilized potential candidates for photocatalytic decomposition of organic contaminants. However, their large band gaps restrict absorption in the visible region, and the photocatalytic degradation efficacy of these semiconductors is still poor [[21], [22], [23], [24], [25], [26]]. To combat this, an enormous volume of work exploring an effective photocatalytic material with improved photocatalytic behavior toward the decomposition of organic contaminants is available [[27], [28], [29]]. Among the different visible light responsive photocatalytic semiconductors identified, bismuth-based semiconductor photocatalysts, such as Bi₂WO₆ [30], BiOBr [31], Bi₂MoO₆ [32], and CaBi₂O₆ [33], appear to be very active materials for the organic contaminates decomposition in an aquatic environment. In particular, BiFeO₃ (BFO)-based materials have attracted significant attention due to their convenient electronic structure and appropriate optical behavior, making them potentially suitable for application in novel solar cells, photodegradation, optoelectronic devices, and sensors [34]. The Fermi-level of BFO lies near the valence band, which makes it a promising visible light catalyst. BFO has a low band gap energy (~2.1–2.2 eV), is chemically stable, non-toxic, relatively inexpensive to produce, and possesses outstanding ferro-electronic properties even at ambient temperatures [35]. Unfortunately, studies have shown that BFO is unsuitable for large-scale photocatalysis applications due to its high rate of e⁻–h⁺ pair reconnection, low quantum yield, and tendency for BFO nanoparticles to aggregate in water [[30], [31], [32], [33]]. To address these challenges, numerous researchers have developed new methods to enhance the photocatalytic efficacy of BFO nanoparticles. These approaches include doping BFO with other metal and non-metal composites and semiconductors, co-catalyst loading, and creating heterostructures to improve the separation of e⁻ and h⁺ [36]. Accordingly, some heterostructure composite photocatalysts have been found to exhibit improved photocatalytic efficiency and photostability: BiFeO₃/BiOI [37], BiFeO₃/AgVO₃ [38], BiFeO₃/BiVO₄ [39], BiFeO₃/BiOCl [40], and CoNiO₂–BiFeO₃–NiS [41].

For many of the same reasons to BFO, cerium vanadate (CeVO₄), abbreviated to CVO, is of equal research interest. CVO is a good visible light semiconductor photocatalyst with non-toxic and environmentally friendly properties that is relatively inexpensive to produce [42]. CVO also possesses a special layered structure with an appropriate bandgap (~1.9 eV) and better photostability characteristics than BFO [43]. Previous reports on CVO-based composite photocatalysts, like Ag@CeVO₄ [44], CeVO₄/BiVO₄ [45], Fe₃O₄/ZnWO₄/CeVO₄ [46], CeVO₄/TiO₂ [47], La₂O₃/CeVO₄@HNTs [48], CeVO₄/g-C₃N₄ [49], and CeVO₄/rGO [50], have demonstrated excellent photocatalytic activity toward the elimination of organic contaminants in wastewater. Therefore, the combination of CeVO₄ with BiFeO₃ is a logical next step and was expected to produce enhanced photocatalytic performance compared to pure BFO or CVO individually by

decreasing the e⁻-h⁺ pairs reconnection. To the best of our knowledge, no study has been reported earlier on the degradation of organic dyes using visible light irradiation of the BFO/CVO photocatalyst.

In the present investigation, we attempted to enhance the photocatalytic ability of BiFeO₃ by coupling it with CeVO₄ as a potential co-catalyst. BiFeO₃/CeVO₄ nanocomposites, abbreviated BFO/CVO herein after, was prepared with the aim of increasing charge separation efficiency, and thus, photocatalytic behavior. A simple one-pot synthesis was utilized to fabricate pure BFO and CVO individually. Then, BFO/CVO nanocomposites are prepared with different weight percentages (10%, 20%, 30%) of BFO by a wet-chemical process. The produced nanocomposites were thoroughly characterized structurally and electrochemically and then explored as photocatalysts for Rhodamine B (RhB) degradation under VLI.

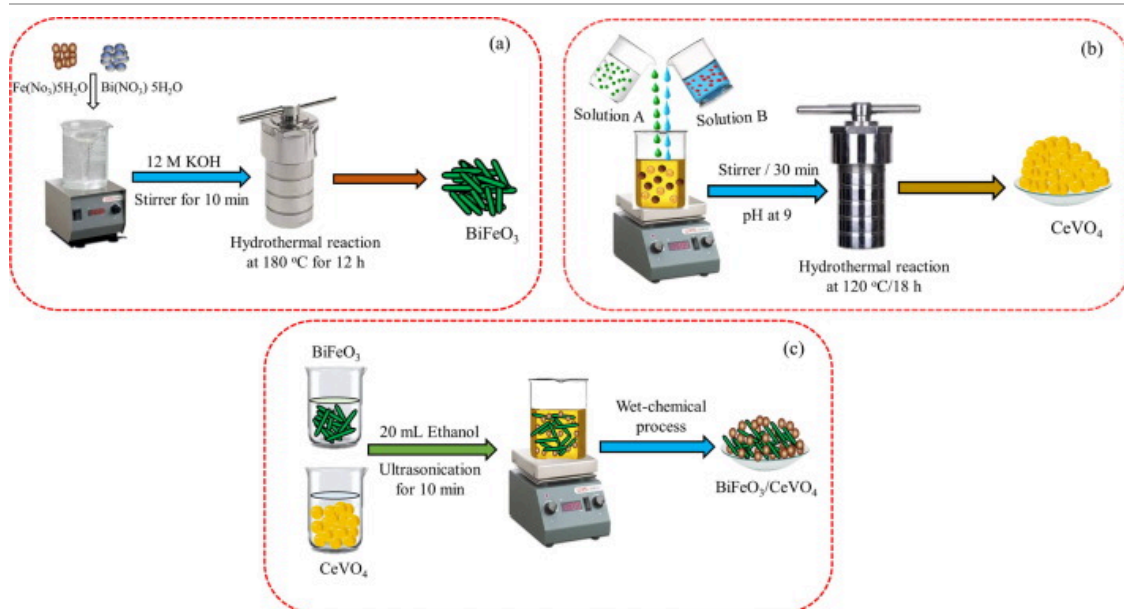
2. Experimental studies

2.1. Materials

Bismuth nitrate pentahydrate (Bi(NO₃)₂·5H₂O), iron nitrate nonahydrate (Fe(NO₃)₃·9H₂O), Triton X-100, and ammonium metavanadate (NH₄VO₃) were obtained from Sigma Aldrich, USA. Potassium hydroxide (KOH), isopropyl alcohol (IPA), cerium nitrate hexahydrate (Ce(NO₃)₆·6H₂O), sodium hydroxide (NaOH), and ammonium oxalate (AO) were acquired from SDFCL chemicals, India. Benzoquinone (BQ), ethanol, and RhB were acquired from Qualigens, India.

2.2. Synthesis of BiFeO₃ nanorods

A straightforward hydrothermal procedure was employed to make the BiFeO₃ (BFO) nanorods. To double-distilled (DD) water (20mL) was added equal ratios of Bi(NO₃)₃·5H₂O (200mmol) and Fe(NO₃)₃·9H₂O (200mmol) and the solution was magnetically stirred. Aqueous KOH (12M, 20mL) was then added over 30min. Thereafter, the reaction vessel was located into an ultrasonication bath for 10min and then stirred for an additional 30min to obtain a homogeneous mixture. The prepared suspension was placed in a Teflon autoclave with a 100mL volume size and was hydrothermally treated at 180°C for 12h (Fig. 1a). After allowing the autoclave to cool to ambient temperature naturally, the as-prepared yellow precipitate was gathered and washed repeatedly using ethanol, DD water, and dried in a hot air oven overnight to obtain BFO nanorods. Fig. 1a provides a schematic presentation of the fabrication approach for BFO.



[Download : Download high-res image \(403KB\)](#)

[Download : Download full-size image](#)

Fig. 1. Schematic presentation of the fabrication process for (a) BiFeO₃ (BFO), (b) CeVO₄ (CVO), and (c) BFO/CVO nanocomposites. BFO and CVO were synthesized separately via a hydrothermal process, and the BFO/CVO composites were obtained via a wet-chemical process under continuous ultrasonication.

2.3. Synthesis of CeVO₄ nanoparticles

Synthesis of the CeVO₄ (CVO) nanoparticles followed literature procedures with minor modifications [43]. To beaker A containing DD water (20 mL) was dissolved NH₄VO₃ (15 mmol). To beaker B containing DD water (20 mL) was dissolved Ce(NO₃)₆H₂O (15 mmol). The solutions in beaker A and beaker B were then simultaneously poured into a reaction vessel and the subsequent mixture was stirred magnetically for 30 min at ambient temperature where the mixture turned from pale yellow to a golden yellow. The reaction solution was stirred for an extra 30 min at 50 °C until a uniform solution was achieved. Aqueous ammonia (0.1 M) was added to maintain a pH level of 9.0. After, the suspension was moved to a Teflon autoclave and the sealed reaction vessel was subject to hydrothermal treatment at 120 °C for 18 h. After allowing the autoclave to cool to ambient temperature certainly, the precipitate was cleaned liberally with DD water and ethanol to eliminate any impurities. The collected product was dried at 60 °C overnight to obtain CVO as a yellow solid. Fig. 1b provides a schematic presentation of the fabrication process for CVO.

2.4. Fabrication of the BFO/CVO nanocomposites

A simple wet-chemical method was used to prepare the BFO/CVO nanocomposite. Various amounts (10, 20, and 30 wt%) of BFO were added to a 50 mL beaker containing 0.5 g of CVO in 20 mL of methanol. The mixture was then ultrasonically agitated for 15 min to ensure complete dispersion. The resulting mixture was magnetically stirred at 80 °C for 60 min, and the obtained BFO/CVO nanocomposites were collected. The different amounts of BFO (10, 20, and 30 wt%) in the BFO/CVO composite were labeled as 10% BFO/CVO, 20% BFO/CVO, and 30% BFO/CVO, respectively. Fig. 1c shows a synthetic scheme for the preparation of the BFO/CVO nanocomposite.

2.5. Characterization

Powder XRD (Bruker-advance D8, wavelength 1.5406 Å) was utilized to authorize the crystalline phase of the BFO/CVO nanocomposites. FT-IR (Perkin-Elmer) measurements were obtained to evaluate the functional groups present in the synthesized samples. The surface structure and elemental purity of optimal materials were obtained by FE-SEM (Thermo Scientific Apreo) and HR-TEM (JEM-2100 Plus). UV-Vis-DRS (Analytik Jena, Specord 210 plus) measurements were obtained to confirm the optical behavior of the samples. Photoluminescence properties of the materials was studied on a Horiba, Fluorolog-QM. The elemental composition of the as-synthesized material was examined via XPS (PHI VersaProbe III Scanning XPS Microprobe).

2.6. Electrochemical studies

The photocurrent response of the catalysts was studied using a three-electrode arrangement on an electrochemical workstation (CHI660E, USA). The working electrode (WE) was the material-loaded FTO substrate, the counter and reference electrodes were a Pt-wire and Ag/AgCl, correspondingly. A photoreactor with a tungsten 250 W halogen lamp (G2E140-AE77-01) light source was employed, and the reaction media was 0.1 M aqueous Na₂SO₄. The FTO WE were fabricated using the doctor blade process: Accurately measured active photocatalyst (5 mg) was ground in a ceramic mortar and mixed with 1:1 v/v Triton X-100 and DD water to form a paste. Thereafter, paste was loaded on an FTO plate (0.5 cm² surface area) and dried at 100 °C in an oven for 3 h.

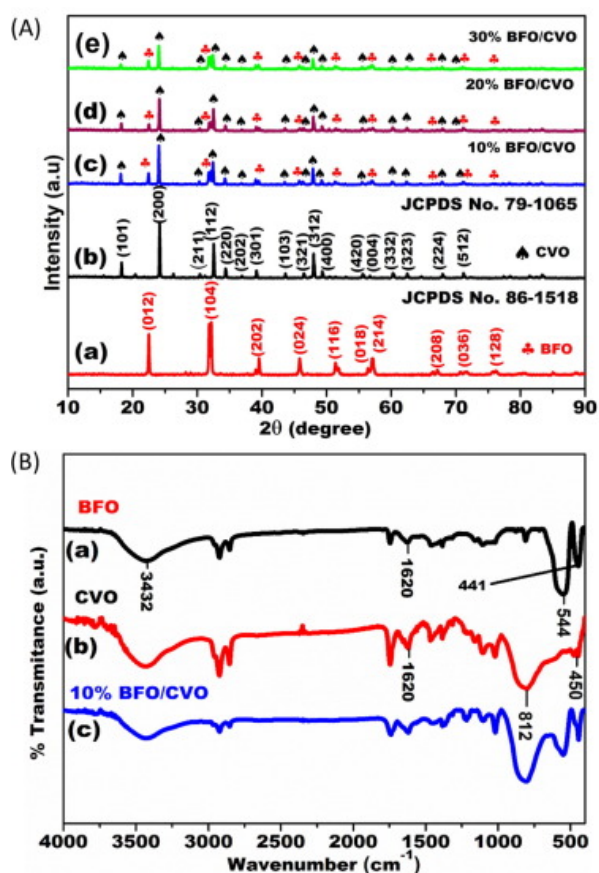
2.7. Photodegradation studies

RhB was selected as a representative organic contaminant to assess the degradation competence of the BFO/CVO nanocomposite. A tungsten 250 W halogen lamp was employed as the irradiation. Active catalyst (75 mg) was dispersed

in an aqueous RhB dye solution (1×10^{-5} M, 75 mL) and the suspension was stirred in the dark for 60 min before being exposed to the light source. During irradiation, aliquots (5 mL) of reaction solution were extracted using a syringe every 15 min and centrifuged to sediment out the particles. The dye solution concentration was measured using a UV-Vis (JASCO V-630) spectrophotometer at an absorbance of 554 nm for RhB.

3. Results and discussion

Bare BFO, bare CVO, and the BFO/CVO composites were confirmed by powder XRD (Fig. 2A). The major peaks for BFO can be noted at 2θ of 22.4°, 31.7°, 39.5°, 45.7°, 51.3°, 56.3°, 57.2°, 66.3°, 71.6°, and 75.6°, and corresponds to the (012), (104), (202), (024), (116), (018), (214), (208), (036), and (128) planes, respectively, of the rhombohedral phase of the BFO (JCPDS NO: 86-1518) [[51], [52]]. Similarly, the tetragonal phase of synthesized CVO was noted at 18.2°, 21°, 30.4°, 32.5°, 34.4°, 36.9°, 39.2°, 43.5°, 46.6°, 48.1°, 49.5°, 55.8°, 56.7°, 60.5°, 62.6°, 68.1°, and 71.5°, matching to (101), (200), (211), (112), (220), (202), (301), (103), (321), (312), (400), (420), (004), (332), (323), (224), and (512) crystalline planes, respectively (JCPDS NO: 79-1065) [53]. The diffraction intensity was significantly reduced by loading varied amounts of BFO material into CVO, which can be attributed to the strong interaction between BFO and CVO in the BFO/CVO composites. This suggests that the BFO sample is well mixed on the CVO surface. Furthermore, the addition of BFO appeared to modify the inter-planer parameters of the CVO crystal.



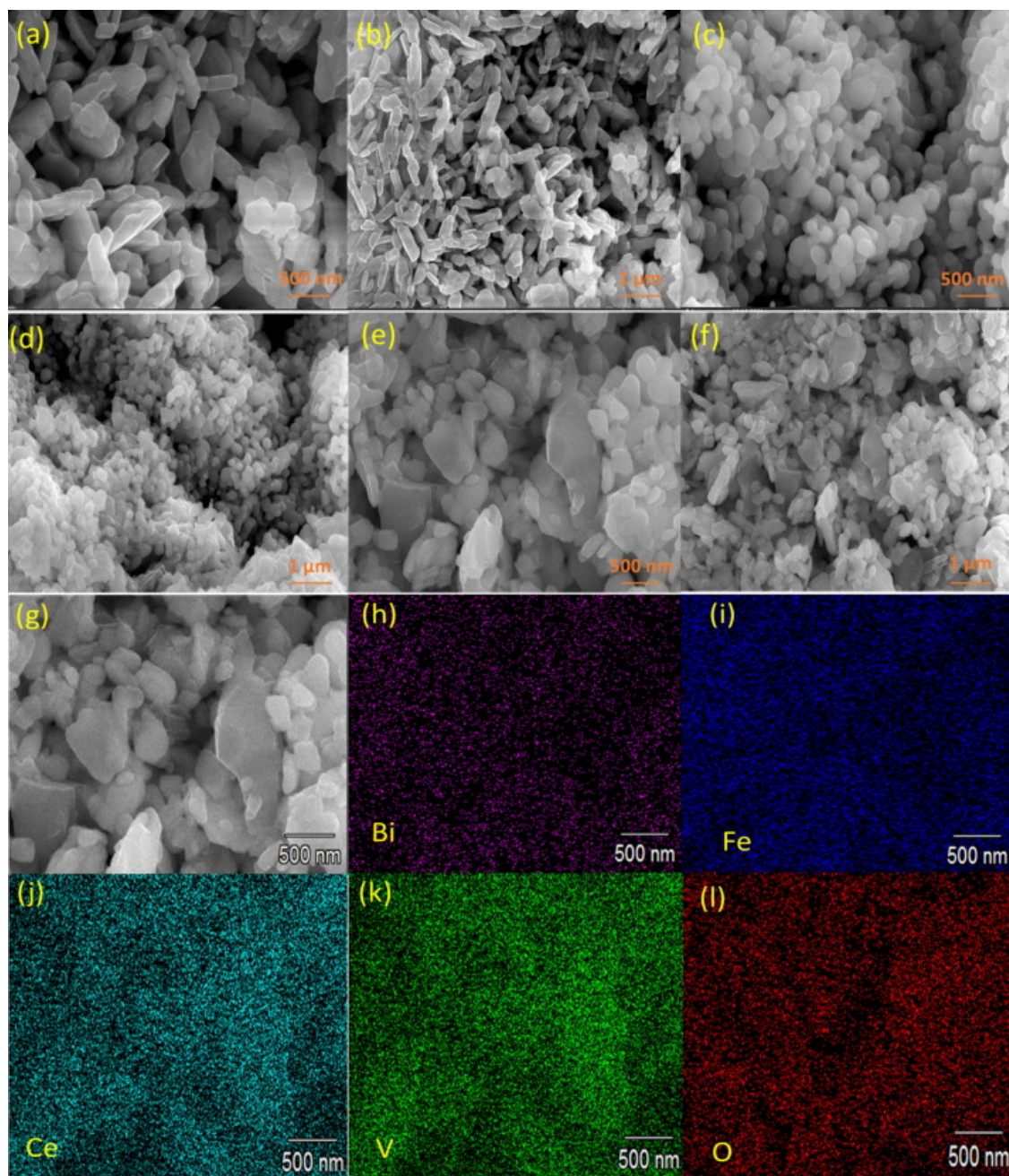
[Download : Download high-res image \(574KB\)](#)

[Download : Download full-size image](#)

Fig. 2. (A) XRD of bare BFO, bare CVO and the various BFO/CVO composites. XRD results confirm the formation of pure BFO in the rhombohedral phase, pure CVO in the tetragonal phase, and (B) FT-IR spectra of optimized bare BFO, bare CVO, and 10% BFO/CVO composite.

The functional groups of the synthesized bare BFO, bare CVO, and 10% BFO/CVO composites were evaluated by FT-IR analysis (Fig. 2B). For bare BFO, the two absorption peaks near 441 and 544 cm⁻¹ were allocated to the Fe-O and O-Fe-O bands, correspondingly [[29], [30]]. For bare CVO, a stretching vibration mode near 450 and 810 cm⁻¹ was accredited to the Ce-O and V-O groups, respectively [[54], [55], [56]]. In addition, two vibration mode peaks near 1620 and 3432 cm⁻¹ can be assigned to the asymmetric and symmetric stretching vibration modes of O-H groups on the BFO and CVO surfaces, respectively. The primary essential representative peaks of both BFO and CVO are clearly present in the BFO/CVO spectra. Therefore, these results prove the existence of both BFO and CVO in the composites.

FE-SEM was used to analyze the morphological properties of the BFO, CVO, and 10% BFO/CVO composite photocatalysts (Fig. 3(a-f)). The BFO (shown in Fig. 3(a & b)) displayed irregular 1D-nanorods overlapping each other. The CVO (shown in Fig. 3(c & d)) consisted of 0D-nanoparticles with a particle size of ~50 nm. The FE-SEM images of the 10% BFO/CVO composite (shown in Fig. 3(e & f)) revealed the presence of numerous 0D-nanoparticles of CVO closely attached to the surface of the 1D-BFO nanorods. Similarly, the EDX spectra of the prepared material supported formation of the appropriate catalysts. As shown in Fig. S1, bare BFO contained Bi, Fe, and O. The EDX spectrum of the CVO sample contained Ce, V, and O (Fig. S2). The EDX spectrum of the optimized 10% BFO/CVO composite displays the colocation of Bi, Fe, Ce, V, and O elements (Fig. S3). The atomic percentages of the obtained materials are given as an inset of Figs. S1-S3. Furthermore, the elemental mapping images of the synthesized 10% BFO/CVO composite material shows a homogeneous mixture of Bi, Ce, Fe, O, and V elements (Fig. 3(g-l)). This proves the successful incorporation of BFO onto the CVO photocatalyst.

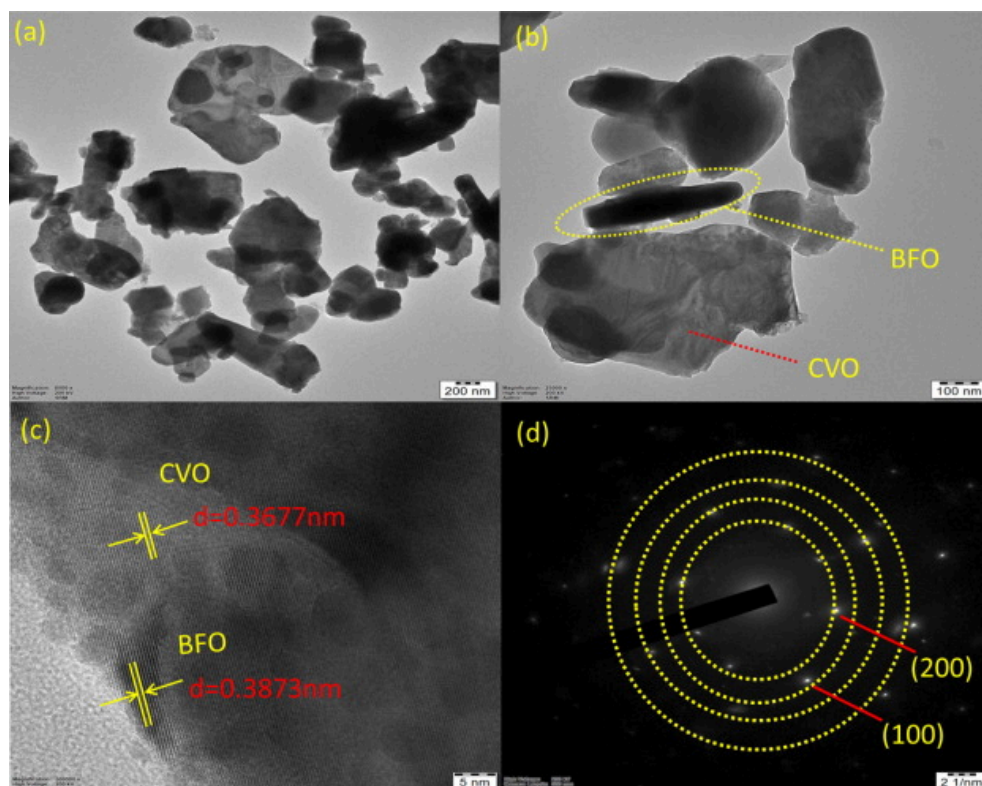


[Download : Download high-res image \(2MB\)](#)

[Download : Download full-size image](#)

Fig. 3. FE-SEM pictures of (a & b) pure BFO, (c & d) CVO, (e & f) 10% BFO/CVO composite, and (g–l) elemental mapping images of 10% BFO/CVO composite.

The 10% BFO/CVO composite was further analyzed to obtain the internal crystal structure through HR-TEM analysis (Fig. 4). The obtained BFO nanorods are mostly overlapping with CVO nanoparticles, thus confirming the close association between BFO and CVO photocatalysts (Fig. 4 a & b). Fig. 4c displays the lattice indexed HR-TEM image of the as-synthesized 10% BFO/CVO composite. Here, the exclusive lattice with a d-spacing value of 0.3871 nm for BFO and 0.3677 nm for CVO are related to their (100) and (200) planes, respectively. These planes match well with the XRD data obtained in this study and the literature [[57], [58]]. Fig. 4d displays the SAED pattern of the BFO/CVO composite, exposing the two peaks that match to the (100) and (200) lattice of BFO and CVO, correspondingly. Thus, these outcomes strongly support the effective interaction of BFO and CVO in the composite.

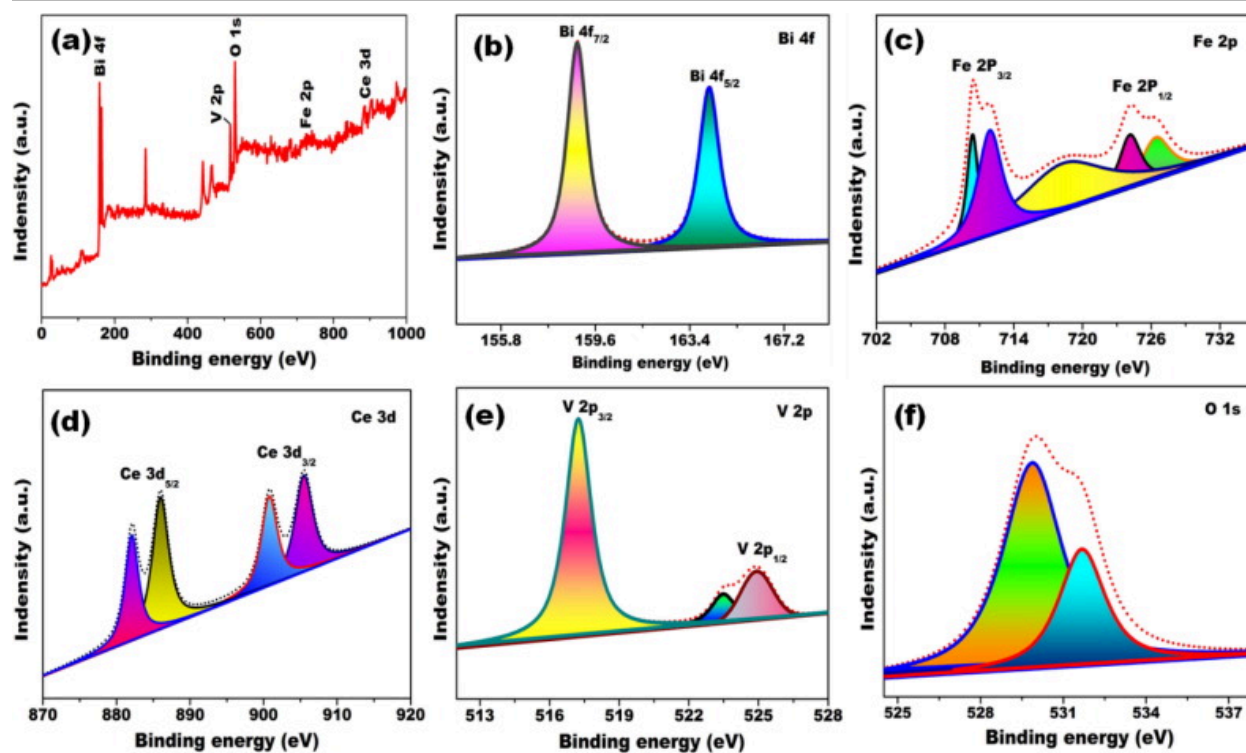


[Download : Download high-res image \(845KB\)](#)

[Download : Download full-size image](#)

Fig. 4. (a–c) HR-TEM pictures and (d) SAED outline of the 10% BFO/CVO composite.

The optimized 10% BFO/CVO composite was studied by XPS to determine the chemical valance states (Fig. 5). Elements, Bi, Fe, Ce, V, and O, can be noted in the full survey with binding energies (BEs) ranging from 0 to 1000eV for the prepared BFO/CVO composite (Fig. 5a). The XPS of Bi 4f displays two peaks at 158.8eV and 164.3eV with 5.5eV separation that resembles to Bi 4f_{7/2} and Bi 4f_{5/2}, correspondingly (Fig. 5b) [59]. As presented in Fig. 5c, the Fe 2p spectrum is separated into five peaks: Two peaks observed at the binding energy of 724.1 eV and 710.2eV can be assigned to Fe 2p_{3/2} and Fe 2p_{1/2}, correspondingly, signifying the existence of Fe³⁺ in the synthesized material. The two peaks located at 718.5eV and 726.6eV are satellite peaks and the peak at 711.9eV corresponds to Fe²⁺ [[59], [60]]. The fitted spectra (Fig. 5d) of Ce 3d shows the two peaks of Ce 3d_{5/2} with assigned BEs of 882.0eV and 885.9eV. The Ce 3d_{3/2} peaks are detected at the binding mode of 900.7eV and 905.5eV, indicating in the presence of Ce³⁺ [61]. The obtained V 2p displayed in Fig. 5e contains two characteristic peaks at 517.2eV and 524.9eV, consistent to the V 2p_{3/2} and V 2p_{1/2}, ascribed to V⁵⁺ [62]. Fig. 5f reveals the O 1s fitted with two peaks at 529.8eV and 531.7eV that are assigned to lattice oxygen adsorption on the sample surface. Thus, XPS studies also support the successful synthesis of the BFO/CVO nanocomposite.

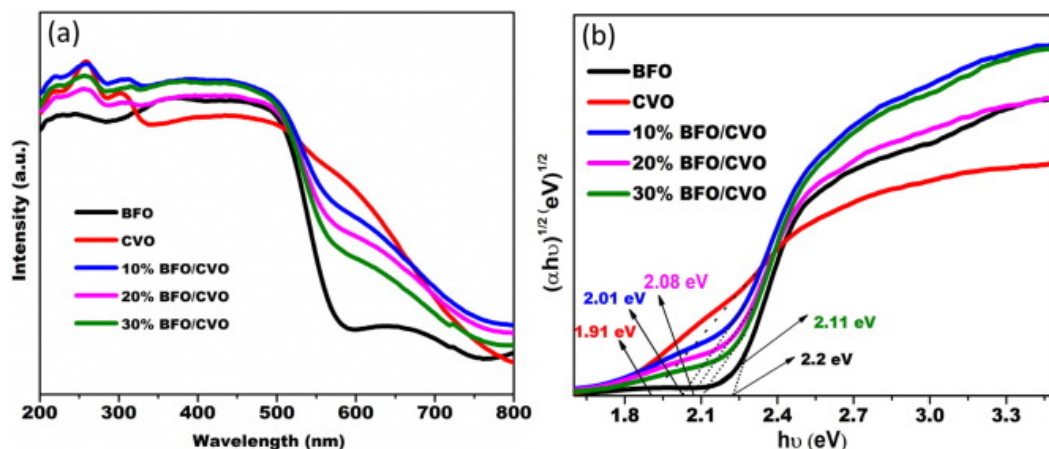


Download : [Download high-res image \(520KB\)](#)

Download : [Download full-size image](#)

Fig. 5. XPS of the prepared 10% BFO/CVO composite: (a) Survey spectrum, (b) Bi 4f, (c) Fe 2p (d) Ce 3d, (e) V 2p, and (f) O 1s core spectra.

Photodegradation efficiency of catalysts can normally be correlated to light absorption efficiency and the optical band gap. The UV–Vis DRS spectra of the bare BFO, bare CVO, and BFO/CVO composites are presented in Fig. 6a. Pristine BFO and CVO materials display absorption edges at 610 and 760nm, correspondingly. Moreover, the absorption edge of the BFO/CVO composite is shifted to a higher visible level as the amount of BFO loading increases. As observed in the spectra of Fig. 6a, the absorption edges of 10%, 20%, and 30% BFO loaded into CVO were 748, 720, and 647nm, respectively. Thus, the fabricated photocatalysts have shown a notable shift in the absorption edge, indicating a significant electronic interaction between BFO and CVO. Application of the Kubelka–Munk equation estimates the band energy gap of the BFO/CVO composites. The E_g values of spectra are plotted from the $(ah\nu)^2$ versus photon energy ($h\nu$) and the attained results are exposed in Fig. 6b. The band gap values of bare BFO, CVO, 10% BFO/CVO, 20% BFO/CVO, and 30% BFO/CVO composites are calculated to be 2.2eV, 1.91eV, 2.01eV, 2.08eV, and 2.11eV, respectively. The 10% BFO/CVO exhibited the lowest band gap energy value for the composites; therefore, the 10% BFO/CVO composite was anticipated to perform the best for the photodecomposition activity toward RhB.



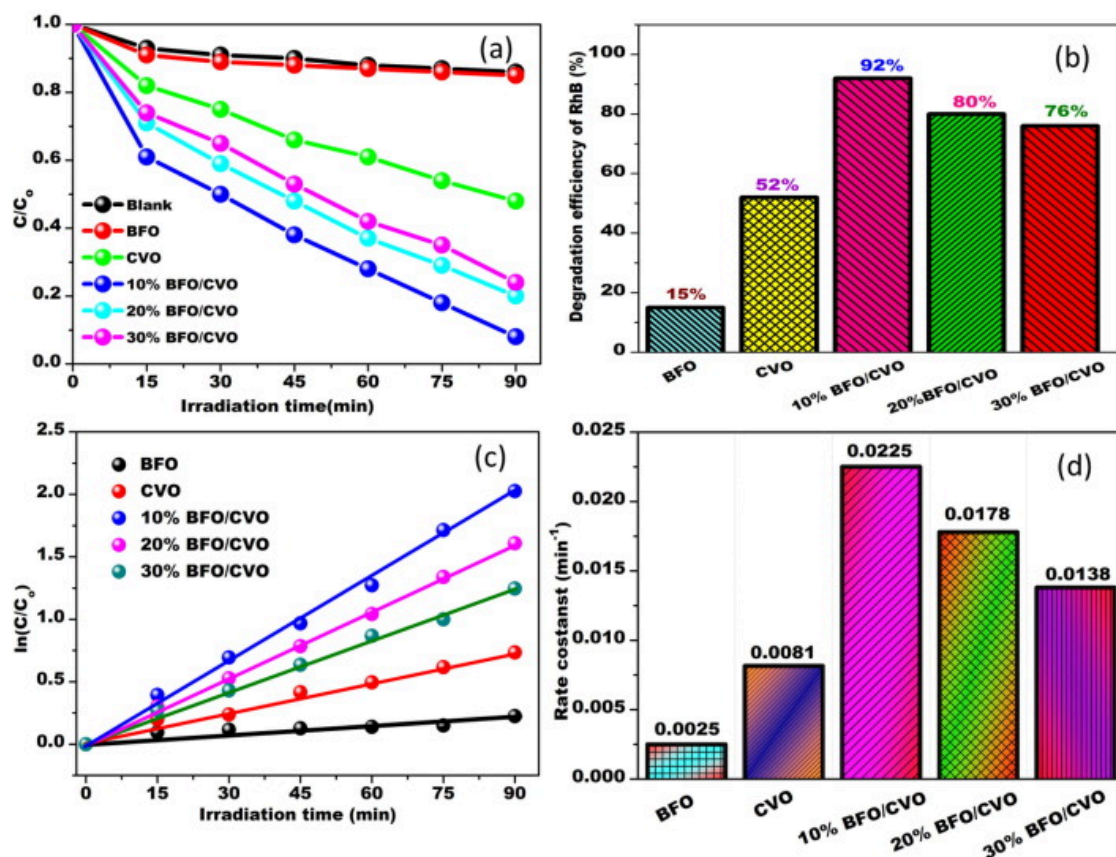
[Download : Download high-res image \(366KB\)](#)

[Download : Download full-size image](#)

Fig. 6. (a) UV-Vis DRS and (b) Kubelka-Munk plot of bare BFO, bare CVO and BFO/CVO composites.

The photocatalytic degradation curves of the bare BFO, bare CVO, and the three BFO/CVO composites are presented in Fig. 7a. As a baseline control experiment, the degradation efficiency of RhB was measured in the absence of any catalyst for 90min under VLI. No significant changes were detected in the concentration of the RhB; likewise, the bare BFO showed negligible degradation activity. However, the bare CVO sample lead to 52% degradation of RhB after 90min under VLI. As expected, the 10% BFO/CVO composite demonstrated the best photocatalytic ability, superior to that of the bare BFO and CVO alone. The photodegradation percentages of RhB after 90min of VLI for BFO, CVO, 10% BFO/CVO, 20% BFO/CVO, and 30% BFO/CVO were 15, 52, 92, 80, and 76%, respectively (Fig. 7b). The 10% BFO/CVO composite's superior performance can be explained by its lower E_g value and higher light absorption in the visible portion. To optimize the degradation rate of the RhB, the as-synthesized materials were fitted to a first-order kinetic rate. As shown in Fig. 7c, the rate constant values of pure BFO, CVO, and the BFO/CVO composites could be obtained from the $\ln(C_0/C)$ vs time plot. As the plot is linear, the decomposition behavior of RhB can be interpreted to follow first-order kinetics. As observed in Fig. 7c and d, the photocatalytic degradation of RhB over BFO/CVO composite photocatalyst followed the pseudo-first-order kinetics relation (equation (1));

$$\ln(C_0/C) = kt \quad (1)$$



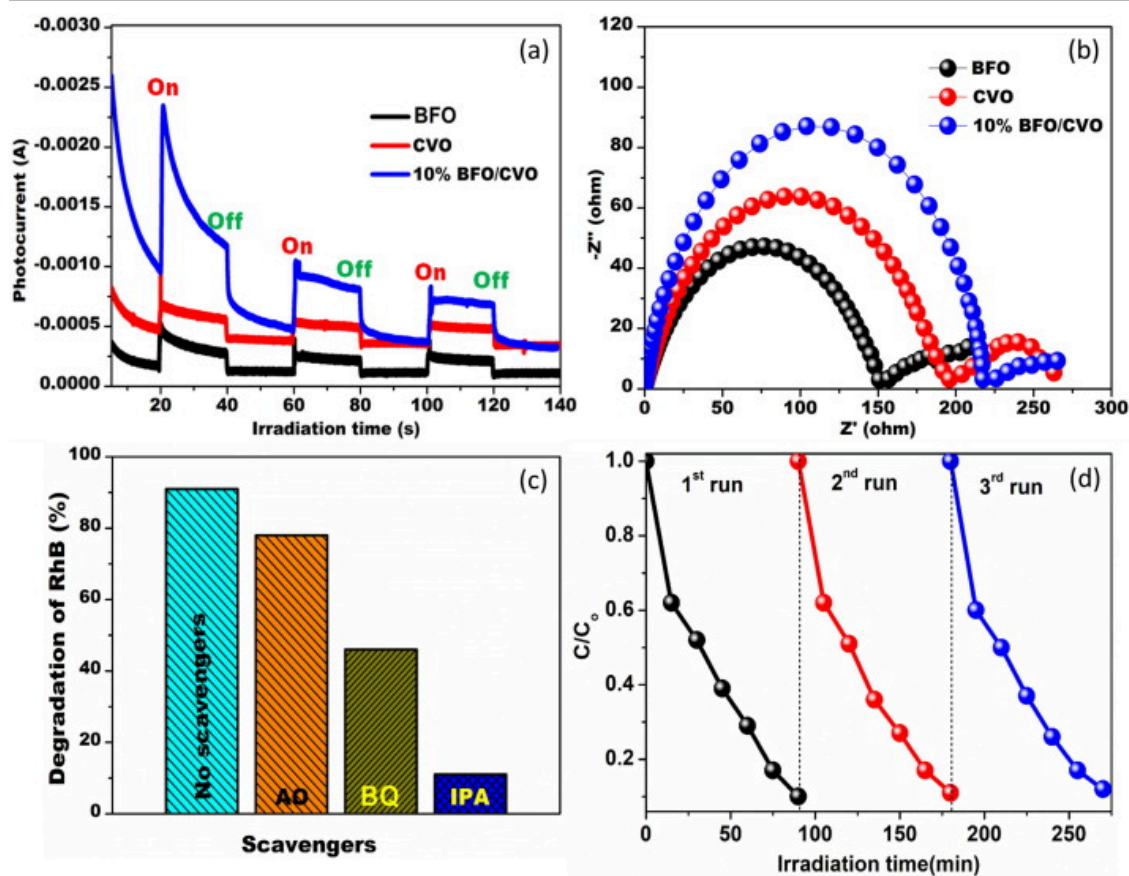
[Download : Download high-res image \(1MB\)](#)

[Download : Download full-size image](#)

Fig. 7. (a) Photodegradation plot, (b) Bar diagram of degradation efficiency, (c) First-order kinetic plot of RhB (1×10^{-5} M) degradation, and (d) Bar graph of rate constants from bare BFO, bare CVO, and the three BFO/CVO composites for the degradation of RhB (1×10^{-5} M) under 90min of VLI.

where k is the rate constant, t is the irradiation time (min), and C_0 and C are the concentration of RhB at initial and different time intervals, respectively. The calculated rate constant value for the 10% BFO/CVO was found to be 0.0225 min^{-1} . From Fig. 7d, it can be observed that the rate constant values for the synthesized catalytic materials varied with the 10% BFO/CVO composite showing the greatest rate constant for the photodegradation activity of RhB. The fabricated photocatalysts were also studied by photoluminescence (PL) spectroscopy with an excitation $\lambda = 325 \text{ nm}$ (Fig. S4). All materials exhibited similar PL spectra at 436nm; however, the intensity of the 10% BFO/CVO composite was notably lower than that of pure BFO and CVO. This low emission suggests less charge carriers recombination; thus, the reconnection rate of the photogenerated carriers is considerably restricted in a BFO/CVO composite. The obtained results clearly indicate that the synthesized 10% BFO/CVO composite provides better charge separation and charge transfer properties.

The photocurrent response of the samples was studied to better understand the observed photocatalytic behaviors of the 10% BFO/CVO composite. Fig. 8a presents the photocurrent curves of the bare BFO, bare CVO, and 10% BFO/CVO samples with on-off cycles of VLI. The 10% BFO/CVO composite delivers an excellent photocurrent response when compared with the corresponding pure BFO and CVO, clearly demonstrating an increase in the charge separation properties that decrease the reconnection rate of the photoexcited charges. EIS was conducted to further evaluate the charge transfer resistance (R_{ct}) of the various materials. Nyquist plots for bare BFO, bare CVO, and the 10% BFO/CVO composite are presented in Fig. 8b. With Nyquist plots, the smaller the semicircle, the smaller the R_{ct} values [[63], [64]]. The 10% BFO/CVO composite had the smallest R_{ct} and implied that the composition of 10% BFO/CVO seems quite beneficial for the charge separation process.



[Download : Download high-res image \(964KB\)](#)

[Download : Download full-size image](#)

Fig. 8. (a) Photocurrent response, (b) Nyquist plots of bare BFO, bare CVO, and 10% BFO/CVO composite, (c) Influence of radical scavengers on 10% BFO/CVO nanocomposite (1 g/L) for mediated photodegradation in RhB (1×10^{-5} M) under 90min of VLI, and (d) Photostability and reusability plots of 10% BFO/CVO composite (1 g/L) for RhB degradation (1×10^{-5} M) under 90min of VLI.

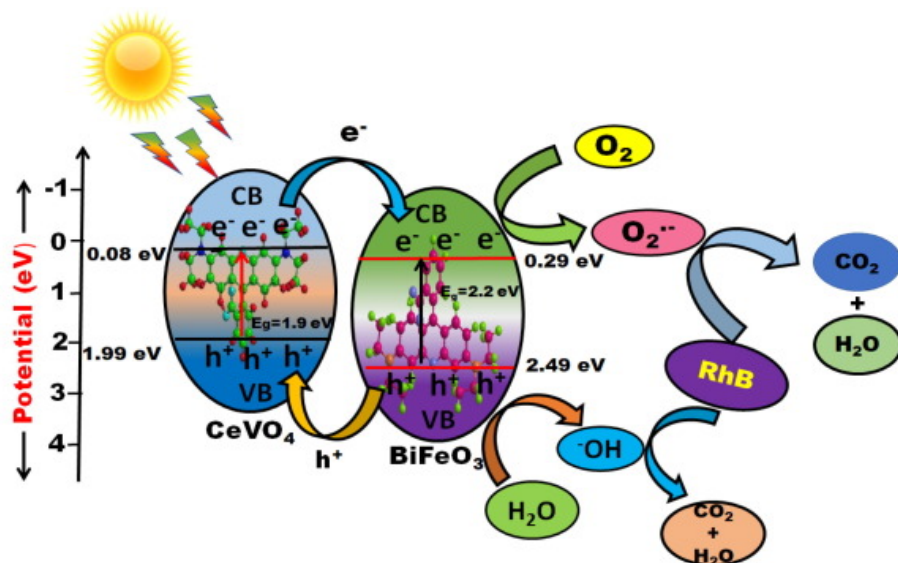
We next studied the 10% BFO/CVO photocatalyzed RhB degradation mechanism using radical scavengers. AO, BQ, and IPA were added to separate reactions as h^+ quenchers, $\cdot O_2^-$, and $\cdot OH$, respectively. As seen in Fig. 8c, when AO (2mM) was added to the reaction mixture, little change was observed in the degradation efficiency, indicating h^+ were not important to the degradation process. When BQ (5mM) was added to a solution, the degradation was reduced to just 36%. When IPA (1mM) was added, the degradation effectiveness was reduced to just 11%, effectively quenching the RhB degradation reaction. These results suggest that the $\cdot OH$ is a significant reactive species in 10% BFO/CVO photocatalyzed degradation of RhB.

The reusability of the fabricated 10% BFO/CVO catalyst was then studied. The same catalyst was used for three cycles of VLI and the findings are presented in Fig. 8d. The decomposition efficacy of the 10% BFO/CVO photocatalyst was observed to weaken slightly after three rounds of RhB degradation. These results are quite promising and suggest that the 10% BFO/CVO composites remain stable during the RhB degradation reaction and can be reused for multiple cycles.

The energy separation and photocatalytic degradation mechanism of the fabricated BFO/CVO composite are presented in Fig. 9. In the proposed reaction mechanism, the composite material absorbs visible light, and electrons are stimulated from the VB to the CB alongside the formation of a h^+ in the VB. The E_{VB} and E_{CB} energy potentials of BFO and CVO can be calculated with Equations (2), (3) [65].

$$E_{VB} = X - E^e + 0.5 E_g \quad (2)$$

$$E_{CB} = E_{VB} - E_g \quad (3)$$



[Download : Download high-res image \(355KB\)](#)

[Download : Download full-size image](#)

Fig. 9. Representative photocatalytic degradation mechanism for 10% BFO/CVO composite under VLI.

where X is referred as the electronegativity of an atom, and E° is the energy of a free electron (4.5 eV). The electronegativities of bare BFO and bare CVO are 5.89 eV and 5.54 eV, correspondingly. The optimal VB and CB potentials of bare BFO are 0.29 eV and 2.49 eV, respectively. Similarly, the as-synthesized CVO has VB and CB potentials of 0.085 eV and 1.99 eV, respectively. Based on the photo-illumination mechanism, both BFO and CVO are excited to produce a photogenerated charge carrier. Due to the more negative potential of the CB of CVO, the photogenerated e^- s are transferred from CVO to BFO while the h^+ are transferred from the VB of BFO to CVO, thereby reducing recombination of the photoinduced charges. Thus, the fabricated BFO/CVO composites, especially with 10% BFO loading, exhibit superior photocatalytic activity compared to the pure components individually.

4. Conclusion

In conclusion, we have designed and reported a novel photo-responsive BiFeO₃/CeVO₄ composite for the decomposition of organic pollutants under VLI. Pure BiFeO₃ (BFO) and CeVO₄ (CVO) were prepared via one-pot hydrothermal approach. A rapid wet-chemical impregnation process was then utilized to produce BFO/CVO composites with BFO loadings of 10, 20, and 30 wt%. Using RhB as a representative organic pollutant, all of the BFO/CVO composites were able to catalyze RhB degradation with visible light irradiation. 10% BFO/CVO demonstrated the good photocatalytic efficiency of 92% within 90 min of visible light illumination with 0.022 min^{-1} rate constant. The effectiveness of this catalyst is believed to derive from photogenerated e^- being transferred from CVO into BFO while the h^+ are transferred from the VB of BFO to CVO, thereby reducing recombination of the photoinduced charges. Through radical scavenger experiments, the major reactive species for 10% BFO/CVO photocatalyzed degradation of RhB were $\cdot\text{OH}$ radicals. These results imply that BiFeO₃/CeVO₄ composites could be suitable photocatalysts for eliminating organic pollutants in wastewater.

CRediT authorship contribution statement

Velu Venugopal: Investigation, Visualization. **Dhandapani Balaji:** Data curation, Conceptualization, Methodology, Investigation, Visualization. **Mani Preeyanghaa:** Data curation, Methodology, Investigation. **Cheol Joo Moon:** Data

curation, Methodology, Investigation. **Bernaurdshaw Neppolian**: Data curation, Methodology, Investigation. **Govarthanan Muthusamy**: Investigation. **Jayaraman Theerthagiri**: Investigation. **Jagannathan Madhavan**: Supervision, Writing – review & editing, Funding acquisition. **Myong Yong Choi**: Supervision, Writing – review & editing, Funding acquisition.

Declaration of Competing Interest

The authors declare that they have no known competing financial interests or personal relationships that could have appeared to influence the work reported in this paper.

Acknowledgements

Dr. J. Madhavan is grateful to Thiruvalluvar University for lab facilities and support. The authors, Ms. M. Preeyanghaa and B. Neppolian, would like to express their appreciation to the Deanship of Scientific Research Chairs, Department of Physics and Nanotechnology, SRM Institute of Science and Technology, for characterization. Prof. M.Y. Choi acknowledges the Korea Basic Science Institute (National research Facilities and Equipment Center) grant funded by the Ministry of Education (No. [2019R1A6C1010042](#), [2021R1A6C102A526](#), [2021R1A6C103A427](#)).

Appendix A. Supplementary material



The following are the Supplementary data to this article:

 [Download : Download Word document \(258KB\)](#)

Supplementary data 1.

[Recommended articles](#)

References

- [1] A.G. Ramu, A. Saruulbuyan, J. Theerthagiri, M.Y. Choi, D. Choi
Atomic layer encapsulation of ferrocene into zeolitic imidazolate framework-67 for efficient arsenic removal from aqueous solutions
Environ. Res., 221 (2023), Article 115289
 [View PDF](#) [View article](#) [View in Scopus](#)  [Google Scholar](#) 
- [2] M. Arumugam, Y. Yu, H.J. Jung, S. Yeon, H. Lee, J. Theerthagiri, S.J. Lee, M.Y. Choi
Solvent-mediated synthesis of BiOI with a tunable surface structure for effective visible light active photocatalytic removal of Cr(VI) from wastewater
Environ. Res., 197 (2021), Article 111080
 [View PDF](#) [View article](#) [View in Scopus](#)  [Google Scholar](#) 
- [3] M.H. Abdellah, S.A. Nosier, A.H. El-Shazly, A.A. Mubarak
Photocatalytic decolorization of methylene blue using TiO₂/UV system enhanced by air sparging
Alex. Eng. J., 57 (2018), pp. 3727-3735
 [View PDF](#) [View article](#) [View in Scopus](#)  [Google Scholar](#) 
- [4] H. Lotfizadeh, S. Rezazadeh, M.R. Fathollahi, J. Jokar, A.A. Mehrizi, B. Soltannia

The effect of silver nanoparticles on the automotive-based paint drying process: an experimental study

Int. J. Adv. Multidiscip. Eng. Sci., 2 (1) (2018), pp. 7-14

[Google Scholar](#) ↗

- [5] H. Lotfizadeh, A.A. Mehrizi, M.S. Motlagh, S. Rezazadeh
Thermal performance of an innovative heat sink using metallic foams and aluminum nanoparticles-
experimental study

Int. Commun. Heat Mass Transfer, 66 (2015), pp. 226-232

 [View PDF](#) [View article](#) [View in Scopus](#) ↗ [Google Scholar](#) ↗

- [6] H. Pourmirzaagha, H.H. Afrouzi, A.A. Mehrizi
Nano-particles transport in a concentric annulus: a lattice Boltzmann approach

J. Theor. Appl. Mech., 53 (3) (2015), pp. 683-695

[CrossRef](#) ↗ [View in Scopus](#) ↗ [Google Scholar](#) ↗

- [7] A.A. Mehrizi, H. Karimi-maleh, M. Naddafi, O. Karaman, F. Karimi, C. Karaman, C.K. Cheng
Evaporation characteristics of nanofuel droplets: a review

Fuel, 319 (2022), Article 123731

 [View PDF](#) [View article](#) [View in Scopus](#) ↗ [Google Scholar](#) ↗

- [8] M. Arumugam, S.J. Lee, T. Begildayeva, S.S. Naik, Y. Yu, H. Lee, J. Theerthagiri, M.Y. Choi
Enhanced photocatalytic activity at multidimensional interface of 1D-Bi₂S₃@2D-GO/3D-BiOI ternary
nanocomposites for tetracycline degradation under visible-light

J. Hazard. Mater., 404 (2021), Article 123868

 [View PDF](#) [View article](#) [View in Scopus](#) ↗ [Google Scholar](#) ↗

- [9] T. Jayaraman, S. Arumugam Raja, A. Priya, M. Jagannathan, M. Ashokkumar
Synthesis of a visible-light active V₂O₅-g-C₃N₄ heterojunction as an efficient photocatalytic and
photoelectrochemical material

New J. Chem., 39 (2015), pp. 1367-1374

[View in Scopus](#) ↗ [Google Scholar](#) ↗

- [10] J. Theerthagiri, S. Salla, R.A. Senthil, P. Nithyadharseni, A. Madankumar, P. Arunachalam, T. Maiyalagan, H.-S. Kim
A review on ZnO nanostructured materials: energy, environmental and biological applications

Nanotechnology, 30 (2019), Article 392001

[CrossRef](#) ↗ [View in Scopus](#) ↗ [Google Scholar](#) ↗

- [11] P.A.M. Arumugam, P. Arunachalam, A.M. Al-Mayouf, M.J. Theerthagiri, M.Y. Choi, Fabrication of visible-light
active BiFeWO₆/ZnO nanocomposites with enhanced photocatalytic activity, Colloids Surf. A: Physicochem. Eng.
Aspects 586 (2020) 124294.

[Google Scholar](#) ↗

- [12] M.A. Khan, W. Hussain, N. Hassan, M. Iiyas, H. Zille, S.Z. Abbas, L. Hui, Fabrication of Ag nanoparticles on a Cu-
substrate with excellent superhydrophobicity, anti-corrosion, and photocatalytic activity, Alex. Eng. J. 61 (2022)
6507-6521.

[Google Scholar](#) ↗

- [13] T. Bavani, A. Selvi, J. Madhavan, M. Selvaraj, V. Vinesh, B. Neppolian, S. Vijayanand, S. Murugesan

One-pot synthesis of bismuth yttrium tungstate nanosheet decorated 3D-BiOBr nanoflower heterostructure with enhanced visible light photocatalytic activity

Chemosphere, 297 (2022), Article 133993

 [View PDF](#) [View article](#) [View in Scopus](#) [Google Scholar](#)

- [14] V. Batra, I. Kaur, D. Pathania, Sonu, V. Chaudhary
Efficient dye degradation strategies using green synthesized ZnO-based nanoplatfoms: a review
Appl. Surf. Sci. Adv., 11 (2022), Article 100314

 [View PDF](#) [View article](#) [View in Scopus](#) [Google Scholar](#)

- [15] C. Li, S. Yu, X. Zhang, Y. Wang, C. Liu, G. Chen, H. Dong
Insight into photocatalytic activity, universality and mechanism of copper/chlorine surface dual-doped graphitic carbon nitride for degrading various organic pollutants in water
J. Colloid Interface Sci., 538 (2019), pp. 462-473

 [View PDF](#) [View article](#) [View in Scopus](#) [Google Scholar](#)

- [16] T. Yang, J. Peng, Y. Zheng, X. He, Y. Hou, L. Wu, X. Fu
Enhanced photocatalytic ozonation degradation of organic pollutants by ZnO modified TiO₂ nanocomposites
Appl. Catal. B, 221 (2018), pp. 223-234

 [View PDF](#) [View article](#) [View in Scopus](#) [Google Scholar](#)

- [17] F.M. Sanakousar, C.C. Vidyasagar, V.M. Jiménez-Pérez, K. Prakash
Recent progress on visible-light-driven metal and non-metal doped ZnO nanostructures for photocatalytic degradation of organic pollutants
Mater. Sci. Semicond. Process., 140 (2022), Article 106390

 [View PDF](#) [View article](#) [View in Scopus](#) [Google Scholar](#)

- [18] R. Wang, X. Xie, C. Xu, Y. Lin, D. You, J. Chen, Z. Li, Z. Shi, Q. Cui, M. Wang
Bi-piezoelectric effect assisted ZnO nanorods/PVDF-HFP spongy photocatalyst for enhanced performance on degrading organic pollutant
Chem. Eng. J., 439 (2022), Article 135787

 [View PDF](#) [View article](#) [View in Scopus](#) [Google Scholar](#)

- [19] E.H. Alosaimi, I.H. Alsohaimi, T.E. Dahan, Q. Chen, A.A. Younes, B. El-Gammal, S. Melhi
Photocatalytic degradation of methylene blue and antibacterial activity of mesoporous TiO₂-SBA-15 nanocomposite based on rice husk
Adsorpt. Sci. Technol. (2021), pp. 1-12

[CrossRef](#) [Google Scholar](#)

- [20] Z.A. Alrowaili, I.H. Alsohaimi, M.A. Betiha, A.A. Essawy, A.A. Mousa, S.F. Alruwaili, H.M. Hassan
Green fabrication of silver imprinted titania/silica nanospheres as robust visible light-induced photocatalytic wastewater purification
Mater. Chem. Phys., 241 (2020), Article 122403

 [View PDF](#) [View article](#) [View in Scopus](#) [Google Scholar](#)

- [21] I.H. Alsohaimi, A.M. Nassar, T.A.S. Elnasr, A.B. Cheba

A novel composite silver nanoparticles loaded calcium oxide stemming from egg shell recycling: a potent photocatalytic and antibacterial activities

J. Clean. Prod., 248 (2020), p. 19274

[Google Scholar ↗](#)

- [22] I.H. Alsohaimi, M.S. Alhumaimess, M. Alzaid, A.A. Essawy, M.R. El-Aassar, R.M. Mohamed, H.M. Hassan
Tailoring confined CdS quantum dots in polysulfone membrane for efficiently durable performance in solar-driven wastewater remediating systems

J. Environ. Manage., 332 (2023), Article 117351

 [View PDF](#) [View article](#) [View in Scopus ↗](#) [Google Scholar ↗](#)

- [23] S. Hussain, M.M. Alam, M. Imran, M.A. Ali, T. Ahamad, A.S. Haidyrah, S.M.R. Alotaibi, M. Shariq
A facile low-cost scheme for highly photoactive Fe₃O₄-MWCNTs nanocomposite material for degradation of methylene blue

Alex. Eng. J., 61 (11) (2022), pp. 9107-9117

 [View PDF](#) [View article](#) [View in Scopus ↗](#) [Google Scholar ↗](#)

- [24] L. Baloo, M.H. Isa, N.B. Sapari, A.H. Jagaba, L.J. Wei, S. Yavari, R. Razali, R. Vasu
Adsorptive removal of methylene blue and acid orange 10 dyes from aqueous solutions using oil palm wastes-derived activated carbons

Alex. Eng. J., 60 (6) (2021), pp. 5611-5629

 [View PDF](#) [View article](#) [View in Scopus ↗](#) [Google Scholar ↗](#)

- [25] H. Mandor, E.Z. El-Ashtoukhy, O. Abdelwahab, N.K. Amin, D.A. Kamel
A flow circulation reactor for simultaneous photocatalytic degradation of ammonia and phenol using N-doped ZnO beads

Alex. Eng. J., 61 (5) (2022), pp. 3385-3401

 [View PDF](#) [View article](#) [View in Scopus ↗](#) [Google Scholar ↗](#)

- [26] A. Alharbi, R.K. Shah, A. Sayqal, A. Subaihi, A.A. Alluhaybi, F.K. Algethami, A.M. Naglah, A.A. Almehizia, H.A. Katouah, H.M. Youssef

Facile synthesis of novel zinc sulfide/chitosan composite for efficient photocatalytic degradation of acid brown 5G and acid black 2BNG dyes

Alex. Eng. J., 60 (2) (2021), pp. 2167-2178

 [View PDF](#) [View article](#) [View in Scopus ↗](#) [Google Scholar ↗](#)

- [27] M. Saeed, K. Albalawi, I. Khan, N. Akram, I.H.A. Abd El-Rahim, S.K. Alhag, A. Ezzat Ahmed Faiza, Synthesis of p-n NiO-ZnO heterojunction for photodegradation of crystal violet dye

Alex. Eng. J., 65 (2023), pp. 561-574

 [View PDF](#) [View article](#) [View in Scopus ↗](#) [Google Scholar ↗](#)

- [28] J. Theerthagiri, K. Karuppasamy, S.J. Lee, R. Shwetharani, H.-S. Kim, S.K.K. Pasha, M. Ashokkumar, M.Y. Choi, Fundamentals and comprehensive insights on pulsed laser synthesis of advanced materials for diverse photo- and electrocatalytic applications, Light: Sci. Appl. 11 (2022) 250.

[Google Scholar ↗](#)

- [29] W. Li, Z. Liu, Y. Dong, L. Wang, Z. Liu, L. Zhang, Z.-A. Qiao
Micellar interface modulation self-assembly strategy towards mesoporous bismuth oxychloride-based materials for boosting photocatalytic pharmaceuticals degradation

Chem. Eng. J., 450 (2022), Article 137897

 [View PDF](#) [View article](#) [View in Scopus](#) [Google Scholar](#)

- [30] L. Zhang, Y. Man, Y. Zhu
Effects of Mo replacement on the structure and visible-light-induced photocatalytic performances of Bi₂WO₆ photocatalyst

ACS Catal., 1 (2011), pp. 841-848

[CrossRef](#) [View in Scopus](#) [Google Scholar](#)

- [31] M. Shang, W. Wang, L. Zhang
Preparation of BiOBr lamellar structure with high photocatalytic activity by CTAB as Br source and template

J. Hazard. Mater., 167 (2009), pp. 803-809

 [View PDF](#) [View article](#) [View in Scopus](#) [Google Scholar](#)

- [32] L. Zhang, T. Xu, X. Zhao, Y. Zhu
Controllable synthesis of Bi₂MoO₆ and effect of morphology and variation in local structure on photocatalytic activities

Appl. Catal. B, 98 (2010), pp. 138-146

 [View PDF](#) [View article](#) [View in Scopus](#) [Google Scholar](#)

- [33] J. Tang, Z. Zou, J. Ye
Efficient photocatalytic decomposition of organic contaminants over CaBi₂O₄ under visible-light irradiation

Angew. Chem. Int. Ed., 43 (2004), pp. 4463-4466

[View in Scopus](#) [Google Scholar](#)

- [34] B. Chen, M. Li, Y. Liu, Z. Zuo, F. Zhuge, Q.-F. Zhan, R.-W. Li
Effect of top electrodes on photovoltaic properties of polycrystalline BiFeO₃ based thin film capacitors

Nanotechnology, 22 (2011), Article 195201

[CrossRef](#) [View in Scopus](#) [Google Scholar](#)

- [35] T. Soltani, M.H. Entezari
Photolysis and photocatalysis of methylene blue by ferrite bismuth nanoparticles under sunlight irradiation

J. Mol. Catal. A Chem., 377 (2013), pp. 197-203

 [View PDF](#) [View article](#) [View in Scopus](#) [Google Scholar](#)

- [36] J. Wu, Z. Fan, D. Xiao, J. Zhu, J. Wang
Multiferroic bismuth ferrite-based materials for multifunctional applications: ceramic bulks, thin films and nanostructures

Prog. Mater. Sci., 84 (2016), pp. 335-402

 [View PDF](#) [View article](#) [View in Scopus](#) [Google Scholar](#)

- [37] A. Malathi, P. Arunachalam, V.S. Kirankumar, J. Madhavan, A.M. Al-Mayouf
An efficient visible light driven bismuth ferrite incorporated bismuth oxyiodide (BiFeO₃/BiOI) composite photocatalytic material for degradation of pollutants

Opt. Mater., 84 (2018), pp. 227-235

 [View PDF](#) [View article](#) [View in Scopus ↗](#) [Google Scholar ↗](#)

- [38] T. Bavani, J. Madhavan, S. Prasad, M.S. AlSalhi, M.J. Aljaafreh
A straightforward synthesis of visible light driven BiFeO₃/AgVO₃ nanocomposites with improved photocatalytic activity

Environ. Pollut., 269 (2021), Article 116067

 [View PDF](#) [View article](#) [View in Scopus ↗](#) [Google Scholar ↗](#)

- [39] B. Samran, S. Iunput, S. Tonnonchiang, S. Chaiwichian, BiFeO₃/BiVO₄ nanocomposite photocatalysts with highly enhanced photocatalytic activity for rhodamine B degradation under visible light irradiation, Phys. B: Condensed Matter. 561 (2019) 23–28.

[Google Scholar ↗](#)

- [40] J. Shang, H. Chen, T. Chen, X. Wang, G. Feng, M. Zhu, Y. Yang, X. Jia
Photocatalytic degradation of rhodamine B and phenol over BiFeO₃/BiOCl nanocomposite

Appl. Phys. A, 125 (2019), p. 133

[View in Scopus ↗](#) [Google Scholar ↗](#)

- [41] B. Harikumar, M.K. Okla, I.A. Alaraidh, A. Mohebaldin, W. Soufan, M.A. Abdel-Maksoud, M. Aufy, A.M. Thomas, L.L. Raju, S.S. Khan

Robust visible light active CoNiO₂–BiFeO₃–NiS ternary nanocomposite for photo-fenton degradation of rhodamine B and methyl orange: Kinetics, degradation pathway and toxicity assessment

J. Environ. Manage., 317 (2022), Article 115321

 [View PDF](#) [View article](#) [View in Scopus ↗](#) [Google Scholar ↗](#)

- [42] L. Yao, E. Guo, K. Sun, Q. Lu, Q. Wang
Formation of one-dimensional CeVO₄ nanobelts as an enhanced photoelectrocatalyst and density functional study

Mater. Lett., 231 (2018), pp. 11-15

 [View PDF](#) [View article](#) [View in Scopus ↗](#) [Google Scholar ↗](#)

- [43] A. Phuruangrat, T. Thongtem, S. Thongtem
Hydrothermal synthesis and characterization of Dy-doped CeVO₄ nanorods used for photodegradation of methylene blue and rhodamine B

J. Rare Earths, 39 (2021), pp. 1211-1216

 [View PDF](#) [View article](#) [View in Scopus ↗](#) [Google Scholar ↗](#)

- [44] Y. Song, R. Wang, X. Li, B. Shao, H. You, C. He
Constructing a novel Ag nanowire@CeVO₄ heterostructure photocatalyst for promoting charge separation and sunlight driven photodegradation of organic pollutants





Chin. Chem. Lett., 33 (2022), pp. 1283-1287







 [View PDF](#) [View article](#) [View in Scopus ↗](#) [Google Scholar ↗](#)

- [45] M. Wang, Y. Guo, Z. Wang, H. Cui, T. Sun, Y. Tang
Simple glycerol-assisted and morphology controllable solvothermal synthesis of CeVO₄/BiVO₄ hierarchical hollow microspheres with enhanced photocatalytic activities

Mater. Chem. Front., 5 (2021), pp. 6522-6529

[CrossRef ↗](#) [View in Scopus ↗](#) [Google Scholar ↗](#)

- [46] M. Amin Marsooli, M. Rahimi Nasrabadi, M. Fasihi-Ramandi, K. Adib, S. Pourmasoud, F. Ahmadi, M. Eghbali, A. Sobhani Nasab, M. Tomczykowa, M.E. Plonska-Brzezinska, Synthesis of magnetic Fe₃O₄/ZnWO₄ and Fe₃O₄/ZnWO₄/CeVO₄ nanoparticles: the photocatalytic effects on organic pollutants upon irradiation with UV-Vis light, *Catalysts* (2020).
[Google Scholar ↗](#)
- [47] L. Yao, X. Li, H. Liu, Z. Li, Q. Lu
One-dimensional hierarchical CeVO₄/TiO₂ heterostructures with enhanced photocatalytic performance
J. Nanopart. Res., 21 (2019), p. 140
[View in Scopus ↗](#) [Google Scholar ↗](#)
- [48] J. Guan, J. Li, Z. Ye, D. Wu, C. Liu, H. Wang, C. Ma, P. Huo, Y. Yan
La₂O₃ media enhanced electrons transfer for improved CeVO₄@halloysite nanotubes photocatalytic activity for removing tetracycline
J. Taiwan Inst. Chem. Eng., 96 (2019), pp. 281-298
 [View PDF](#) [View article](#) [View in Scopus ↗](#) [Google Scholar ↗](#)
- [49] K. Leeladevi, M. Arunpandian, J.V. Kumar, T. Chellapandi, M. Thirupathi, G. Madhumitha, J.-W. Lee, E.R. Nagarajan
Fabrication of 3D pebble-like CeVO₄/g-C₃N₄ nanocomposite: a visible light-driven photocatalyst for mitigation of organic pollutants
Diam. Relat. Mater., 116 (2021), Article 108424
 [View PDF](#) [View article](#) [View in Scopus ↗](#) [Google Scholar ↗](#)
- [50] K. Yu, L. Li, C. Zang, B. Zhao, F. Chen
BiFeO₃/MoS₂ nanocomposites with the synergistic effect between ≡Mo^{VI}/≡Mo^{IV} and ≡Fe^{III}/≡Fe^{II} redox cycles for enhanced Fenton-like activity
Colloids Surf. A: Physicochem. Eng. Asp., 578 (2019), Article 123607
 [View PDF](#) [View article](#) [View in Scopus ↗](#) [Google Scholar ↗](#)
- [51] Q.Q. Liu, C.Y. Fan, H. Tang, T.D. Ma, J.Y. Shen
One-step synthesis of recycled 3D CeVO₄/rGO composite aerogels for efficient degradation of organic dyes
RSC Adv., 6 (2016), pp. 85779-85786
[View in Scopus ↗](#) [Google Scholar ↗](#)
- [52] S.-M. Lam, Z.H. Jaffari, J.-C. Sin, H. Zeng, H. Lin, H. Li, A.R. Mohamed, D.-Q. Ng
Surface decorated coral-like magnetic BiFeO₃ with Au nanoparticles for effective sunlight photodegradation of 2,4-D and E. coli inactivation
J. Mol. Liq., 326 (2021), Article 115372
 [View PDF](#) [View article](#) [View in Scopus ↗](#) [Google Scholar ↗](#)
- [53] P. Ju, Y. Yu, M. Wang, Y. Zhao, D. Zhang, C. Sun, X. Han
Synthesis of EDTA-assisted CeVO₄ nanorods as robust peroxidase mimics towards colorimetric detection of H₂O₂
J. Mater. Chem. B, 4 (2016), pp. 6316-6325
[View in Scopus ↗](#) [Google Scholar ↗](#)

- [54] S. Ashrafi, M. Mousavi-Kamazani, S. Zinatloo-Ajabshir, A. Asghari
Novel sonochemical synthesis of Zn₂V₂O₇ nanostructures for electrochemical hydrogen storage
Int. J. Hydrogen Energy, 45 (2020), pp. 21611-21624
 [View PDF](#) [View article](#) [View in Scopus](#) [Google Scholar](#)
- [55] I. Othman, J. Hisham Zain, M. Abu Haija, F. Banat
Catalytic activation of peroxymonosulfate using CeVO₄ for phenol degradation: an insight into the reaction pathway
Appl. Catal. B, 266 (2020), Article 118601
 [View PDF](#) [View article](#) [View in Scopus](#) [Google Scholar](#)
- [56] S. Mishra, M. Priyadarshinee, A.K. Debnath, K.P. Muthe, B.C. Mallick, N. Das, P. Parhi
Rapid microwave assisted hydrothermal synthesis cerium vanadate nanoparticle and its photocatalytic and antibacterial studies
J. Phys. Chem. Solid, 137 (2020), Article 109211
 [View PDF](#) [View article](#) [View in Scopus](#) [Google Scholar](#)
- [57] K.P. Remya, D. Prabhu, R.J. Joseyphus, A.C. Bose, C. Viswanathan, N. Ponpandian
Tailoring the morphology and size of perovskite BiFeO₃ nanostructures for enhanced magnetic and electrical properties
Mater. Des., 192 (2020), Article 108694
 [View PDF](#) [View article](#) [View in Scopus](#) [Google Scholar](#)
- [58] X. Yang, W. Zuo, F. Li, T. Li
Surfactant-free and controlled synthesis of hexagonal CeVO₄ nanoplates: photocatalytic activity and superhydrophobic property
ChemistryOpen, 4 (2015), pp. 288-294
[CrossRef](#) [View in Scopus](#) [Google Scholar](#)
- [59] Y. Zhang, Y. Wang, J. Qi, Y. Tian, M. Sun, J. Zhang, T. Hu, M. Wei, Y. Liu, J. Yang
Enhanced magnetic properties of BiFeO₃ thin films by doping: analysis of structure and morphology
Nanomaterials (2018)
[Google Scholar](#)
- [60] S. Mandal, C.K. Ghosh, D. Sarkar, U.N. Maiti, K.K. Chattopadhyay
X-ray photoelectron spectroscopic investigation on the elemental chemical shifts in multiferroic BiFeO₃ and its valence band structure
Solid State Sci., 12 (2010), pp. 1803-1808
 [View PDF](#) [View article](#) [View in Scopus](#) [Google Scholar](#)
- [61] Z. Li, L. Cheng, S. Zhang, Z. Wang, C. Fu
Enhanced photocatalytic and magnetic recovery performance of Co-doped BiFeO₃ based on MOFs precursor
J. Solid State Chem., 279 (2019), Article 120978
 [View PDF](#) [View article](#) [View in Scopus](#) [Google Scholar](#)
- [62] G. Lu, Z. Lun, H. Liang, H. Wang, Z. Li, W. Ma

In situ fabrication of BiVO₄-CeVO₄ heterojunction for excellent visible light photocatalytic degradation of levofloxacin

J. Alloy. Compd., 772 (2019), pp. 122-131

 [View PDF](#) [View article](#) [View in Scopus ↗](#) [Google Scholar ↗](#)

- [63] T. Begildayeva, J. Theerthagiri, S.J. Lee, Y. Yu, M.Y. Choi, Unraveling the synergy of anion modulation on Co electrocatalysts by pulsed laser for water splitting: intermediate capturing by in situ/operando Raman studies, *Small* (2022) 2204309.

[Google Scholar ↗](#)

- [64] S. Naik Shreyanka, J. Theerthagiri, S.J. Lee, Y. Yu, M.Y. Choi
Multiscale design of 3D metal–organic frameworks (M–BTC, M: Cu Co, Ni) via PLAL enabling bifunctional electrocatalysts for robust overall water splitting

Chem. Eng. J., 446 (2022), Article 137045

 [View PDF](#) [View article](#) [View in Scopus ↗](#) [Google Scholar ↗](#)

- [65] J. Theerthagiri, R.A. Senthil, A. Malathi, A. Selvi, J. Madhavan, M. Ashokkumar
Synthesis and characterization of a CuS–WO₃ composite photocatalyst for enhanced visible light photocatalytic activity

RSC Adv., 5 (2015), pp. 52718-52725

[View in Scopus ↗](#) [Google Scholar ↗](#)

Cited by (14)

3D-Zn²/SnO⁴ nanobolt coupled with ZnO-SnO² nanocomposites for ameliorated the hazardous dye degradation based on a dual Z–scheme system

2024, *Process Safety and Environmental Protection*

[Show abstract](#) 

Synergistic effects of co-doping and rGO reinforcement to boost the structural, electrical, optical, and photocatalytic properties of manganese ferrite

2024, *Ceramics International*

[Show abstract](#) 

Cobalt oxide coupled with graphitic carbon nitride composite heterojunction for efficient Z-scheme photocatalytic environmental pollutants degradation performance

2023, *Environmental Research*

[Show abstract](#) 

N-Hydroxysuccinamide functionalized iron oxide nanoparticles conjugated with 5-fluorouracil for hyperthermic therapy of malignant liver cancer cells by DNA repair disruption

2023, *International Journal of Biological Macromolecules*

[Show abstract](#) 

Research progress in green synthesis of manganese and manganese oxide nanoparticles in biomedical and environmental applications – A review

2023, Chemosphere

[Show abstract](#) 

Synthesis of solar-driven Cu-doped graphitic carbon nitride photocatalyst for enhanced removal of caffeine in wastewater

2023, Environmental Research

[Show abstract](#) 



[View all citing articles on Scopus](#) 

Peer review under responsibility of Faculty of Engineering, Alexandria University.

© 2023 THE AUTHORS. Published by Elsevier BV on behalf of Faculty of Engineering, Alexandria University.



All content on this site: Copyright © 2024 Elsevier B.V., its licensors, and contributors. All rights are reserved, including those for text and data mining, AI training, and similar technologies. For all open access content, the Creative Commons licensing terms apply.





Ultra-efficient, low-cost and carbon-supported transition metal sulphide as a platinum free electrocatalyst towards hydrogen evolution reaction at alkaline medium

Kumar Premnath^a, Jagannathan Madhavan^a  , Saradh Prasad^{b c} , Mamduh J. Aljaafreh^b ,
Mohamad S. AlSalhi^{b c}  , Show Pou Loke^d 

Show more 

 Share  Cite

<https://doi.org/10.1016/j.ijhydene.2021.09.120> 

[Get rights and content](#) 

Highlights

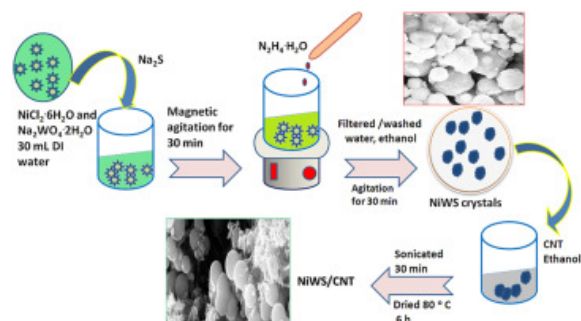
- The electrocatalyst prepared by one-step co-precipitation reduction process.
- Synergistic effects of heteroatom's with carbon are highlighted in energy application.
- NiWS/CNT showed highest activity towards HER. (175 mV current density).
- This finding offered an outstanding Pt-free electrocatalyst for energy application.
- NiWS/CNT can be used an alternative for water splitting process.

Abstract

Hydrogen (H₂) is the future energy carrier and it is quite challenging to produce at a large-scale on economic basis. The water splitting technique has achieved a good place in H₂ production. To generate efficient electrocatalysts for the Hydrogen evolution reaction (HER), low-cost synthetic designs are necessary. In our study, a one-step co-precipitation reduction process was used to synthesize NiWS electrocatalyst. The crystalline structure, phase purity, elemental composition and the surface morphology of the as-prepared samples have been examined by different characterization techniques. These techniques have proved that the elemental presence and formation of NiWS with high crystalline nature (rhombohedral). Furthermore, the performance of the electrocatalyst towards HER has been evaluated through

electrochemical methods. On analysis, NiWS/CNT showed an excellent electrochemical activity of 175 mV, and pure NiWS showed 201 mV at 10 mA/cm² in an alkaline electrolyte. These over-potential values are lower than HER in acid and neutral electrolytes. Further, the as-prepared NiWS/CNT proved to be a highly stable and efficient platinum-free electrocatalyst for HER.

Graphical abstract



[Download : Download high-res image \(238KB\)](#)

[Download : Download full-size image](#)

Introduction

Recent developments in energy production and electrocatalysts synthesis have always been a fascinating area to researchers. Though all forms of energy are indispensable for human life, fuel energy and electrical energy are considered important. Due to the increasing energy demand and environmental pollution, comprehensive efforts in search of renewable and environmentally compatible alternative energy resources are gaining significant research value. On this subject, splitting of water using sunlight or electricity made from renewable sources is considered as one of the promising and appealing processes [1,2]. However, approximately 95% of H₂ is presently generated using coal gasification and steam methane reforming that depend on traditional fuel resources such as fossil fuel. Whereas water electrolysis is used to produce a mere 4% of H₂ [3,4]. So to improve the H₂ production from the water-splitting process, cheap and highly deserved electrocatalysts are required in hydrogen evolution reaction (HER). The milestone HER catalyst relies primarily on employing platinum (Pt), which is a scanty and exorbitant noble metal. These barriers have challenged researchers to explore Pt-free electrocatalysts for HER applications.

So far, various transition metals with carbides, phosphides, and chalcogenides (sulfides, selenides and tellurides) have been successfully examined as electrode materials by various synthesis protocols [5,6]. Among the earth-abundant materials, metal sulfides, and transition metal chalcogenides have been recognized as efficient electrocatalysts. These materials exhibit higher electrocatalytic performance, toxic-free nature, bio-compatible (in most cases), superiority stability, and high abundance, thus making them advantageous alternatives for the electrocatalytic production of H₂ [7,8]. The metal tellurides are the chalcogenides that consists of tellurium as an electronegative element with different electropositive metals [9,10]. Tellurium, selenium and polonium are metalloids, whereas sulfur and oxygen are nonmetals in the oxygen family (16 A group of the periodic table). These characteristic properties of elements in 16 A group play an essential role for structural dependent applications of metal oxides, sulfides, selenides and tellurides [11,12].

In recent research reports, the most discussed transition-metal dichalcogenides (TMDs) with a general formula of MX₂ (M=Ni, Fe, Mo, Co and W, where X=S or Se) compounds are reported as capable electrocatalysts for HER [13,14]. Based on the molecular orbital theory, the TMDs possess proper surface, proton and hydride acceptor sites, which aids them

to function as a good bi-functional electrocatalyst [15]. This helps in promoting active electron transfer between the surface site and the adsorbed reaction intermediates.

More recently, nickel-based composites have been elevated to the massive scale of research owing to its controllable electrocatalytic activity by the synergistic action of the alloy compounds [16,17], with a special mention of nickel sulfide as the finest catalyst with high activity and excellent electron transferability in both the media of alkaline and neutral. Nickel compounds were reported to achieve much higher activity with the best composite combinations of NiX, where X=Se, S, C, P [18,19]. Similarly, nickel-doped composites also have a superior effect than other transition metals such as Co, Mo, Fe, Mn, W. In addition, Ni-based binary metals have modified electron density with Fermi level and proper metal-H-bond binding energy. From the recent research reports, many substoichiometric types of tungsten oxides with oxygen vacancies are found. The formation of plentiful oxygen vacancies sites induces the formation of metallic phases. Here in, the tungsten has been composited with nickel for good electrochemical active catalyst [20,21]. The revolutionary developments of carbon research evolved with the innovation of carbon nanotubes (CNTs) [22], [23], [24]. Owing to its extraordinary electrocatalytic performance and large surface areas [25], [26], [27], tungsten carbon (W-WC/CNT) electrode exhibited an optimal HER performance with an overpotential of 155mV at 10mA/cm² and a lowest Tafel slope 56 mV/dec [28]. In another study, NiP catalyst activated with the addition of CNT, (NiP@CNT) exhibited 165mV and 78 mV/dec Tafel slope with too long stability of up to 20h [29]. Facile construction of N-doped Mo₂C@CNT composites with 3D nanospherical structures exhibited an excellent HER performance with less overpotential of 183mV at 10mA/cm² and smaller Tafel slope of 73 mV/dec [30]. Carbon nanomaterials activated carbon, carbon fiber, graphene, carbon nanotubes are being actively used in electrode materials due to their high specific surface area, excellent electrical conductivity, low cost and abundant availability. The pore structure of carbon excellently supports to increase the catalytic activity of transition metal based composites [31]. In this present investigation, nickel sulphide has been composited with tungsten, then the catalytic activity has been increased with the addition of CNTs supports. This composition is explored as an efficient electrocatalyst with high current density at low overpotentials at different pH electrolytes.

Section snippets

Materials

Nickel chloride hexahydrate (NiCl₂·6H₂O, 98.9% - GRM1394) was purchased from Himedia laboratory Mumbai, India. Sodium tungstate dehydrates (Na₂WO₄·2H₂O, 99.0% - GRM1082) were purchased from Himedia laboratory Mumbai, India. Sodium sulfide nonahydrate (Na₂S·9H₂O, 99.0% - GRM1572) was purchased from Himedia laboratory Mumbai. Hydrazine hydrate (N₂H₄·H₂O, 97.5% -ASH2558) was bought from Avra Hyderabad India. Sulphuric acid (H₂SO₄, 99.1% - CL6C670881) from Merck, Mumbai, India. Potassium hydroxide...

Characterization studies

The XRD patterns of the synthesized pure NiWS and composite NiWS/CNT are depicted in Fig. 1a–d. The carbon nanotubes (CNT) show diffraction peaks at 27.53° and 43.44° as shown in Fig. 1a. The precursor NiS obtained peaks at 2θ values 19.50°, 27.53°, 31.08°, 35.10°, 36.8°, 43.44° and 54.72° (Fig. 1b) are indexed to the planes of (110), (101), (300), (021), (220), (211) and (321) respectively, the spectra exhibiting rhombohedral phase, (JCPDS No. 86–2281), NiS 2 theta peaks are well correlated...

Conclusions

Fabrication of advanced electrocatalysts for sustainable H₂ production from water splitting is crucial in energy research, as H₂ will be the future fuel on economy grounds. Therefore in the present investigation, we have reported on nickel tungsten sulfide composite with CNT which was synthesized by a simple one-step co-precipitation reduction method. The synthesized composite was found to exhibit a rhombohedral phase as confirmed by XRD. The FESEM results revealed the tiny crystal morphology...

Declaration of competing interest

The authors declare that they have no known competing financial interests or personal relationships that could have appeared to influence the work reported in this paper....

Acknowledgements

The authors extend their appreciation to the Researchers Supporting Project Number (RSP-2021/68), King Saud University, Riyadh, Saudi Arabia....

[Special issue articles](#) [Recommended articles](#)

References (50)

R. Jiang *et al.*

[Electrochemically synthesized N-doped molybdenum carbide nanoparticles for efficient catalysis of hydrogen evolution reaction](#)

Electrochim Acta (2018)

F. Zhang *et al.*

[Revealing the catalytic micro-mechanism of Mon, WN and WC on hydrogen evolution reaction Revealing the catalytic micro-mechanism of Mon, WN and WC on hydrogen evolution reaction](#)

Int J Hydrogen energy (2021)

M.A. Ghanem *et al.*

[Mesoporous cobalt hydroxide prepared using liquid crystal template for efficient oxygen evolution in alkaline media](#)

Electrochim Acta (2016)

S. Yoo *et al.*

[Encapsulation of Pt nanocatalyst with N-containing carbon layer for improving catalytic activity and stability in the hydrogen evolution reaction](#)

Int J Hydrogen energy (2021)

C. Tang *et al.*

[NiS₂ nanosheets array grown on carbon cloth as an efficient 3D hydrogen evolution cathode](#)

Electrochim Acta (2015)

J. Wang *et al.*

[NiS₂ nanosheet array: a high-active bifunctional electrocatalyst for hydrazine oxidation and water reduction toward energyefficient hydrogen production](#)

Mater Today Energy (2017)

J. Theerthagiri *et al.*

[Growth of iron diselenide nanorods on graphene oxide nanosheets as advanced electrocatalyst for hydrogen evolution reaction](#)

Int J Hydrogen Energy (2017)

K. Premnath *et al.*

[Hydrothermally synthesized nickel molybdenum selenide composites as cost-effective and efficient trifunctional electrocatalysts for water splitting reactions](#)

Int J Hydrogen Energy (2019)

S. Yoo *et al.*

[Encapsulation of Pt nanocatalyst with N-containing carbon layer for improving catalytic activity and stability in the hydrogen evolution reaction](#)

Int J Hydrogen energy (2021)

J. Liang *et al.*

[Effective conversion of heteroatomic model compounds in microalgae-based bio-oils to hydrocarbons over \$\beta\$ -Mo₂C/CNTs catalyst](#)

J Mol Catal Chem (2016)



View more references

Cited by (9)

[The impact and performance of carbon-supported platinum group metal electrocatalysts for fuel cells](#)

2024, International Journal of Electrochemical Science

[Show abstract](#)

[Renovated FeCoP-NC nanospheres wrapped by CoP-NC nanopetals: As a tremendously effectual and robust MOF-assisted electrocatalyst for hydrogen energy production](#)

2024, Environmental Research

[Show abstract](#)

[Pyrite copper nickel sulfide for stable hydrogen evolution reaction in alkaline media](#)

2024, International Journal of Hydrogen Energy

[Show abstract](#)

[Baby diaper's super absorbent polymer derived carbon templated NiCuP@NiCu nanostructures for green hydrogen production](#)

2024, International Journal of Hydrogen Energy

[Show abstract](#)

Zn_xNi_{1-x}Se₂ nanoparticles grown on functionalized nickel foam as binder-free electrocatalysts for HER in acidic and alkaline media

2023, Surfaces and Interfaces

[Show abstract](#) 

Self-assembled NiMn₂O₄ shell on nanoporous Ni(Mn) core for boosting alkaline hydrogen production

2023, Applied Surface Science

Citation Excerpt :

...As shown in Fig. 4a, the electrochemical performances of catalysts are evaluated in 1 M KOH using a three electrode setup with a scan rate of 10 mV s⁻¹. As expected, Ov-NMO/np-Ni₃₀(Mn) affords an overpotential of 130 mV at the cathodic current density of 10 mA cm⁻², which is ranked only second to commercial Pt/C (90 mV), but superior to that of Ov-NMO/np-Ni₂₅(Mn) (181 mV), Ov-NMO/np-Ni₂₀(Mn) (266 mV), NMO/np-Ni₃₀(Mn) (199 mV), NMO/np-Ni₂₅(Mn) (228 mV), NMO/np-Ni₂₀(Mn) (270 mV) and other reported alkaline HER catalysts (Fig. 4h and Table S3) [41–44]. It also reflects that the presence of OV could indeed improve electrocatalytic activities of shell-core materials in this study...

[Show abstract](#) 

[View all citing articles on Scopus](#) 

[View full text](#)

© 2021 Hydrogen Energy Publications LLC. Published by Elsevier Ltd. All rights reserved.



All content on this site: Copyright © 2024 Elsevier B.V., its licensors, and contributors. All rights are reserved, including those for text and data mining, AI training, and similar technologies. For all open access content, the Creative Commons licensing terms apply.

